Exoplanery searches with gravitational microlensing: polarization issues

А.Ф.Захаров (Alexander F. Zakharov)
Institute of Theoretical and Experimental Physics,   Moscow,

e-mail: zakharov@itep.ru

- **Main references: G. Ingrosso , F. De Paolis, P. Jetzer, S. Calchi Novati , A.A. Nucita, A.F. Zakharov   (MNRAS, 2009); (GRG, 2010), (MNRAS, 2012)**
-
- **9th SCSLSA, Banja Koviljaca, 16 May 2013**

Gravitational lensing: From micro to nano

Alexander F. Zakharov

Institute of Theoretical and Experimental Physics, B. Cheremushkinskaya, 25, 117259 Moscow, Russia
Bogoliubov Laboratory for Theoretical Physics, JINR, 141980 Dubna, Russia

**A R T I C L E   I N F O**

A B S T R A C T

Different regimes of gravitational lensing depend on lens masses and roughly correspond to angular distance between images. If a gravitational lens has a typical stellar mass, this regime is named a microlensing because a typical angular distance between images is about microarcseconds in the case when sources and lenses are located at cosmological distances. An angular distance depends on a lens mass as a square root and therefore, if a lens has a typical Earth-like planet mass of $10^{-6} M_\odot$, such a regime is called nanolensing. Thus, generally speaking, one can call a regime with a planet mass lens a nanolensing (independently on lens and source locations). So, one can name searches for planets with gravitational lens method a gravitational nanolensing. There are different methods for finding exoplanets such as radial spectral shifts, astrometrical measurements, transits, pulsar timing etc. Gravitational microlensing (including pixel-lensing) is among the most promising techniques if we are interested to find Earth-like planets at distances about a few astronomical units from the host star.

1 nano angular second

2.5 cm coin from the Neptune orbit (4.5* 10^{9} km) (about 30 AU).

Millimetron is a future mission for space–ground interferometry. 12 m radio antenna has to be placed at the L2 point
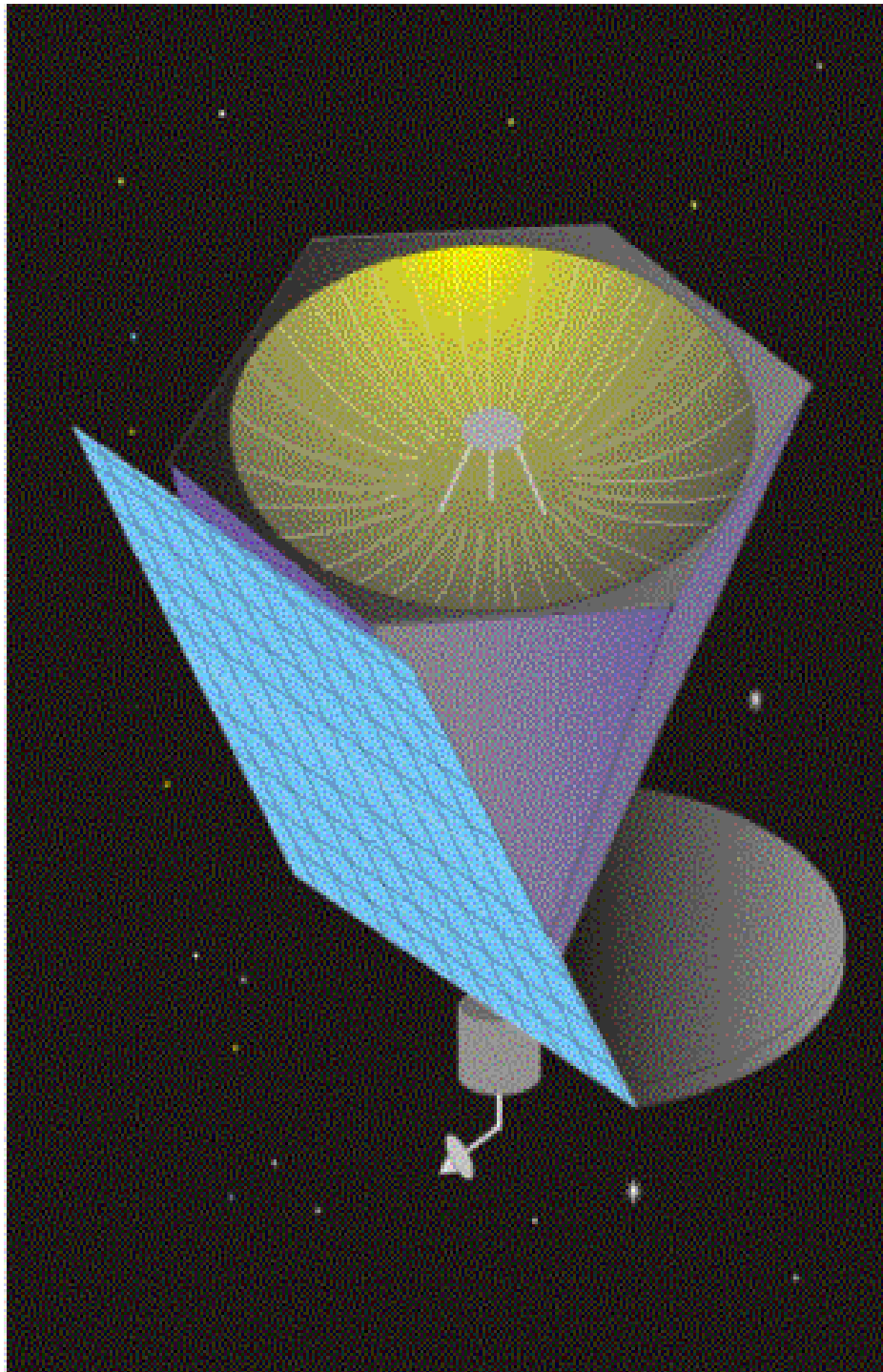
MILLIMETRON

antenna diameter 12 m

range of wavelength 0.01 - 20 mm

bolometric sensitivity
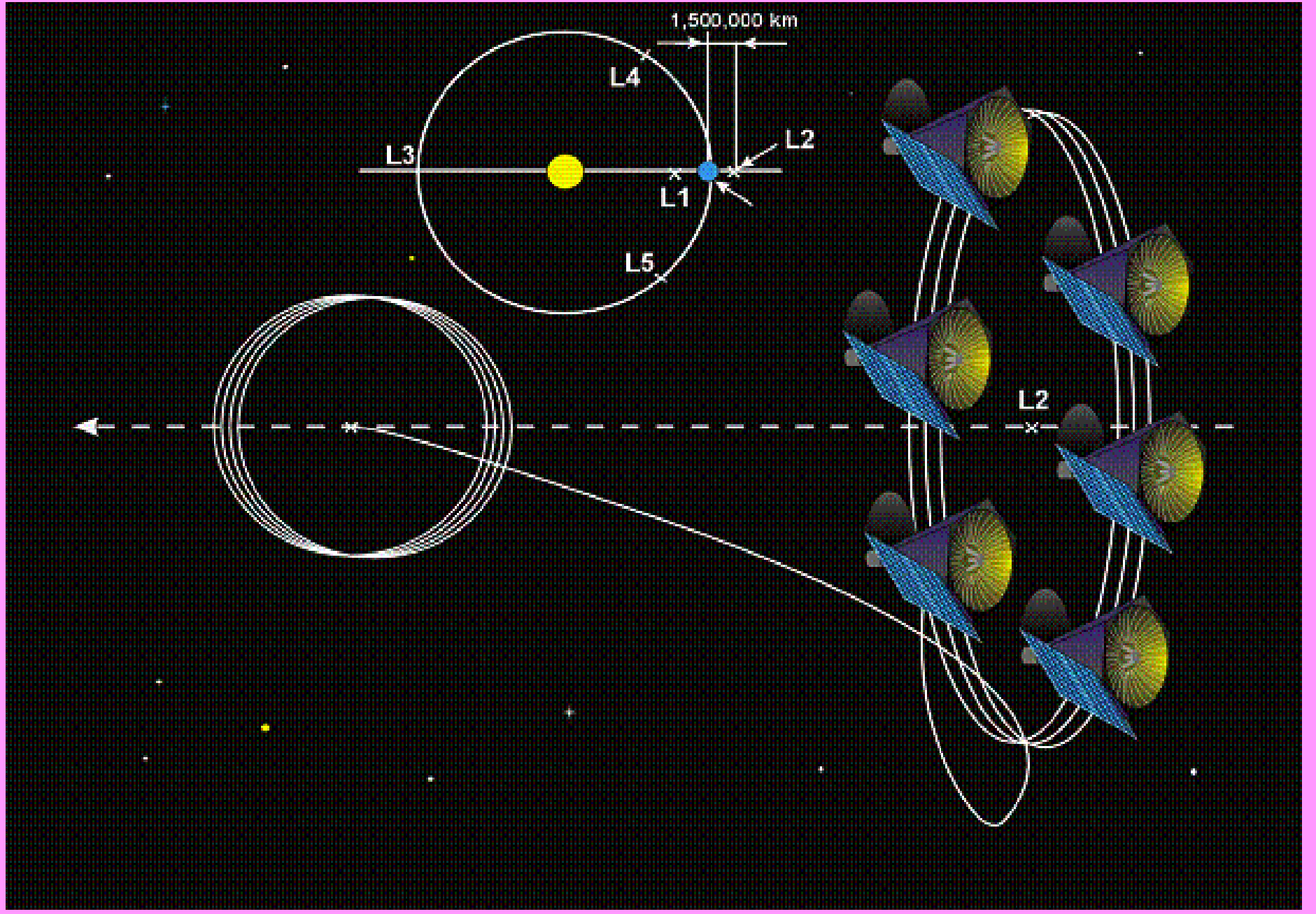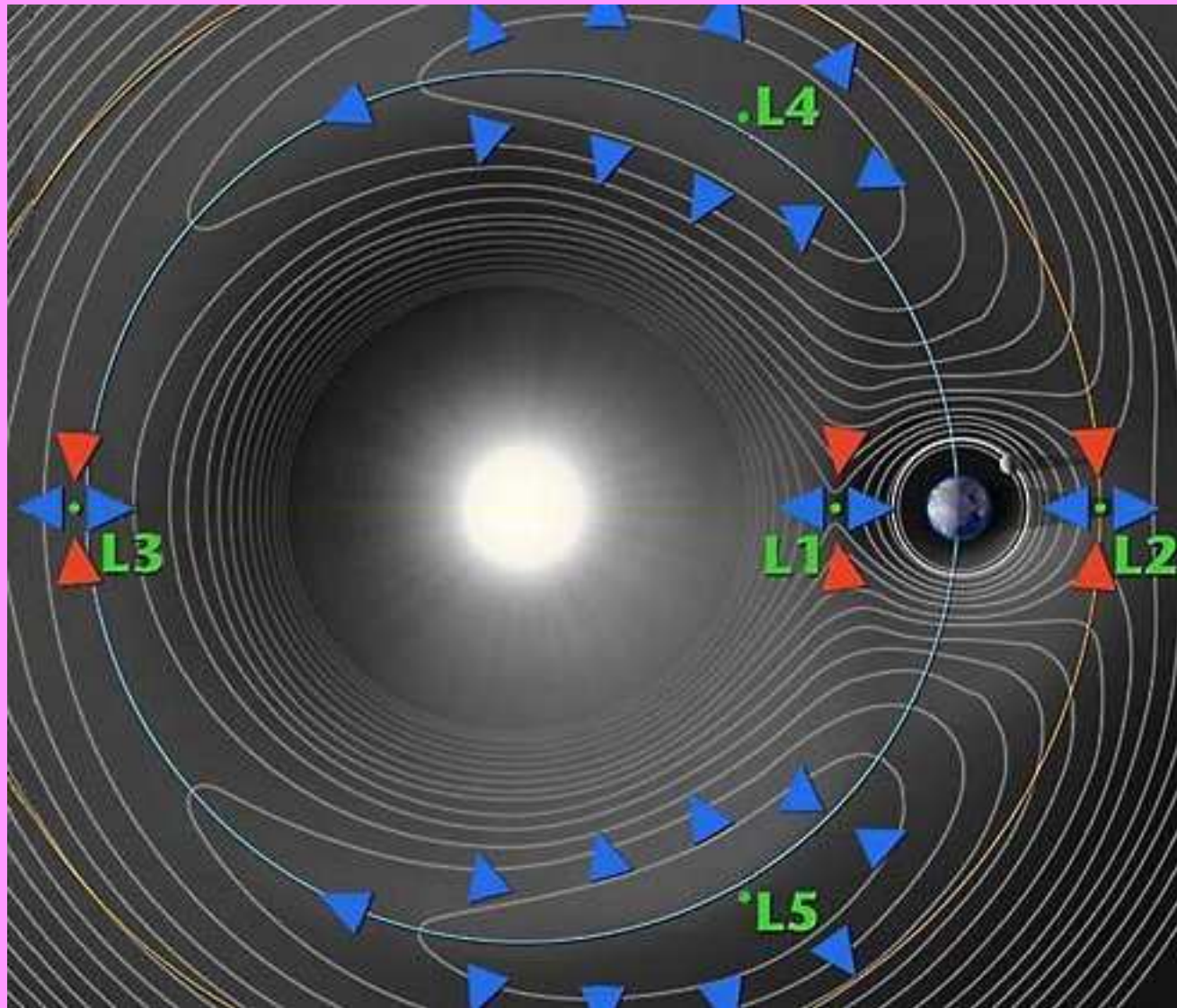(wavelength 0.3 mm, 1 h of integration)

$5 \cdot 10^{-9}$ Jy (sigma)

interferometry sensitivity
space-ground (ALMA)
(wavelength 0.5 mm, bandwidth 16 GHz
integration of 300 s)

10^{-4} Jy (sigma)

beam of the interferometer

10^{-9} arcsec

Outline

- History (GL, ML, local ML)
- Binary lenses (planets)
- Pixel microlensing
- Polarization issues for exoplanetary searches
- Conclusions

History

$$\Theta = \frac{2GM}{c^2 R} \qquad (1)$$

or

$$\Theta \sim 0.87" \qquad (2)$$

for $M = M_\odot$ and $R = R_\odot$.

Newton (Optics, 1704): "Does body act on the light, is the action stronger for smaller distances?"

In 1801 J. Soldner presented his derivation of expression (1) for publication.

In 1911 A. Einstein derived the(1) in SR.

In 1915, 1916 A. Einstein derived GR expression for the bending angle of light

$$\Theta = \frac{4GM}{c^2 R} \qquad (3)$$

or

$$\Theta \sim 1.75" \qquad (4)$$

and Einstein's prediction was confirmed by A. Eddington in 1919.

aber, wie man sich leicht überzeugt, auf der erwähnten Annahme beruhen.

Damit haben wir die Untersuchung des Meridianinstruments abgeschlossen. Die Untersuchung der Winkelmessung in den zur Meridianebene normalen Ebenen bringt, wie man sich leicht überzeugt, keine neuen Resultate.

Zusammenfassend können wir also sagen: der Winkelmessung liegt die Annahme der euklidischen Kinematik des starren Körpers zu Grunde. Die Verwendung optischer Hilfsapparate (Fernrohr, Mikroskop usw.) bringt keine neuen optischen Annahmen mit sich. Die »Starrheit« der Instrumente wird mit Hilfe unserer Annahme 2 und der Unabhängigkeit der Abbildungsgesetze von der Richtung geprüft. Diese letztere ist zwar noch nicht unmittelbar überprüft, kann aber durch den Ausfall des *Michelson*schen Versuches gestützt werden.

Wien, 1924 Febr. 15. *Fr. Zerner.*

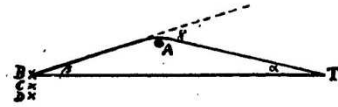## Über eine mögliche Form fiktiver Doppelsterne. Von *O. Chwolson.*

Es ist gegenwärtig wohl als höchst wahrscheinlich anzunehmen, daß ein Lichtstrahl, der in der Nähe der Oberfläche eines Sternes vorbeigeht, eine Ablenkung erfährt. Ist γ diese Ablenkung und γ_0 der Maximumwert an der Oberfläche, so ist $\gamma_0 \geq \gamma \geq 0$. Die Größe des Winkels ist bei der Sonne $\gamma_0 = 1{.}7$; es dürften aber wohl Sterne existieren, bei denen γ_0 gleich mehreren Bogensekunden ist; vielleicht auch noch mehr. Es sei A ein großer Stern (Gigant), T die Erde, B ein entfernter Stern; die Winkeldistanz zwischen A und B, von T aus gesehen, sei α, und der Winkel zwischen A und T, von B aus gesehen, sei β. Es ist dann

$$\gamma = \alpha + \beta\,.$$

Ist B sehr weit entfernt, so ist annähernd $\gamma = \alpha$. Es kann also α gleich mehreren Bogensekunden sein, und der Maximumwert von α wäre etwa gleich γ_0. Man sieht den Stern B von der Erde aus an zwei Stellen: direkt in der Richtung TB und außerdem nahe der Oberfläche von A, analog einem Spiegelbild. Haben wir mehrere Sterne B, C, D, so würden die Spiegelbilder umgekehrt gelegen sein wie in

Petrograd, 1924 Jan. 28.

einem gewöhnlichen Spiegel, nämlich in der Reihenfolge D, C, B, wenn von A aus gerechnet wird (D wäre am nächsten zu A).

Der Stern A würde als fiktiver Doppelstern erscheinen. Teleskopisch wäre er selbstverständlich nicht zu trennen. Sein Spektrum bestände aus der Übereinanderlagerung zweier, vielleicht total verschiedenartiger Spektren. Nach der Interferenzmethode müßte er als Doppelstern erscheinen. Alle Sterne, die von der Erde aus gesehen rings um A in der Entfernung $\gamma_0 - \beta$ liegen, würden von dem Stern A gleichsam eingefangen werden. Sollte zufällig TAB eine gerade Linie sein, so würde, von der Erde aus gesehen, der Stern A von einem Ring umgeben erscheinen.

Ob der hier angegebene Fall eines fiktiven Doppelsternes auch wirklich vorkommt, kann ich nicht beurteilen.

O. Chwolson.

Antwort auf eine Bemerkung von *W. Anderson.*

Daß ein Elektronengas einer Substanz mit negativem Brechungsvermögen optisch äquivalent sein müßte, kann bei dem heutigen Stand unserer Kenntnisse nicht zweifelhaft sein, da dasselbe einer Substanz von verschwindend kleiner Eigenfrequenz äquivalent ist.

Aus der Bewegungsgleichung

$$\varepsilon X = \mu\, d^2x/dt^2$$

eines Elektrons von der elektrischen Masse ε und der ponderabeln Masse μ folgt nämlich für einen sinusartig pendelnden Prozeß von der Frequenz ν die Gleichung

$$\varepsilon X = -(2\pi\nu)^2\, \mu x\,.$$

Berücksichtigt man, daß εx das »Moment« eines schwingenden Elektrons ist, so erhält man für die Polarisation $p = n\varepsilon x$ eines Elektronengases mit n Elektronen pro Volumeinheit

$$p = -\varepsilon^2 n/[\mu\,(2\pi\nu)^2]\cdot X\,.$$

Hieraus folgt, daß die scheinbare Dielektrizitätskonstante

$$D = 1 + 4\pi p/X = 1 - \varepsilon^2 n/(\pi\mu\,\nu^2)$$

ist. $\sqrt{D}$ ist in diesem Falle der Brechungsexponent, also jedenfalls kleiner als 1. Es erübrigt sich bei dieser Sachlage, auf das Quantitative einzugehen.

Es sei noch bemerkt, daß ein Vergleich des Elektronengases mit einem Metall unstatthaft ist, weil die bei der elementaren Theorie der Metalle zugrundegelegte »Reibungskraft« bei freien Elektronen fehlt; das Verhalten der letzteren ist allein durch die Einwirkung des elektrischen Feldes und durch die Trägheit bedingt.

Berlin, 1924 April 15. *A. Einstein.*

Zur Bemerkung von *W. Anderson* AN 5269.

In his note entitled »Zu Prof. *Einstein*s Bemerkung AN 5233«, *W. Anderson* makes use of the well-known formula for the index of refraction of a medium containing both free of an electron gas is greater than unity, and that the conductivity is large. This assumption seems to be based on an erroneous conception of dielectric constant and conductivity. In fact, if *Hea-*

DISCUSSION

LENS–LIKE ACTION OF A STAR BY THE DEVIATION OF LIGHT IN THE GRAVITATIONAL FIELD

SOME time ago, R. W. Mandl paid me a visit and asked me to publish the results of a little calculation, which I had made at his request. This note complies with his wish.

The light coming from a star A traverses the gravitational field of another star B, whose radius is R_o. Let there be an observer at a distance D from B and at a distance x, small compared with D, from the extended central line $\overrightarrow{AB}$. According to the general theory of relativity, let α_o be the deviation of the light ray passing the star B at a distance R_o from its center.

For the sake of simplicity, let us assume that $\overrightarrow{AB}$ is large, compared with the distance D of the observer from the deviating star B. We also neglect the eclipse (geometrical obscuration) by the star B, which indeed is negligible in all practically important cases. To permit this, D has to be very large compared to the radius R_o of the deviating star.

It follows from the law of deviation that an observer situated exactly on the extension of the central line $\overrightarrow{AB}$ will perceive, instead of a point-like star A, a luminius circle of the angular radius β around the center of B, where

$$\beta = \sqrt{\alpha_o \frac{R_o}{D}}.$$

It should be noted that this angular diameter β does not decrease like $1/D$, but like $1/\sqrt{D}$, as the distance D increases.

Of course, there is no hope of observing this phenomenon directly. First, we shall scarcely ever approach closely enough to such a central line. Second, the angle β will defy the resolving power of our instruments. For, α_o being of the order of magnitude of one second of arc, the angle R_o/D, under which the deviating star B is seen, is much smaller. Therefore, the light coming from the luminous circle can not be distinguished by an observer as geometrically different from that coming from the star B, but simply will manifest itself as increased apparent brightness of B.

The same will happen, if the observer is situated at a small distance x from the extended central line $\overrightarrow{AB}$. But then the observer will see A as two point-like light-sources, which are deviated from the true geometrical position of A by the angle β, approximately.

The apparent brightness of A will be increased by the lens-like action of the gravitational field of B in the ratio q. This q will be considerably larger than unity only if x is so small that the observed positions of A and B coincide, within the resolving power of our instruments. Simple geometric considerations lead to the expression

$$q = \frac{l}{x} \cdot \frac{1 + \frac{x^2}{2l^2}}{\sqrt{1 + \frac{x^2}{4l^2}}},$$

where

$$l = \sqrt{\alpha_o D R_o}.$$

If we are interested mainly in the case $q \gg 1$, the formula

$$q = \frac{l}{x}$$

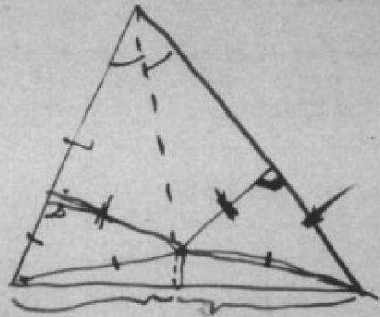is a sufficient approximation, since $\frac{x^2}{l^2}$ may be neglected.

Even in the most favorable cases the length l is only a few light-seconds, and x must be small compared with this, if an appreciable increase of the apparent brightness of A is to be produced by the lens-like action of B.

Therefore, there is no great chance of observing this phenomenon, even if dazzling by the light of the much nearer star B is disregarded. This apparent amplification of q by the lens-like action of the star B is a most curious effect, not so much for its becoming infinite, with x vanishing, but since with increasing distance D of the observer not only does it not decrease, but even increases proportionally to $\sqrt{D}$.

ALBERT EINSTEIN

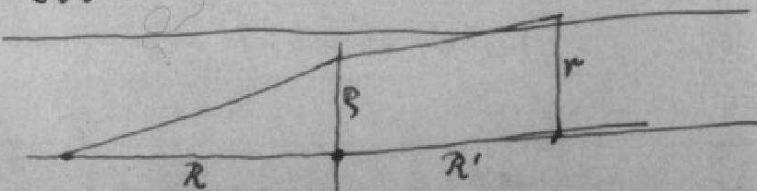INSTITUTE FOR ADVANCED STUDY,
PRINCETON, N. J.

Alle Dreiecke sind gleichschenklig.

Hestenberg
Berlin-Halensee,
Joachim Friedrichstr. 33.

$$r = \rho \frac{R+R'}{R} - \frac{R'\alpha}{\rho} \qquad \Big|\; \rho^? \text{ nach unten}$$
$$\text{negativ. Dann gilt}$$
$$\text{auch für starkabgebogene}$$
$$\text{Strahl.}$$

$$r_0 = \rho_0 - \frac{1}{\rho_0} \quad \cdots (1)$$

$$\boxed{\rho_0^2 = \rho^2 \frac{R+R'}{R R'\alpha}}$$

Einsetzl.

$$r = \cdot - \frac{R\alpha}{\rho} = \cdot - \frac{R\alpha}{\rho_0}\sqrt{\frac{R+R'}{R R'\alpha}}$$

$$= \cdot - \frac{1}{\rho_0}\sqrt{\frac{R}{R'}(R+R')\alpha}$$

$$\boxed{r_0 = r\sqrt{\frac{\cdot R'}{R'(R+R')\alpha}}}$$
$$\boxed{\rho_0 = \rho\sqrt{\frac{R+R'}{R R'\alpha}}}\Bigg\} (2)$$

1) gibt zwei Wurzeln für ρ_0.
Von hier an Index weggelassen.

$$2 + r^2 = \rho^2 + \frac{1}{\rho^2}$$
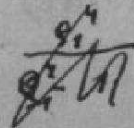
$$f = \varphi + \frac{\pi^2}{\varphi}$$

$$df = \left(1 - \frac{\pi^2}{\varphi^2}\right)d\varphi = \left(1 - \frac{1}{\varphi^4}\right)d\varphi$$

$$\mathcal{H}\,df = \pm H\,d\varphi$$

$$\mathcal{H} = \pm \frac{H}{1 - \frac{1}{\varphi^4}}$$

$$\mathcal{H}_{tot} = H\left\{\frac{1}{1-\frac{1}{\varphi^4}} + \frac{1}{\frac{1}{\varphi_2^4}-1}\right\}\cdots (3)$$

Klammer gibt relative Helligkeit.
(um $\alpha = 1$)

$$r = \frac{1}{x} - x$$

$$\{\ \} = \frac{1}{1-x_1^4} + \frac{1}{x_2^4-1}$$
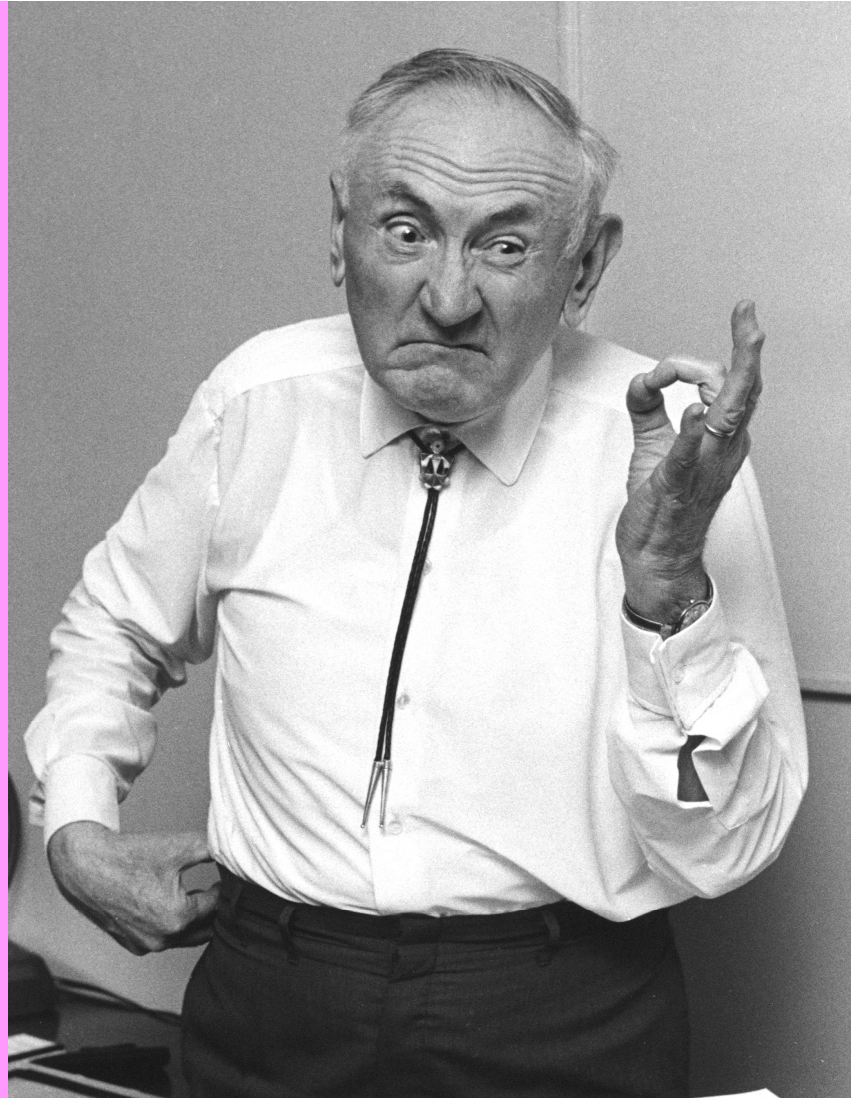
- Fritz Zwicky → GL+DM

В.К. Зворыкин с иконоскопом конструкции 1937 г.

Nebulae as Gravitational Lenses

Einstein recently published[1] some calculations concerning a suggestion made by R. W. Mandl, namely, that a star B may act as a "gravitational lens" for light coming from another star A which lies closely enough on the line of sight behind B. As Einstein remarks the chance to observe this effect for stars is extremely small.

Last summer Dr. V. K. Zworykin (to whom the same idea had been suggested by Mr. Mandl) mentioned to me the possibility of an image formation through the action of gravitational fields. As a consequence I made some calculations which show that extragalactic *nebulae* offer a much better chance than *stars* for the observation of gravitational lens effects.

In the first place some of the massive and more concentrated nebulae may be expected to deflect light by as much as half a minute of arc. In the second place nebulae, in contradistinction to stars, possess apparent dimensions which are resolvable to very great distances.

Suppose that a distant globular nebula A whose diameter is 2ξ lies at a distance, a, which is great compared with the distance D of a nearby nebula B which lies exactly in front of A. The image of A under these circumstances is a luminous ring whose average apparent radius is $\beta = (\gamma_0 r_0/D)^{\frac{1}{2}}$, where γ_0 is the angle of deflection for light passing at a distance r_0 from B. The apparent width of the ring is $\Delta\beta = \xi/a$. The apparent total brightness of this luminous ring is q times greater than the brightness of the direct image of A. In our special case $q = 2la/\xi D$, with $l = (\gamma_0 r_0 D)^{\frac{1}{2}}$. In actual cases the factor q may be as high as $q = 100$, corresponding to an increase in brightness of five magnitudes. The surface brightness remains, of course, unchanged.

The discovery of images of nebulae which are formed through the gravitational fields of nearby nebulae would be of considerable interest for a number of reasons.

(1) It would furnish an additional test for the general theory of relativity.

(2) It would enable us to see nebulae at distances greater than those ordinarily reached by even the greatest telescopes. Any such *extension* of the known parts of the universe promises to throw very welcome new light on a number of cosmological problems.

(3) The problem of determining nebular masses at present has arrived at a stalemate. The mass of an average nebula until recently was thought to be of the order of $M_N = 10^9 M_\odot$, where $M_\odot$ is the mass of the sun. This estimate is based on certain deductions drawn from data on the intrinsic brightness of nebulae as well as their spectrographic rotations. Some time ago, however, I showed[2] that a straightforward application of the virial theorem to the great cluster of nebulae in Coma leads to an average nebular mass four hundred times greater than the one mentioned, that is, $M_N' = 4 \times 10^{11} M_\odot$. This result has recently been verified by an investigation of the Virgo cluster.[3] Observations on the deflection of light around nebulae may provide the most direct determination of nebular masses and clear up the above-mentioned discrepancy.

A detailed account of the problems sketched here will appear in *Helvetica Physica Acta*.
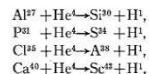
<div align="right">F. ZWICKY</div>

Norman Bridge Laboratory,
  California Institute of Technology,
    Pasadena, California,
      January 14, 1937.

[1] A. Einstein, Science **84**, 506 (1936).
[2] F. Zwicky, Helv. Phys. Acta **6**, 124 (1933).
[3] Sinclair Smith, Astrophys. J. **83**, 23 (1936).

Emergence of Low Energy Protons from Nuclei

In some experiments recently described[1] the emission of protons in alpha-particle induced transmutations has been studied. In several cases the interesting fact was noticed that protons of relatively low energy were emitted in considerable numbers. Thus for each of the reactions

$$Al^{27} + He^4 \rightarrow Si^{30} + H^1,$$
$$P^{31} + He^4 \rightarrow S^{34} + H^1,$$
$$Cl^{35} + He^4 \rightarrow A^{38} + H^1,$$
$$Ca^{40} + He^4 \rightarrow Sc^{43} + H^1,$$

a group of protons of maximum range 20 cm or less is found and the yield is in general large (more than one-third of the total number of protons emitted). In each case protons of range 10 cm are observed with no apparent diminution of the probability of emission. The question arises as to how these low energy protons get out of the composite nucleus.

In recent experiments in this laboratory the excitation curve for the emission of neutrons from argon under alpha-particle bombardment has been plotted and the nuclear radius found to be 7.3×10^{-13} cm which is in accord with Bethe's revised radii for the radioactive elements[2] and may be taken as a basis for calculation of the nuclear radii of Si^{30}, S^{34}, A^{38}, Ca^{42} and Sc^{43}. Other evidence (e.g., scattering experiments) indicates, if anything, smaller radii than those found in this way. In Table I are given the radii so calculated, together with the heights of the corresponding proton barriers and the range of a proton just able to surmount them. It will be seen that in every case the experimentally observed ranges are smaller than necessary to scale the barrier. It therefore appears that we can draw one of two significant conclusions from the experimental data. Either *barriers to emerging protons are abnormally low* or *the composite nucleus containing the final product element and the proton has a finite lifetime sufficiently long to enable the proton to leak through the barrier*. The latter view, which is in accordance with Bohr's conception of transmutation,[3]

TABLE I.

PRODUCT NUCLEUS	NUCLEAR RADIUS ($\times 10^{13}$cm)	PROTON BARRIER HEIGHT (Mev)	RANGE TO SCALE BARRIER (cm)	EXPERIMENTALLY FOUND RANGE
Si^{30}	6.7	3.0	14.0	<10
S^{34}	6.9	3.3	16.5	<10
A^{38}	7.2	3.6	19.0	<10
Ca^{42}	7.4	3.9	22.0	14
Sc^{43}	7.5	4.0	23.0	<10

Constraints on DM objects from GL
(Wambsganss(1993))

Prefix	Deflection angle (")	Mass $M/M_\odot$	Lens	Time delay
kilo	10^3	10^{18}	supercluster	
macro	10^0	10^{12}	galaxy	months
milli	10^{-3}	10^6	MBH	min
micro	10^{-6}	10^0	star	10^{-4} sec
nano	10^{-9}	10^{-6}	planet	10^{-10} sec
pico	10^{-12}	10^{-12}	???	10^{-16} sec
femto	10^{-15}	10^{-18}	comet	10^{-22} sec

Плоскость источника

Плоскость линзы
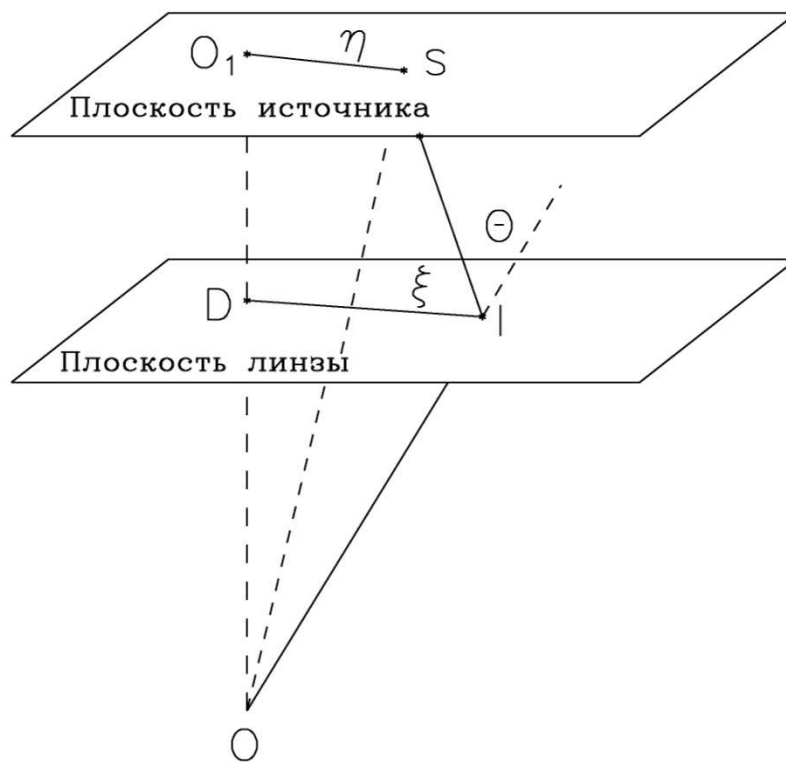
Notations and expressions

$$\vec{\eta} = D_s \vec{\xi}/D_d - D_{ds}\vec{\Theta}(\vec{\xi}). \qquad (5)$$

For Schwarzschild GL

$$\vec{\Theta}(\vec{\xi}) = 4GM\vec{\xi}/(c^2\xi^2). \qquad (6)$$

If $\vec{\eta} = \vec{0}$ then

$$\xi_0 = \sqrt{\frac{4GM}{c^2} \times \frac{D_d D_{ds}}{D_s}}$$

is Einstein − Chwolson radius and

$$\theta_0 = \xi_0/D_d \qquad (7)$$

is Einstein − Chwolson angle. If we introduce dimensionless variables $\vec{x} = \vec{\xi}/\xi_0, \vec{y} = D_s\vec{\eta}/(\xi_0 D_d)$ then

$$\vec{y} = \vec{x} - \vec{x}/x^2. \qquad (8)$$

The Eq. (8) has two roots

$$\vec{x}^{\pm} = \vec{y}\left(\frac{1}{2} \pm \sqrt{\frac{1}{4} + \frac{1}{y^2}}\right) \qquad (9)$$

and

$$l = |x^-| + |x^+| = 2y\sqrt{\frac{1}{4} + \frac{1}{y^2}}. \qquad (10)$$

If we introduce $\vec{\theta} := \vec{\xi}/D_d, \vec{\beta} = \vec{\eta}/D_s$ then the magnification of GL mapping is

$$\mu := \frac{\Delta\omega}{\Delta\omega_0} := \left|\det \frac{\partial\vec{\beta}}{\partial\vec{\theta}}\right|^{-1} = \left|\det \frac{\partial\vec{y}}{\partial\vec{x}}\right|^{-1} \qquad (11)$$

and

$$\mu_{\pm} = \frac{1}{4}\left(\frac{y}{\sqrt{4+y^2}} + \frac{\sqrt{4+y^2}}{y} \pm 2\right). \qquad (12)$$

Therefore,

$$\mu_{\text{total}} = \mu_+ + \mu_- = \frac{y^2+2}{y(y^2+4)^{1/2}}, \qquad (13)$$

thus $\mu_{\text{total}} \to 1/y$ (for $y \to 0$) and $\mu_{\text{total}} \to 1 + 1/y^4$ (for $y \to \infty$).

If $M \sim M_\odot$ and $D_d \sim 10$ kpc then

$$\theta_0 = 0.902\text{mas}\left(\frac{M}{M_\odot}\right)^{1/2}\left(\frac{10\text{ kpc}}{D_d}\right)\left(1 - \frac{D_d}{D_s}\right)^{1/2};$$

and angular velocity

$$\dot{\theta} = \frac{d\theta}{dt} = 4.22\left(\frac{v}{200\text{ km/s}}\right)\left(\frac{10\text{ kpc}}{D_d}\right)\frac{\text{mas}}{\text{yr}}. \qquad (14)$$
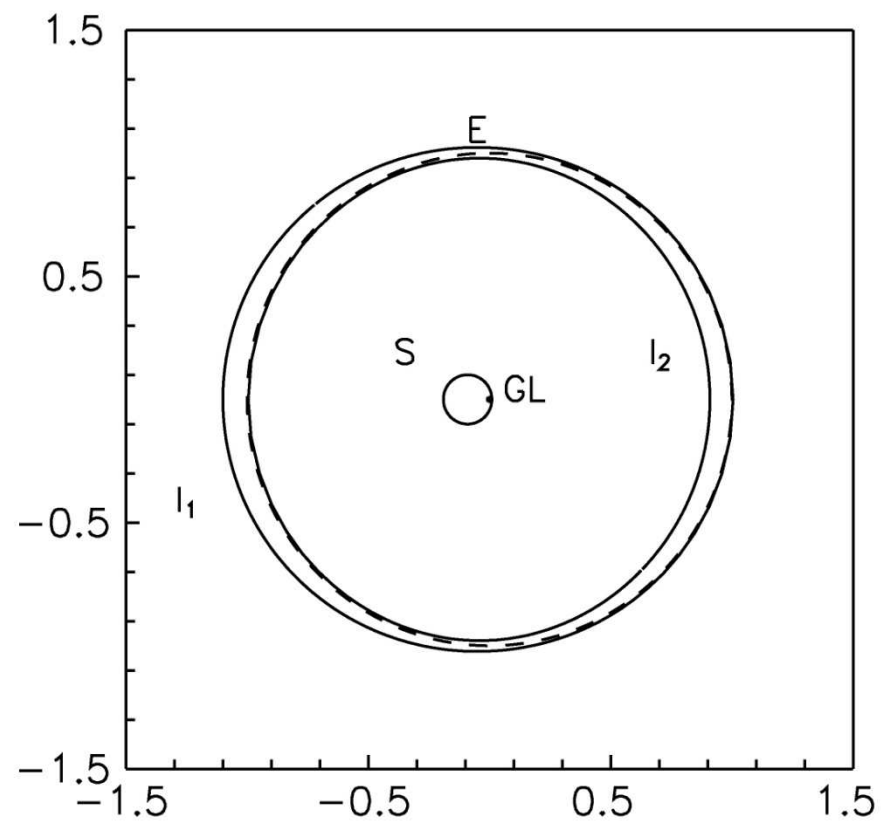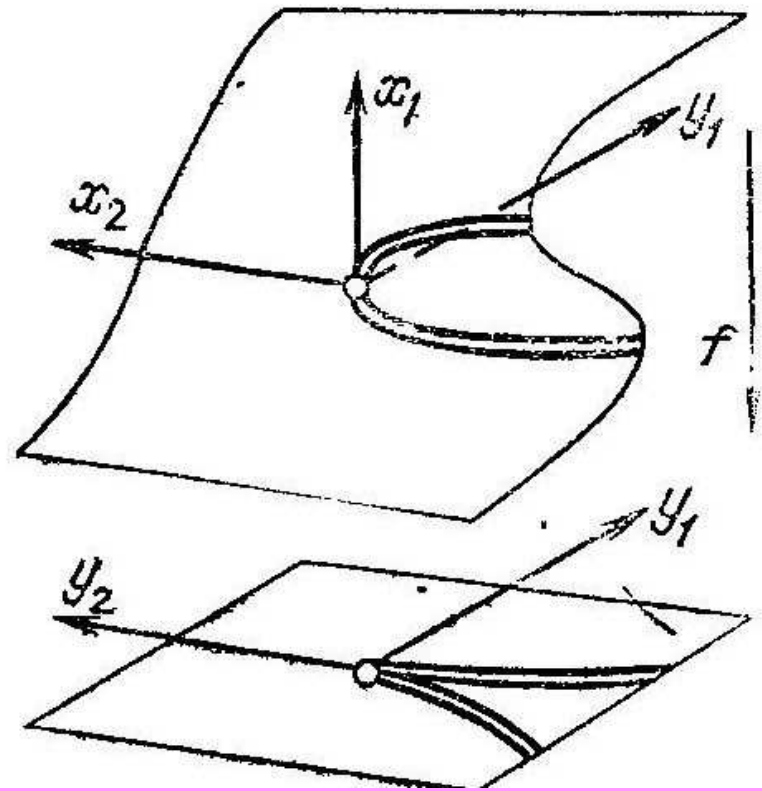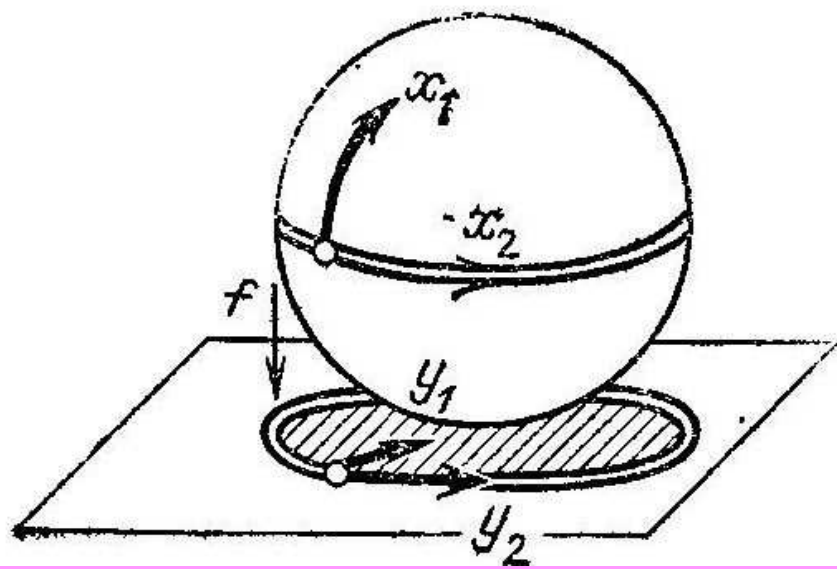
Therefore a typical duration is

$$t_0 = \frac{\theta_0}{\dot{\theta}} = .214\left(\frac{M}{M_\odot}\right)^{1/2}\left(\frac{D_d}{10\ kpc}\right)^{1/2} \times \qquad (15)$$
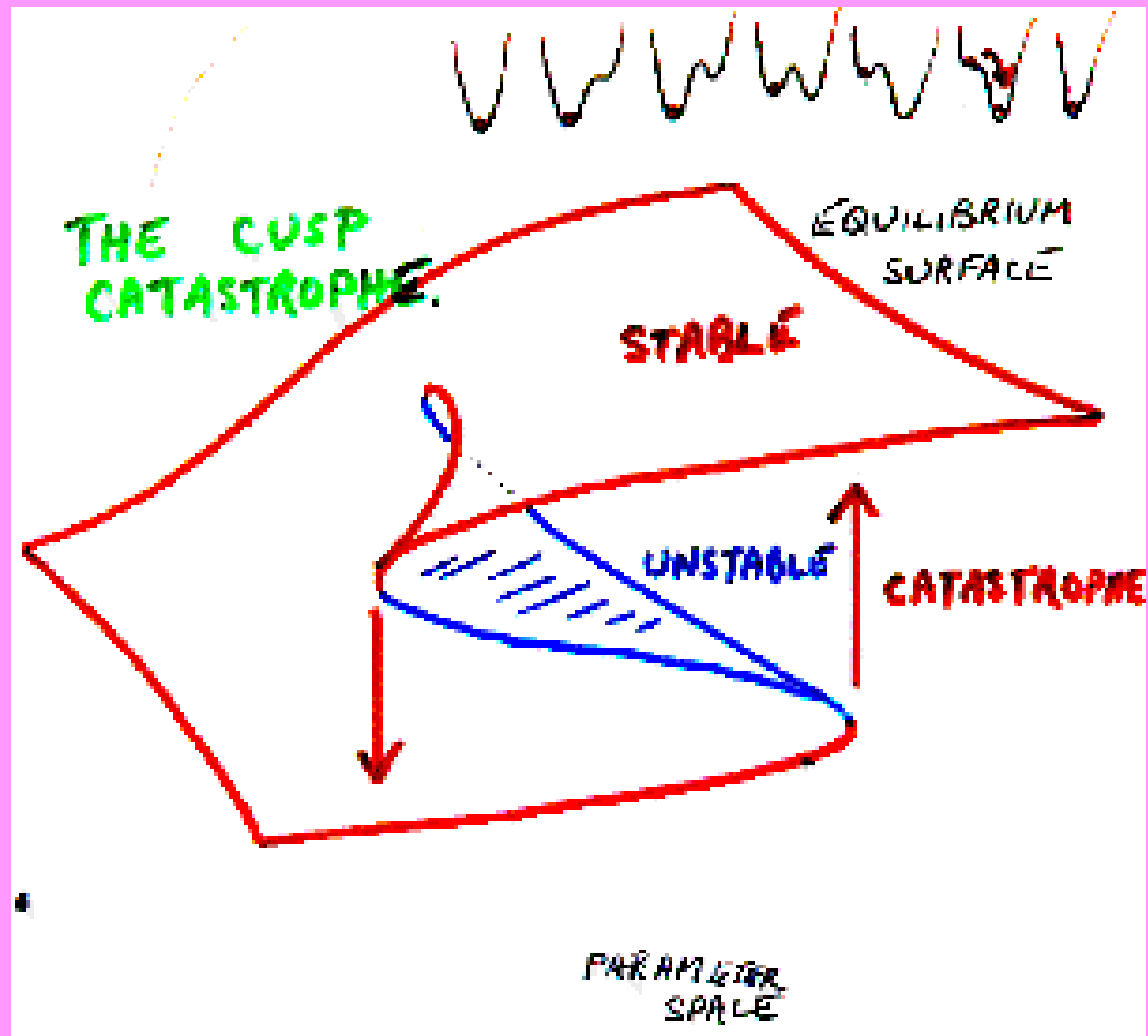
$$\times \left(1 - \frac{D_d}{D_s}\right)^{1/2}\left(\frac{200\text{ km/s}}{v}\right)\text{yr}. \qquad (16)$$

THE CUSP CATASTROPHE.

EQUILIBRIUM SURFACE

STABLE

UNSTABLE

CATASTROPHE

PARAMETER SPACE
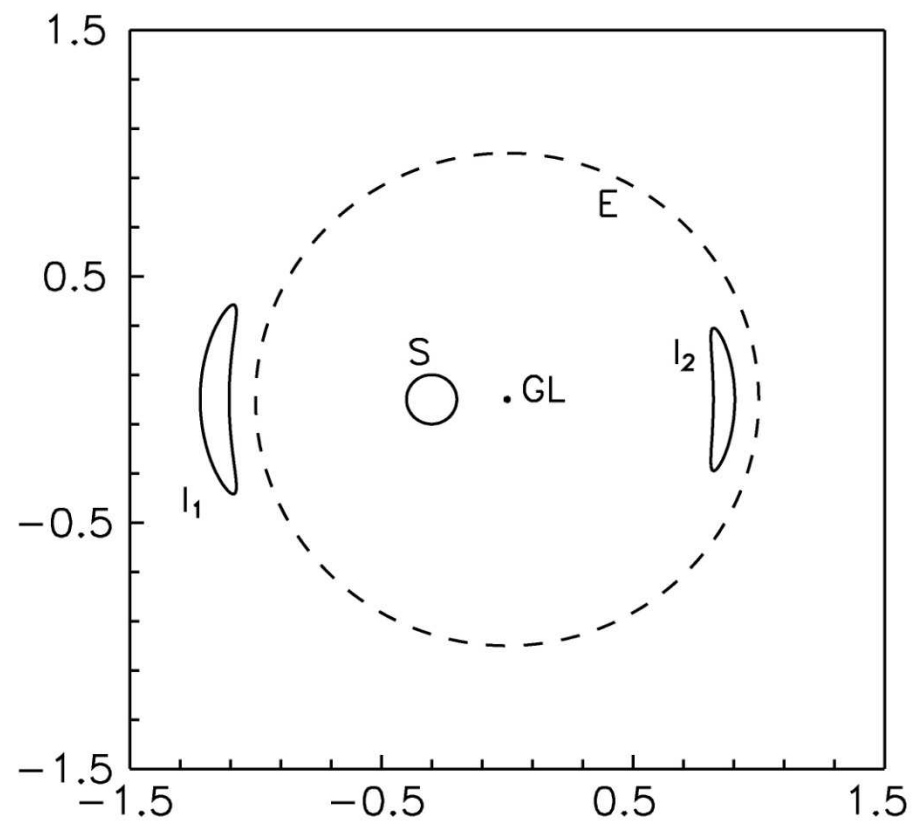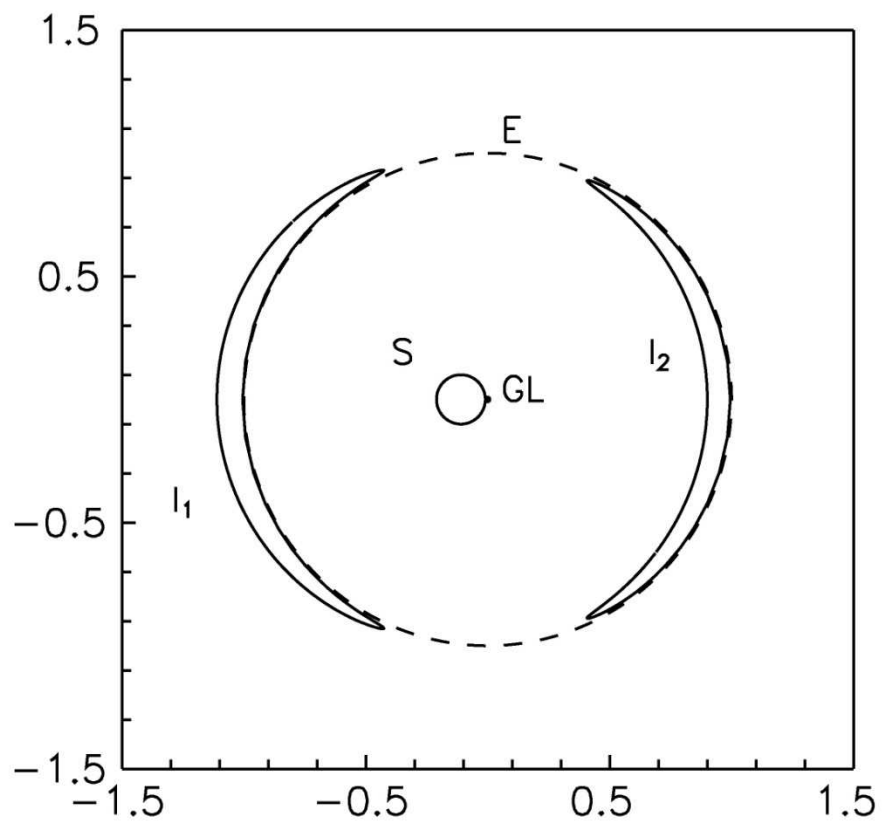
Let us consider the following elementary case of the general situation. Namely we add together the monopole field of a point mass and the gravitational field of another point mass located at a distance $\mathbf{r}_2$ from the primary point mass. So, the gravitational lens potential has the following form

$$\varphi(\mathbf{r}) = \frac{GM}{r} + \frac{Gm}{|\mathbf{r} - \mathbf{r}_2|} \ .$$

Therefore, in the gravitational field of the system of fixed gravity points the deflection angle of a light ray is approximately equal to

$$\mathbf{\Theta}(\xi) = \frac{4GM}{c^2} \frac{\xi}{\xi^2} + \frac{4Gm}{c^2} \frac{\xi - \xi_2}{|\xi - \xi_2|^2} \ ,$$

where ξ and ξ_2 are variables of length dimensionality, ξ is the light ray impact parameter with respect to the primary point mass, and ξ_2 is the lens plane projection of the distance between the points. One can choose the coordinates in the following way: the position of the second point mass is defined by the expression $\xi_2 = (a, 0)$.

Light motion in the gravitational field of two fixed gravity points and the respective gravitational lens equation are very complicated [13]. We simplify the expression for the deflection angle $\mathbf{\Theta}(\xi)$ as far as possible for the analysis of major optical effects of the formation of images, their intensities etc. For this simplification we decompose $\mathbf{\Theta}(\xi)$ into a Taylor series with respect to ξ, leaving terms up to the first order in ξ inclusively:

$$\mathbf{\Theta}(\xi) = \frac{2r_g\xi}{\xi^2} - \mu \frac{2r_g\xi_2}{\xi_2^2} + \mu \frac{2r_g\xi}{\xi_2^2} - \mu \frac{4r_g\xi_2(\xi_2\xi)}{\xi_2^4} \ ,$$

where μ is the mass ratio. We write the gravitational lens equation for the case

$$\mathbf{\eta} = \frac{D_s}{D_d} \xi - 2r_g D_{ds} \frac{\xi}{\xi^2} + \mu D_{ds} \frac{2r_g\xi_2}{\xi_2^2}$$

$$+ \mu D_{ds} \frac{2r_g\xi}{\xi_2^2} - \mu D_{ds} \frac{4r_g\xi_2(\xi_2\xi)}{\xi_2^4} \ .$$

then the visible image position characterized by the vector ξ is shifted and does not lie on the line connecting the gravitational lens center and the light source as in the case of a spherically symmetric gravitational field.

We also introduce the following variables

$$\mathbf{y} = \frac{\boldsymbol{\eta}}{R_{\mathrm{E}}}\frac{D_d}{D_s} + \mu\,\frac{D_{ds}D_d}{R_{\mathrm{E}}D_s}\frac{2r_g\xi_2}{\xi_2^2}\quad\text{and}\quad \mathbf{x} = \frac{\xi}{R_{\mathrm{E}}}\,,$$

which are normalized on the Einstein–Chwolson radius $R_{\mathrm{E}}^2 = 4GMD_{ds}D_d/(c^2 D_s)$ and respective distances. Thus, the gravitational lens equation (the relation between $\mathbf{y}$ and $\mathbf{x}$) has the following form:

$$\mathbf{y} = \mathbf{x} - \frac{\mathbf{x}}{|x|^2} + \gamma\begin{pmatrix} 1 & 0 \\ 0 & -1 \end{pmatrix}\mathbf{x}\,,$$

where $\gamma = \mu(R_{\mathrm{E}}/a)^2$ is a parameter characterizing the action of the second mass on the light ray. To obtain a simpler form of the gravitational lens equation we change variables again

$$\mathbf{X} = \mathbf{x}\sqrt{1+\gamma}\,,\qquad \mathbf{Y} = \frac{\mathbf{y}}{\sqrt{1+\gamma}}\,. \tag{14}$$

We rewrite the gravitational lens equation using these variables. The equation looks more compact and clear now, and has the following form:

$$\mathbf{Y} = \begin{pmatrix} 1 & 0 \\ 0 & \varLambda \end{pmatrix}\mathbf{X} - \frac{\mathbf{X}}{|\mathbf{X}|^2}\,, \tag{15}$$

where

$$\varLambda = \frac{1-\gamma}{1+\gamma}\,.$$

The amplification factor $\varLambda$ is equal to the inverse of the determinant (the inverse of the Jacobian of the gravitational lens mapping):

$$\varLambda = \left|\frac{\partial\mathbf{y}}{\partial\mathbf{x}}\right|^{-1}\,,$$

but the critical curves for the gravitational lens (the geometric locus on the lens plane, where the amplification factor is equal to infinity) and caustic curves (the geometric locus on the source plane, where the amplification factor is equal to infinity) are determined from the condition of vanishing determinant, namely

$$\det \varLambda = \det\frac{\partial\mathbf{Y}}{\partial\mathbf{X}} = 0\,.$$

but the critical curves for the gravitational lens (the geometric locus on the lens plane, where the amplification factor is equal to infinity) and caustic curves (the geometric locus on the source plane, where the amplification factor is equal to infinity) are determined from the condition of vanishing determinant, namely

$$\det A = \det \frac{\partial \mathbf{Y}}{\partial \mathbf{X}} = 0 .$$

We rewrite the condition for the components $\mathbf{X}$ in the explicit form:

$$\Lambda(X_1^2 + X_2^2)^2 + (\Lambda - 1)(X_1^2 - X_2^2) - 1 = 0 . \tag{16}$$

These curves are called Cassini ovals [14]. This condition looks clearer in polar coordinates on the lens plane. We introduce the following notation for polar coordinates:

$$X_1 = \rho \cos \phi , \qquad X_2 = \rho \sin \phi .$$

Using the coordinates ρ, ϕ we rewrite the equation for Cassini ovals:

$$\Lambda \rho^4 + (\Lambda - 1)\rho^2 \cos 2\phi - 1 = 0 .$$

If we use the gravitational lens mapping then the map of the oval onto the source plane will form a caustic curve. To obtain the mapping equation we substitute the equation of the Cassini oval into the gravitational lens equation and obtain

$$Y_1 = \lambda \cos^3 \phi, \qquad Y_2 = -\lambda \sin^3 \phi. \tag{18}$$

So, the critical curve (Cassini oval) is close to a unit circle, but the caustic curve is an astroid in the approximation used.

If we suppose that one point mass is much greater than the other $(m_2 \ll m_1)$, and the major semiaxis is equal to the Einstein–Chwolson radius $a = R_E$, we will have $\lambda = 2m_2/m_1$. The caustic curve (the astroid) for such a case is shown in Fig. 5. If we use the normalized variables $\mathbf{X}$ the Einstein–Chwolson radius will be equal to unity, but the transverse caustic size will be m_2/m_1 times smaller.
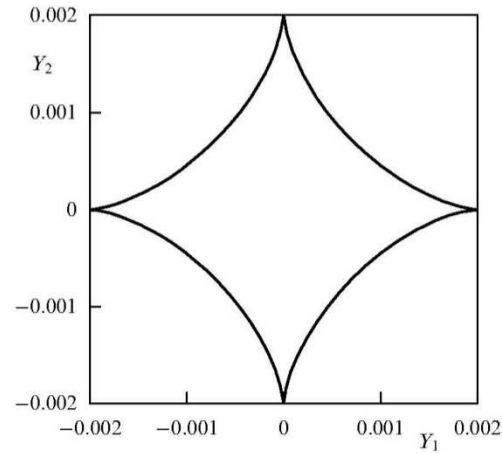
Figure 5. Caustic curve for the case of two point masses when one of the masses is much greater than the other ($\mu = 0.001$, $a = R_E$).

Research Note

The gravitational lens equation near cusps

P. Schneider and A. Weiss

Max-Planck-Institut für Astrophysik, Karl-Schwarzschild-Str. 1, W-8046 Garching bei München, Federal Republic of Germany

Abstract. The behaviour of the gravitational lens mapping near cusps is studied, both analytically and numerically, paying particular attention to magnification probabilities. We demonstrate that the three images of a point source inside a cusp satisfy the relation that the sum of the magnifications of the two images with the same parity equals, up to a sign, the magnification of the third image (of opposite parity). This property will then be used to show that the asymptotic magnification cross-section for point sources, in the limit $\mu_s \to \infty$, derived previously for folds only, is also valid in the presence of cusps. The next order term of such an expansion, which is due to sources just outside of cusps, is derived. We apply these relations to a special gravitational lens model and show that these asymptotic relations are indeed very good approximations for the large-μ_s cross-sections. For the study of the magnification of extended sources near cusps, we generalize the ray-shooting method to allow for very small sources. The magnification cross-sections for extended sources are then compared to those for point sources. A magnification contour plot for extended sources near a cusp is obtained. Since the largest magnifications of sources occur near cusps, this paper may directly apply to studies of the amplification bias in source counts.

Key words: gravitational lensing, Catastrophe Theory

1. Introduction

The gravitational deflection of light, in the approximation of gravitational lens theory, can be described by a mapping $f : \mathbb{R}^2 \to \mathbb{R}^2$ from the lens plane (or a small part of the observer's sky) to the source plane (or the corresponding part of the sphere of constant source redshift). In the case of a single geometrically-thin deflector, this is a gradient mapping (for an introduction to gravitational lens theory, see Blandford & Narayan 1986, hereafter BN; Blandford & Kochanek 1987; Schneider, Ehlers & Falco 1992, hereafter SEF). The behaviour of such a gradient mapping near critical points, i.e., points where the Jacobian of the lens mapping vanishes, is investigated and classified by Catastrophe Theory (e.g., Poston & Steward 1978; Gilmore 1981; for applications in gravitational lensing, see BN; Kovner 1987a; SEF, Chap. 6). In

Send offprint requests to: P. Schneider

a generic lens mapping, the critical points form closed, smooth, non-intersecting curves (so-called critical curves), and their image curves under the mapping f are the so-called caustics. They are also closed curves, but can intersect each other, self-intersect, and are not necessarily smooth, but can have cusps.

Caustics are an important ingredient in gravitational lens theory, for several reasons. First, the number of images of a source changes by ± 2 if, and only if, the source position changes across a caustic. Hence, knowing the structure of the caustics allows a qualitative understanding of the lens mapping, at least concerning image multiplicities. Also, if one considers families of lens mapping, Catastrophe Theory allows to predict the parameter values of the models at which the caustic structure changes, thus allowing a classification of parametrized lens models (for an example, see Erdl & Schneider 1992). Second, the magnification of a source, which is due to the area distortion of the lens mapping (i.e., the inverse of the Jacobian) becomes largest if the source is near a caustic. In particular, to determine the probability distribution for very large magnification of sources, one has to consider the lens mapping near caustics only.

A generic lens mapping has only two types of singularities, folds and cusps. At fold points, the caustic is smooth. A source on the "positive side" of a fold has two images close to, and on opposite sides of the corresponding critical curve. By approaching the caustic, the two critical images move closer together, thereby brightening. At the point where the source crosses the caustic, the two images attain (formally) infinite magnification (in practice, a finite source size leads to finite values of the magnification, but if we had a sufficiently compact source, wave optics effects would limit the magnification; see Chap. 7 of SEF and references therein), merge and disappear thereafter. The magnification of a point source scales like $1/\sqrt{y}$, where y is the distance of the source from the caustic. Considering folds only, the magnification probability of point sources in the limit of high magnifications, $\mu \to \infty$, behaves like μ^{-2}, and the constant of proportionality can be derived as a particular integral over the critical curves of the lens mapping (see BN, SEF, and Sect. 2.4 below).

The derivation of this probability distribution neglects the fact that cusps show a different behaviour. The standard argument implicitly used is that "cusps form a set of measure zero in the set of all critical points"; one therefore expects that cusps do neither change the shape, nor the amplitude of the $p(\mu) \propto \mu^{-2}$ law. Cusps are isolated points, connected by folds. A source close
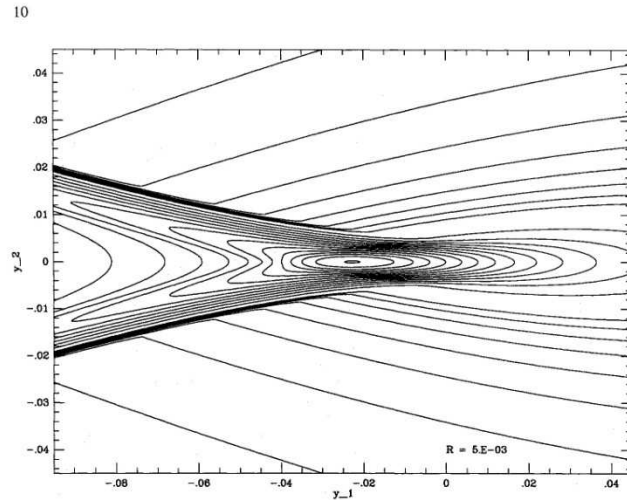
Fig. 5. Magnification contours around a generic cusp. The source radius chosen for this plot was $5\,10^{-3}$. The contour levels range from 3 to 10 in steps of one, and then to 80 (central contour) in steps of 5.

be the following: select a region in the source plane such that all points with magnification $> \mu_0$ lie inside the selected region (this region, in the case of the Chang-Refsdal lens, is preferentially chosen as a rectangle). Then, distribute N point sources inside this region (with area $\mathscr{A}$), calculate their magnifications from the lens equation, assign to each point a differential cross-section $d\sigma = \mathscr{A}/N$ and add up these differential cross-sections. If the N points are distributed randomly, we can easily estimate the number of points required for a given accuracy. If $\mathscr{A} \sim 4$, and $\sigma(10^3) \sim 4 \times 10^{-6}$ (typical values for the Chang-Refsdal lens), then $N_{1000} \sim 10^{-6} N$ points will have magnification $> 10^3$. If the cross-section is to be determined to within an accuracy of 10^{-3}, we would need $N = 10^{12}$ points — a hopeless task. The situation is slightly better if the points are not distributed randomly, but on a regular grid. Nevertheless, even then the computing time would be much too large for calculating accurate cross-sections for large μ_p.

To overcome these difficulties, we use a hierarchical method, based on the idea 'to use the computing time for interesting source positions'. For example, we want to distribute a higher density of points in regions where the magnification is large. Ideally, the number of source positions should be the same for each logarithmic bin of magnification, so that the statistical accuracy is smooth over the whole μ-interval considered. We now describe such a method applicable to point sources; a similar method has been used for extended sources, as described in the next subsection.

Consider the area $\mathscr{A}$ to be divided up into N squares. If the magnification at the center of a square is μ_p, we assign to this square a differential cross-section $d\sigma(\mu_p) = \mathscr{A}/N$. If this particular square is 'interesting' (we will specify this below), we can divide it into four subsquares and again calculate the magnification at the center of each subsquare (the corresponding differential cross-section then is $\mathscr{A}/(4N)$). If one or more of these subsquares appears again 'interesting', further divisions can be made; we can go down this hierarchy as far as desired.

Squares are 'interesting' if they have high magnification, if the gradient across the square is large, or if a caustic crosses the square (these conditions are not mutually exclusive, of course). We have defined numerical criteria according to the preceding prescription of 'interesting'; for example, if the magnification of a square at hierarchy level n is larger than μ_n, the square is further divided (it was found that $\mu_{n+1} = \mu_n \, 10^{0.15}$ is a good splitting criterium). Further, if the magnification factors at the corners of a square differed by more than 0.5, subdivision was applied. For the calculations shown in this paper, 14 hierarchy levels were used.

The solutions of the lens equation, and thus the point source magnification, can be calculated for the Chang-Refsdal lens, using the equations of Sect. 3. For each source position, one has to solve the fourth-order equation (3.3b), insert the real solutions into (3.3a), and calculate the magnification of each individual image. In connection with the hierarchical splitting of the source plane as described above, we have implemented an efficient and reliable method to solve Eq. (3.3a). This method will be described next; however, another method of solving the lens equation, to be described later, turned out to be superior in the situation considered here.

The Chang-Refsdal-equation in the form of Eq. (3.3b) can in principle be solved by any reasonable root-finder for polynomials or other well-behaved functions. Indeed, some of the root-solvers (e.g. from Press et al., 1986) worked well for most of the tested source positions, but with no exception all failed for those being close to cusps. The reason lies in the fact that at cusps a terrace point in the fourth-order polynomial $f(u)$ (given by (3.3b)) develops into a pair of extrema, or, in other words, a single root changes into three. All tested standard root-solvers gave the wrong number of roots of $f(u)$ on either side of the cusp! Numerically, a root cannot be found with an accuracy higher than $\approx 10^{-8}$ for coefficients of (3.3b) of the order of one by propagation of the machine inaccuracy into the powers of u.

On the magnification of gravitational lens images near cusps

Alexander F. Zakharov[1,2]

[1] Institute of Theoretical and Experimental Physics, B.Cheremushkinskaya, 25, 117259, Moscow, Russia
[2] Max-Planck-Institut für Astrophysik, Karl-Schwarzschild-Strasse 1, D-85740 Garching, Germany

Abstract. On the base of the gravitational lens equation obtained by Schneider & Weiss the magnification of images near a cusp is investigated. Using the symmetrical polynomials on the roots of the polynomial of the third degree we slightly generalize the Schneider & Weiss statement on the magnification near different solutions of the gravitational lens equation. The analytical expressions for magnifications of different images near the cusp are presented.

Key words: gravitational lensing

1. Introduction

It is well known that the mapping of two-dimensional surfaces into a plane gives only two types of stable singularities: folds and cusps (pleats). There are also similar singularities of caustics in gravitational lens optics. Schneider & Weiss (1986; 1992) studied the gravitational lens mapping near the cusps. Mandzhos (1993) investigated the mutual coherence by solving analytically the gravitational lens equation near the cusp. In turn, we study the magnification near the cusp and obtain a useful analytical expression for it.

2. Basic equations

We recall the basic equations from Schneider & Weiss (1992) before considering their gravitational lens equation near the cusp. As is shown in Schneider, Ehlers & Falco (1992), hereafter SEF, the gravitational lens equation may be written in the following form: let the distance between an observer and a source be D_s, the distance between an observer and the gravitational lens be D_d, and D_{ds} be the distance between the gravitational lens and a source. If we suppose a small angle of deflection then we have the following simple expression for the lens equation (SEF)

$$\boldsymbol{\eta} = D_s\,\boldsymbol{\xi}/D_d + D_{ds}\,\boldsymbol{\beta}(\boldsymbol{\xi}),$$

Send offprint requests to: A.F. Zakharov

where the vectors $\boldsymbol{\eta}, \boldsymbol{\xi}$ define the coordinates in source plane and in the lens plane respectively (SEF),

$$\boldsymbol{\beta}(\boldsymbol{\xi}) = 4G/c^2 \int \rho\,(\boldsymbol{R})\,(\boldsymbol{\xi} - \boldsymbol{R})\,/\,|\,\boldsymbol{\xi} - \boldsymbol{R}|^2\, \mathrm{dXdY},$$

where $\boldsymbol{R} = \{X, Y\}$ is the point vector in the lens plane, $\rho(\boldsymbol{R})$ is the surface mass density of the gravitational lens. We introduce the following variables (SEF)

$$\boldsymbol{x} = \boldsymbol{\xi}/R_0, \quad \boldsymbol{y} = D_s\,\boldsymbol{\eta}/(R_0 D_d),$$

where $R_0 = \sqrt{2 r_g D_d D_{ds}/D_s}$ is the Einstein - Chwolson radius (see Historical Remarks in SEF). We also introduce the following notation for the scaled (SEF) angle

$$\boldsymbol{\alpha} = \boldsymbol{\beta}\,D_{ds} D_d/(D_s R_0).$$

In the modelling of gravitational lenses, the surface mass density is normalized with the critical surface mass density (Wamsganss 1990)

$$\rho_{cr} = \frac{c^2 D_s}{4\pi G D_d D_{ds}}.$$

For typical lensing situations the critical surface mass density is of the order of $\rho_{cr} = 10^4 M_\odot pc^{-2}$ (Wamsganss 1990). Therefore, if we define the scaled surface mass density by the following expression (SEF)

$$\sigma = \rho/\rho_{cr},$$

then we have the expression for the angle $\boldsymbol{\alpha}$

$$\boldsymbol{\alpha}(\boldsymbol{x}) = \int \sigma\,(\boldsymbol{x}')(\boldsymbol{x} - \boldsymbol{x}')/|\boldsymbol{x} - \boldsymbol{x}'|^2\, d^2 x'.$$

As Schneider (1985) showed, we may introduce the scalar potential ψ, such, that

$$\boldsymbol{\alpha}(\boldsymbol{x}) = \nabla \psi\,(\boldsymbol{x}),$$

where

$$\psi(\mathbf{x}) = \int \sigma(\mathbf{x}') \ln |\mathbf{x} - \mathbf{x}'| \, d^2 x'.$$

Then (SEF)

$$\mathbf{y} = \mathbf{x} - \boldsymbol{\alpha}(\mathbf{x}) \qquad (1)$$

If we introduce (as in SEF)

$$\phi(\mathbf{x}, \mathbf{y}) = (\mathbf{x} - \mathbf{y})^2/2 - \psi(\mathbf{x}),$$

we can write the lens equation in the form (Schneider 1985)

$$\nabla \phi(\mathbf{x}, \mathbf{y}) = 0.$$

It is easy to see that mapping $\mathbf{x} \mapsto \mathbf{y}$ is a Lagrange mapping (Arnold 1979), since that is gradient mapping (Arnold 1983). Really, if we consider the function

$$S = \mathbf{x}^2/2 - \psi(\mathbf{x}),$$

then

$$\mathbf{y} = \nabla S.$$

Singularities of Lagrange's mappings are described in Arnold's paper (1972), and in Arnold's review (1983), and their bifurcations are described in Arnold's paper (1976).

Equation (1) defined the mapping of points on the lens plane into points on the source plane. Using the Jacobian matrix we define the local mapping (SEF):

$$\delta \mathbf{y} = A \, \delta \mathbf{x},$$

$$A = \begin{pmatrix} \partial y_1/\partial x_1 & \partial y_1/\partial x_2 \\ \partial y_2/\partial x_1 & \partial y_2/\partial x_2 \end{pmatrix} = \begin{pmatrix} 1 - \psi_{11} & -\psi_{12} \\ -\psi_{21} & 1 - \psi_{22} \end{pmatrix}, \qquad (2)$$

where

$$\psi_{ij} = \frac{\partial^2 \psi}{\partial x_i \partial x_j} \quad (i, j = 1, 2). \qquad (3)$$

Let us consider lenses which are systems of point masses. Outsides the points where the masses are located, we have the following equality (SEF)

$$\psi_{22} = -\psi_{11}, \qquad (4)$$

since the potential obeys the Laplace equation.

The magnification of an image at $\mathbf{x}$ is

$$\mu(\mathbf{x}) = 1/\det A(\mathbf{x}),$$

since the distortion of the transformation is determined by the Jacobian matrix. The singular points of the mapping are characterized by

$$\det A(\mathbf{x}) = 0$$

(where the mapping is not one-to-one). The set is formed by so-called critical curves (SEF).

Since $\det A(\boldsymbol{\gamma}^{(c)}) = 0$ (at points on the critical curve), it is possible to find coordinates with $\phi_{11} \neq 0, \phi_{12} = \phi_{22} = 0$. As shown in Schneider & Weiss (1992), the lens equation near the cusp can be represented as

$$y_1 = c x_1 + \frac{b}{2} x_2^2,$$
$$y_2 = b x_1 x_2 + a x_2^3, \qquad (5)$$

where $a = \frac{1}{6}\phi_{2222}, b = \phi_{122}, c = \phi_{11}$ and $c \neq 0, b \neq 0, 2ac - b^2 \neq 0$. It was shown in SEF that additional terms do not affect the local properties of the mapping. It is possible to see that by the direct comparison of terms (for example the term with ϕ_{112} is smaller than the term with ϕ_{11}) or using Newton's polygon or Bruno's truncating rules (see for example Bruno 1989). Similar to Schneider & Weiss (1992), we introduce the notations

$$\hat{x}_1 = \frac{c}{b} x_1, \quad \hat{x}_2 = x_2, \quad \hat{y}_1 = y_1/b, \quad \hat{y}_2 = \frac{c}{b^2} y_2, \qquad (6)$$

then we have

$$\hat{y}_1 = \hat{x}_1 + \frac{1}{2}\hat{x}_2^2,$$
$$\hat{y}_2 = \hat{x}_1 \hat{x}_2 + s\hat{x}_2^3,$$

where $s = ac/b^2$. We also introduce $S = 1 - 2s$, $\tilde{y}_1 = 2\hat{y}_1/3S$, $\tilde{y}_2 = \hat{y}_2/S$; then we have (Schneider & Weiss 1992)

$$\hat{x}_1 = \frac{3S}{2}\tilde{y}_1 - \frac{1}{2}\hat{x}_2^2, \qquad (7)$$
$$\hat{x}_2^3 - 3\tilde{y}_1\hat{x}_2 + 2\tilde{y}_2 = 0. \qquad (8)$$

3. Statement on the magnifications of images near cusps

We recall that (Schneider & Weiss 1992)

$$\hat{\mu} = (\det \hat{A})^{-1}, \quad \hat{\mu} = b^2 \mu, \qquad (9)$$
$$\det A = b^2 \det \hat{A} = b^2[\hat{x}_1 + (3s - 1)\hat{x}_2^2]. \qquad (10)$$

Consider the magnifications for different images of one point inside the cusp. We show below that the following equality is valid for all sources inside the cusp

$$\hat{\mu}^{(1)} + \hat{\mu}^{(2)} + \hat{\mu}^{(3)} = 0. \qquad (11)$$

It is clear from Eq.(11) that we have the statement of Schneider & Weiss (1992) that

$$|\hat{\mu}^{(1)}| = |\hat{\mu}^{(2)} + \hat{\mu}^{(3)}|. \qquad (12)$$

It should be mentioned that Eq. (11) follows from Schneider and Weiss Eq.(2.3) (Eq. (12) of our paper) plus their comment on the parities after their Eq.(2.33b). We use the following expression for magnifications

$$\mu^{(i)} = \frac{1}{\hat{x}_1^{(i)} + (3s-1)(\hat{x}_2^{(i)})^2} \qquad (13)$$

or using Eq.(7)

$$\mu^{(i)} = \frac{2}{S[\tilde{y}_1 - (\hat{x}_2^{(i)})^2]} \qquad (14)$$

Therefore it is necessary to prove that

$$\frac{1}{\tilde{y}_1 - (\hat{x}_2^{(1)})^2} + \frac{1}{\tilde{y}_1 - (\hat{x}_2^{(2)})^2} + \frac{1}{\tilde{y}_1 - (\hat{x}_2^{(3)})^2} = 0 \qquad (15)$$

or that

$$3\tilde{y}_1^2 - 2\tilde{y}_1[(\hat{x}_2^{(1)})^2 + (\hat{x}_2^{(2)})^2 + (\hat{x}_2^{(3)})^2] +$$
$$+[(\hat{x}_2^{(1)}\hat{x}_2^{(2)})^2 + (\hat{x}_2^{(1)}\hat{x}_2^{(3)})^2 + (\hat{x}_2^{(2)}\hat{x}_2^{(3)})^2] = 0. \qquad (16)$$

Vieta's theorem applied to Eq.(8) yields

$$\hat{x}_2^{(1)} + \hat{x}_2^{(2)} + \hat{x}_2^{(3)} = 0,$$
$$\hat{x}_2^{(1)}\hat{x}_2^{(2)} + \hat{x}_2^{(1)}\hat{x}_2^{(3)} + \hat{x}_2^{(2)}\hat{x}_2^{(3)} = -3\tilde{y}_1.$$

If we express the symmetric power polynomials in terms of symmetric elementary polynomials we have

$$(\hat{x}_2^{(1)})^2 + (\hat{x}_2^{(2)})^2 + (\hat{x}_2^{(3)})^2 = 6\tilde{y}_1, \qquad (17)$$
$$(\hat{x}_2^{(1)}\hat{x}_2^{(2)})^2 + (\hat{x}_2^{(1)}\hat{x}_2^{(3)})^2 + (\hat{x}_2^{(2)}\hat{x}_2^{(3)})^2 = 9\tilde{y}_1^2, \qquad (18)$$

Thus we obtain (16). Similarly we have

$$q_1 = \hat{\mu}^{(1)}\hat{\mu}^{(2)}\hat{\mu}^{(3)} = \frac{2}{(3S)^3(\tilde{y}_1^3 - \tilde{y}_2^2)}, \qquad (19)$$

$$p_1 = \hat{\mu}^{(1)}\hat{\mu}^{(2)} + \hat{\mu}^{(1)}\hat{\mu}^{(3)} + \hat{\mu}^{(2)}\hat{\mu}^{(3)} = \frac{-3\tilde{y}_1}{(3S)^2(\tilde{y}_1^3 - \tilde{y}_2^2)}. \qquad (20)$$

Therefore we get an equation of third degree for the magnification of different images of a point inside the cusp

$$\tilde{\mu}^3 + \tilde{p}_1\tilde{\mu} + \tilde{q}_1 = 0, \qquad (21)$$

where $\tilde{\mu} = \hat{\mu}/S$, $\tilde{p}_1 = p_1(3S)^2$, $\tilde{q}_1 = q_1(3S)^3$. If $\tilde{y}_1^3 > \tilde{y}_2^2$ then the discriminant for the pure cubic equation

$$D = \left(\frac{\tilde{p}_1}{3}\right)^3 + \left(\frac{\tilde{q}_1}{2}\right)^2 = \frac{-\tilde{y}_2^2}{(\tilde{y}_1^3 - \tilde{y}_2^2)^3}.$$

is negative and we have three solutions of the Eq.(21) (see for example, Bronstein & Semendjajew 1980). Namely, we have
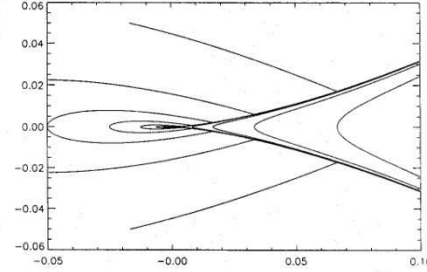
Fig. 1. Magnification contours around a cusp for the sum of absolute values of magnifications of all images. The contour levels are $10 * 2^i$, $-1 \le i \le 14$

for a point inside the cusp region

$$\tilde{\mu}^{(1)} = -\frac{2}{3}\sqrt{\frac{\tilde{y}_1}{\tilde{y}_1^3 - \tilde{y}_2^2}} \cos\left\{\frac{\cos^{-1}\left[\sqrt{\frac{\tilde{y}_1^3 - \tilde{y}_2^2}{\tilde{y}_1^3}}\right]}{3}\right\}, \qquad (22)$$

$$\tilde{\mu}^{(2)} = -\frac{2}{3}\sqrt{\frac{\tilde{y}_1}{\tilde{y}_1^3 - \tilde{y}_2^2}} \cos\left\{\frac{\cos^{-1}\left[\sqrt{\frac{\tilde{y}_1^3 - \tilde{y}_2^2}{\tilde{y}_1^3}}\right]}{3} + \frac{2\pi}{3}\right\}, \qquad (23)$$

$$\tilde{\mu}^{(3)} = -\frac{2}{3}\sqrt{\frac{\tilde{y}_1}{\tilde{y}_1^3 - \tilde{y}_2^2}} \cos\left\{\frac{\cos^{-1}\left[\sqrt{\frac{\tilde{y}_1^3 - \tilde{y}_2^2}{\tilde{y}_1^3}}\right]}{3} + \frac{4\pi}{3}\right\} \qquad (24)$$

and we have only one solution for a point outside the cusp region

$$\tilde{\mu}^{(1)} = \frac{\sqrt[3]{\sqrt{\tilde{y}_2^2 - \tilde{y}_1^3} + \tilde{y}_2} + \sqrt[3]{\sqrt{\tilde{y}_2^2 - \tilde{y}_1^3} - \tilde{y}_2}}{\sqrt{\tilde{y}_2^2 - \tilde{y}_1^3}}. \qquad (25)$$

It is possible to calculate the magnifications of the images from the direct solution of the gravitational lens equation near a cusp. Namely, we solve Eq.(8) and use Eqs.(7),(9),(10). After that we also obtain the expressions for magnifications.

4. Discussion

In Fig. 1 we present the contours for the sum of absolute values of magnifications of images near the cusp. Note that the algebraic sum of the values is equal to zero and that there are three real solutions of the gravitational lens equation in the cusp region. The contours are plotted by using expressions (22-25). It is possible to compare Fig. 1 with the similar figure from Schneider & Weiss (1992) that was obtained using the ray - shooting method (see, for example, Wamsganss 1990). Figure 1 shows clearly the cusp type singularity.

EXTENDED-SOURCE EFFECT AND CHROMATICITY IN TWO-POINT-MASS MICROLENSING

ONDŘEJ PEJCHA[1] AND DAVID HEYROVSKÝ

Institute of Theoretical Physics, Charles University, Prague, Czech Republic; pejcha@astronomy.ohio-state.edu, and heyrovsky@utf.mff.cuni.cz

ABSTRACT

We explore the sensitivity of two-point-mass gravitational microlensing to the extended nature of the source star, as well as the related sensitivity to its limb darkening. We demonstrate that the sensitive region, usually considered to be limited to a source-diameter-wide band along the caustic, is strongly expanded near cusps, most prominently along their outer axis. In the case of multicomponent caustics, facing cusps may form a region with a non-negligible extended-source effect spanning the gap between them. We demonstrate that for smaller sources the size of the sensitive region extending from a cusp measured in units of source radii increases, scaling as the inverse cube root of the radius. We study the extent of different sensitivity contours and show that for a microlensed Galactic bulge giant the probability of encountering at least a 1% extended-source effect is higher than the probability of caustic crossing by 40–60% when averaged over a typical range of lens-component separations, with the actual value depending on the mass ratio of the components. We derive analytical expressions for the extended-source effect and chromaticity for a source positioned off the caustic. These formulae are more generally applicable to any gravitational lens with a sufficiently small source. Using exactly computed amplifications we test the often used linear-fold caustic approximation and show that it may lead to errors on the level of a few percent even in near-ideal caustic-crossing events. Finally, we discuss several interesting cases of observed binary and planetary microlensing events and point out the importance of our results for the measurement of stellar limb darkening from microlensing light curves.

Key words: binaries: general – gravitational lensing – planetary systems – stars: atmospheres
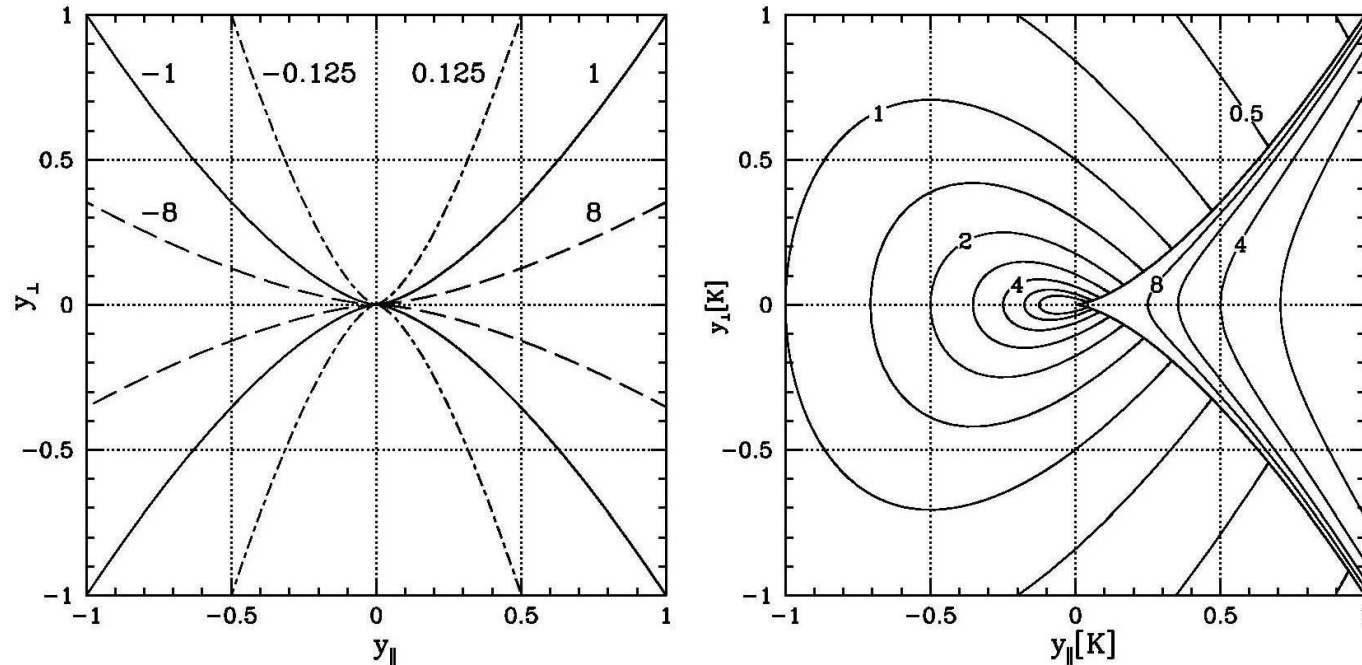
Figure 16. Geometry of a generic cusp caustic given by Equation (A2). Left panel: cusps for six values of K, with $K > 0$ curves drawn bold and $K < 0$ thin. Cusps with $|K| = 1$, 8, and 0.125 are marked by solid, dashed, and dot-dashed lines, respectively. Right panel: amplification contours for lensing by a generic cusp (bold curve). Contour values in units of $|K b|^{-1}$ are spaced by a factor of $2^{1/2}$; outside the cusp levels range from the outermost $2^{-3/2}$ to the innermost 2^3, inside the cusp from the rightmost $2^{3/2}$ to the leftmost 2^3. With axes marked in units of K, the right panel is valid for an arbitrary cusp.

APPENDIX

AMPLIFICATION OF IMAGES FORMED BY A CUSP

As shown by Schneider & Weiß (1992), the lens equation

a function of the image position (Schneider & Weiß 1992). Zakharov (1995, 1999) presented an elegant alternative method for obtaining image amplifications as a function of the source position, without explicitly solving the lens equation. From the general properties of the roots of the image equation, Zakharov derived a simple cubic equation for the amplification, the roots of which are the amplifications of the images. We reproduce the main results here because of a few typos appearing in the original papers. A point source satisfying $y_\perp^2 < K^{-1} y_\parallel^3$ lies inside the cusp and has three images with amplifications
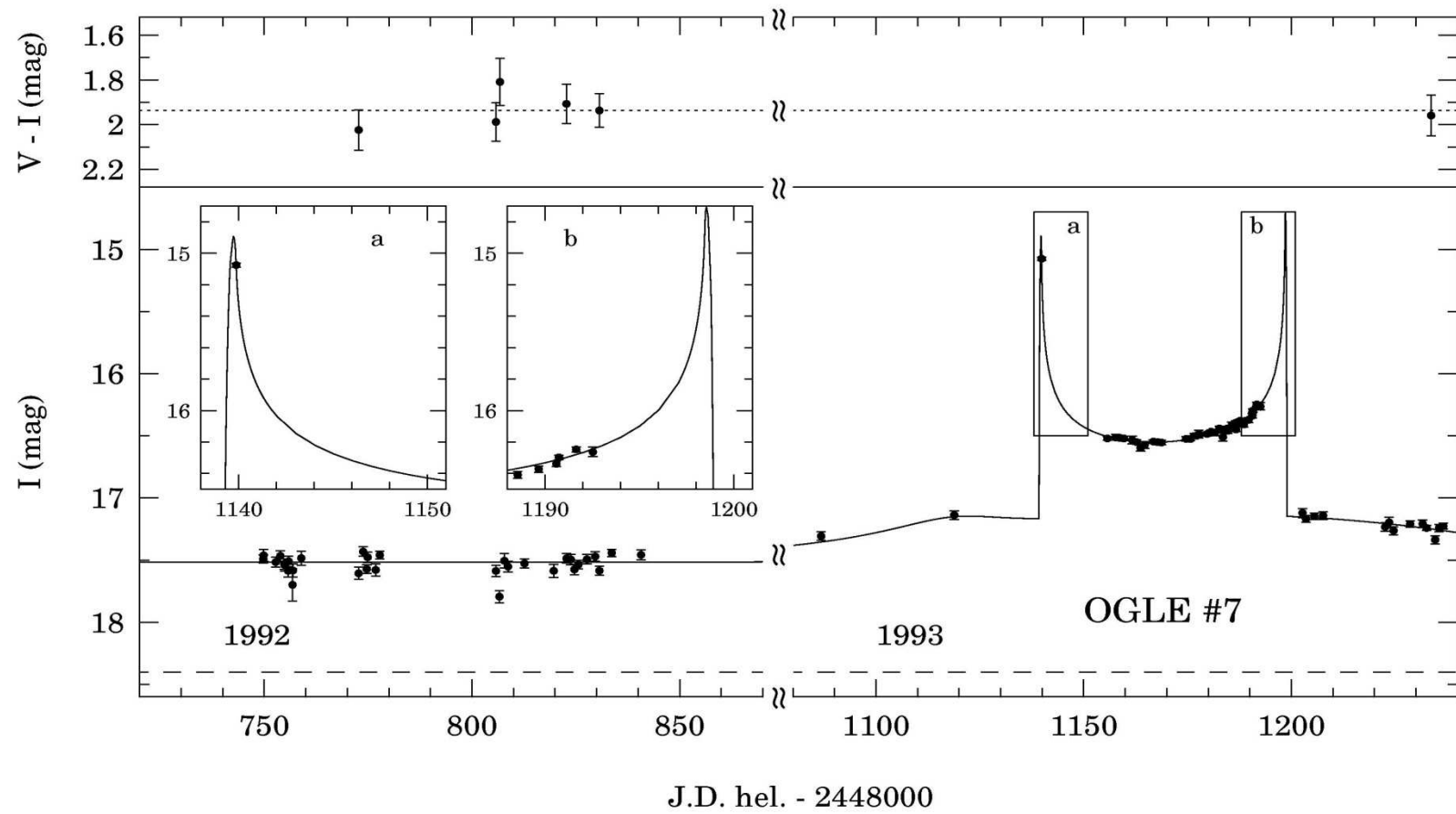
star
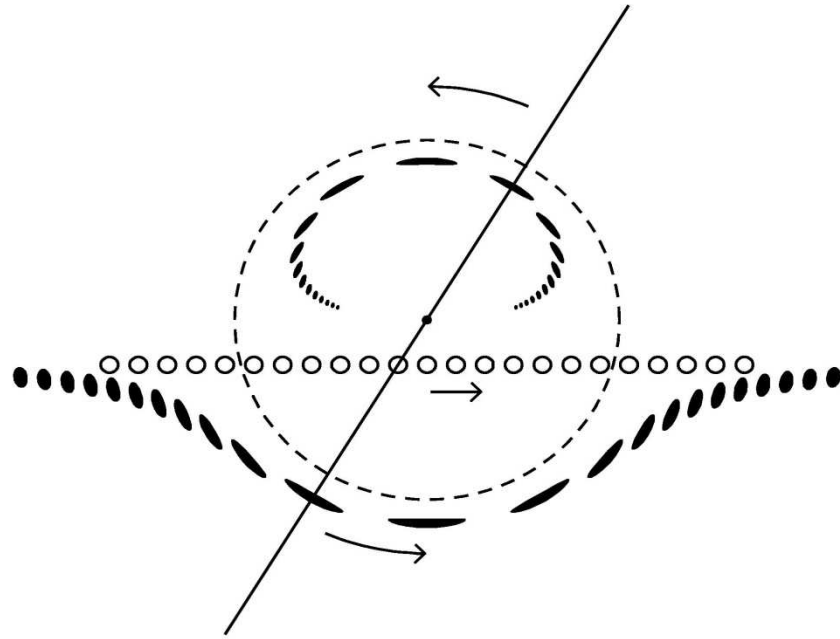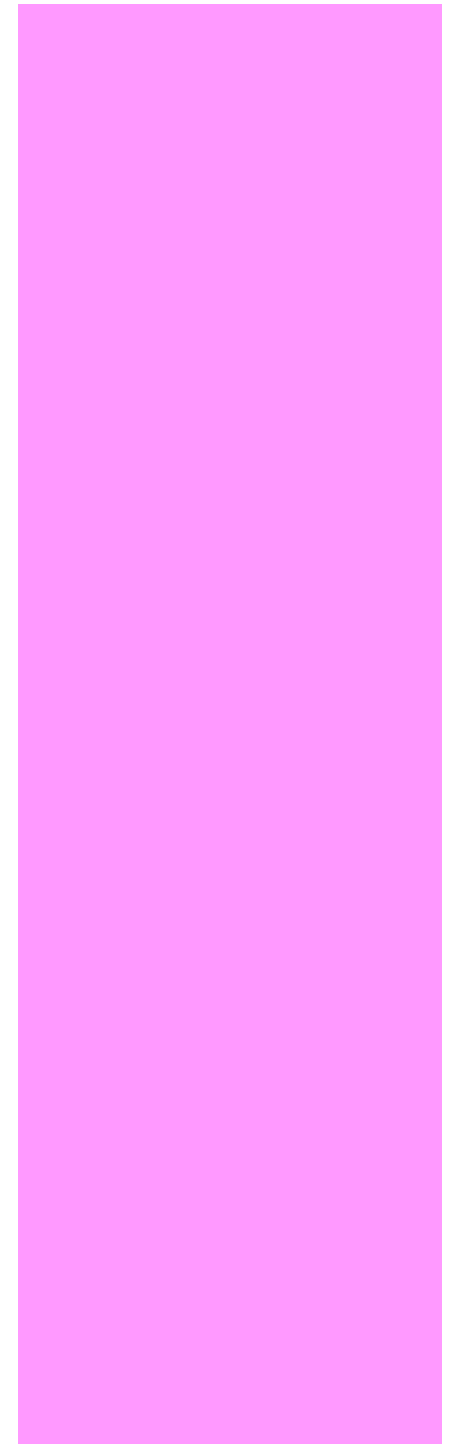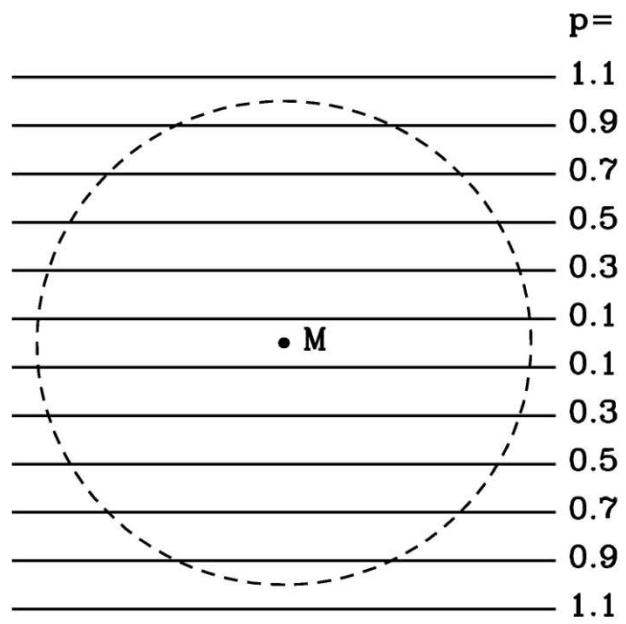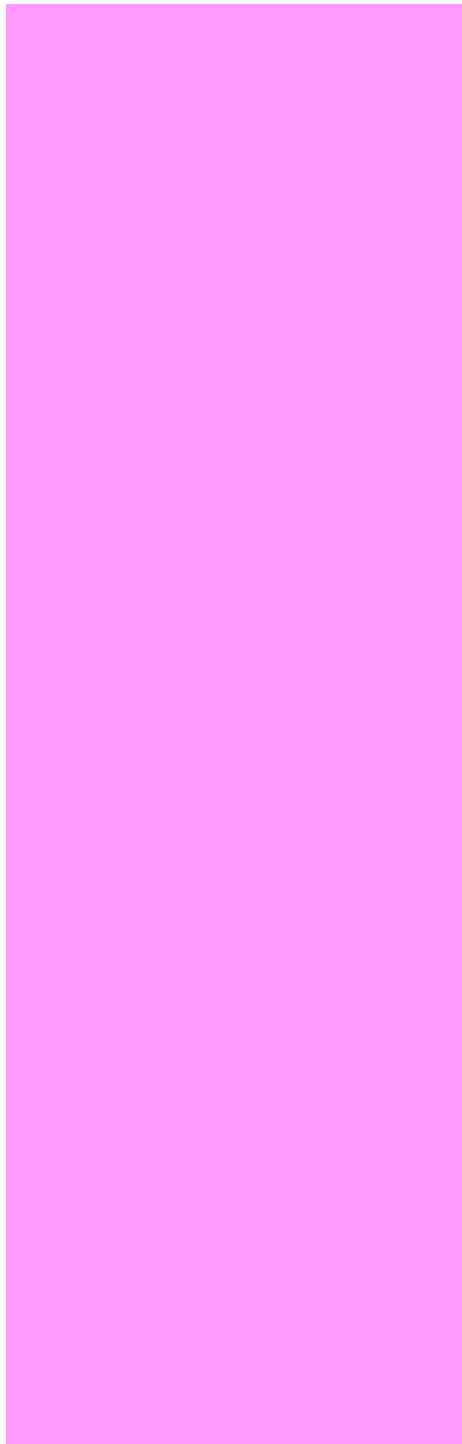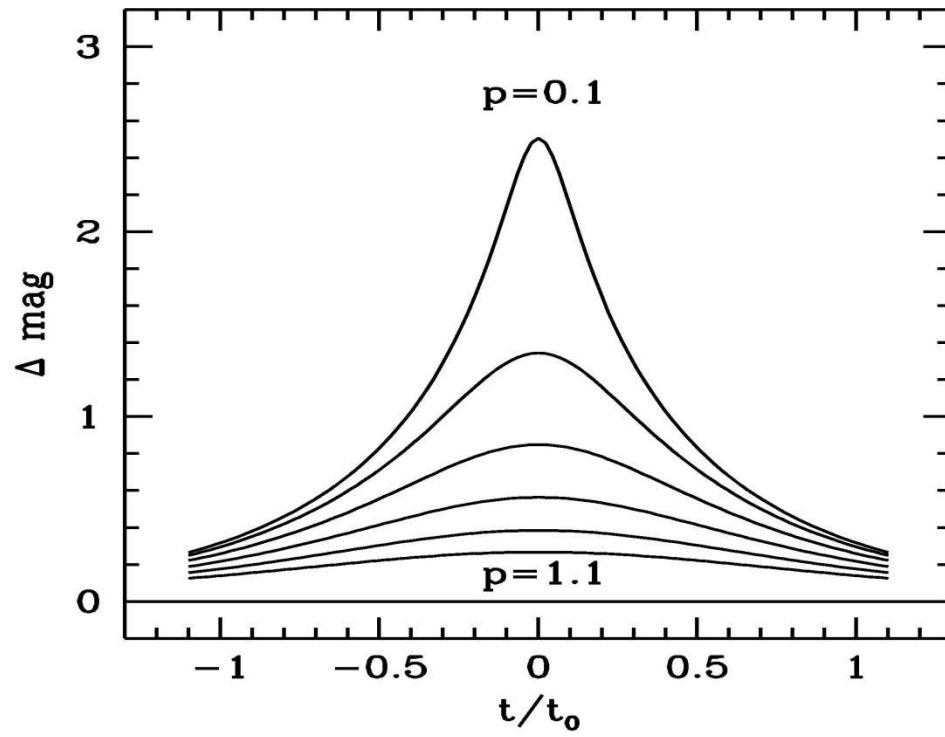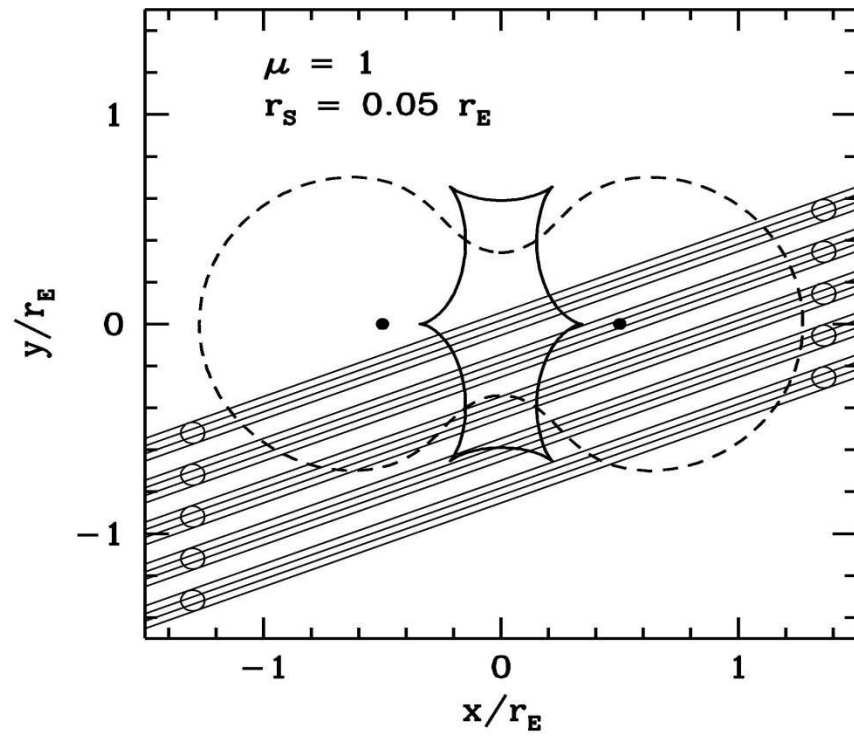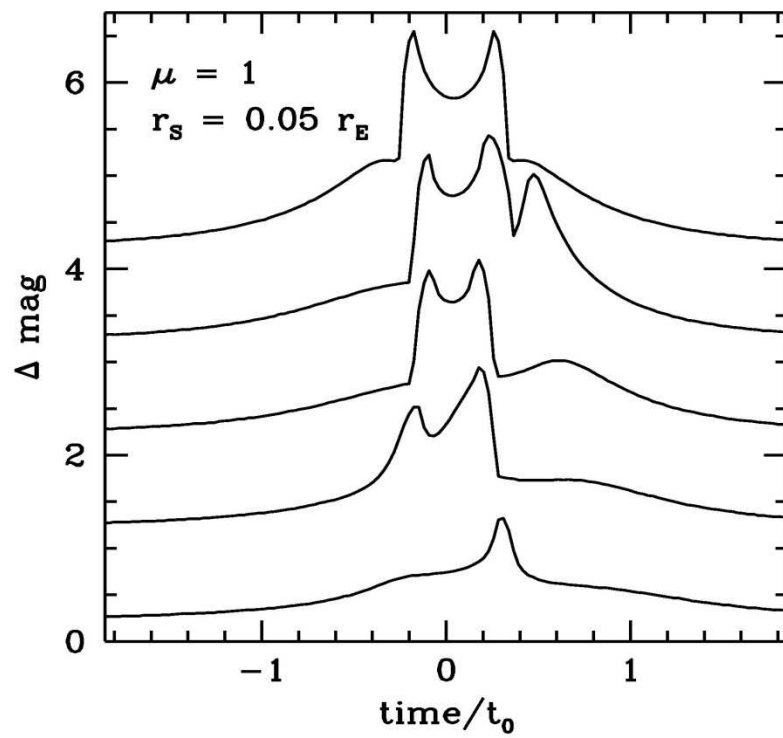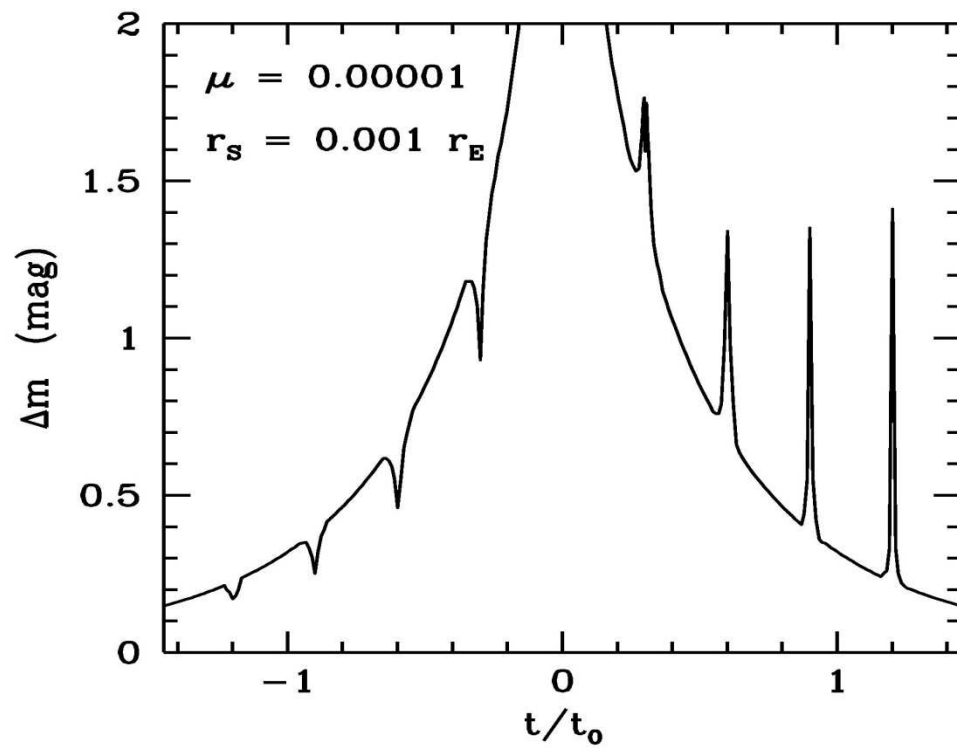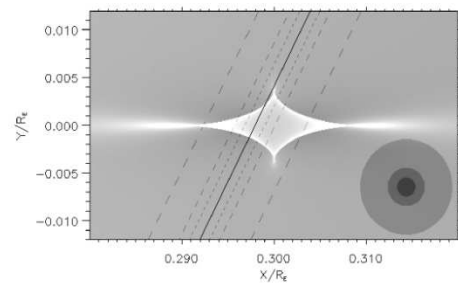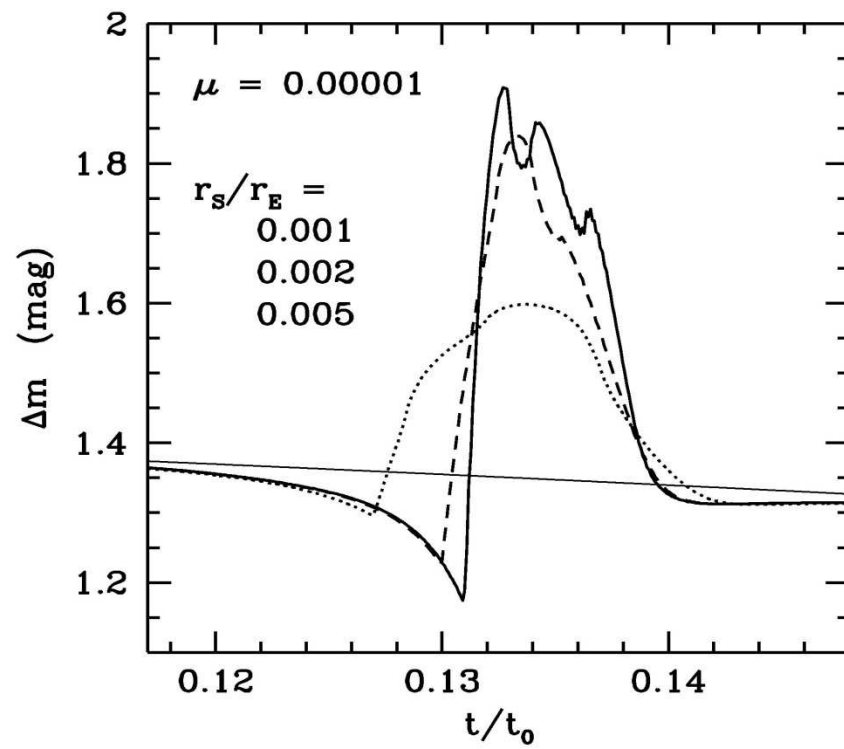
planet

Magnification
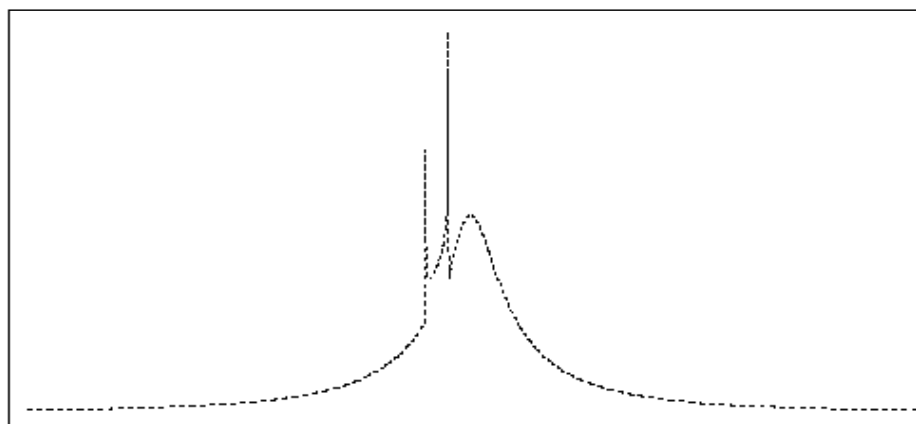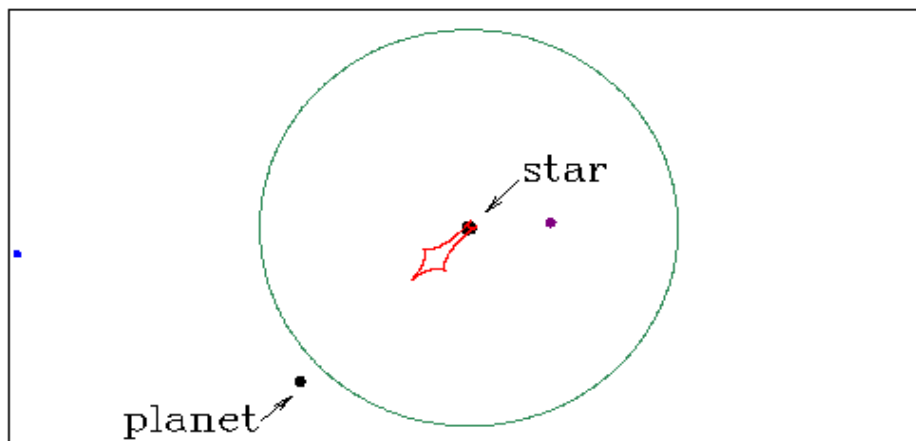
Time

Planet discovery with ML with the lowest mass

(J.-P. Beaulieu et al. Nature, 2006)

Planet discovery with ML with the lowest mass in 2006 (now people find a planet with a mass about 2 Earth masses, see Mayor et al.)
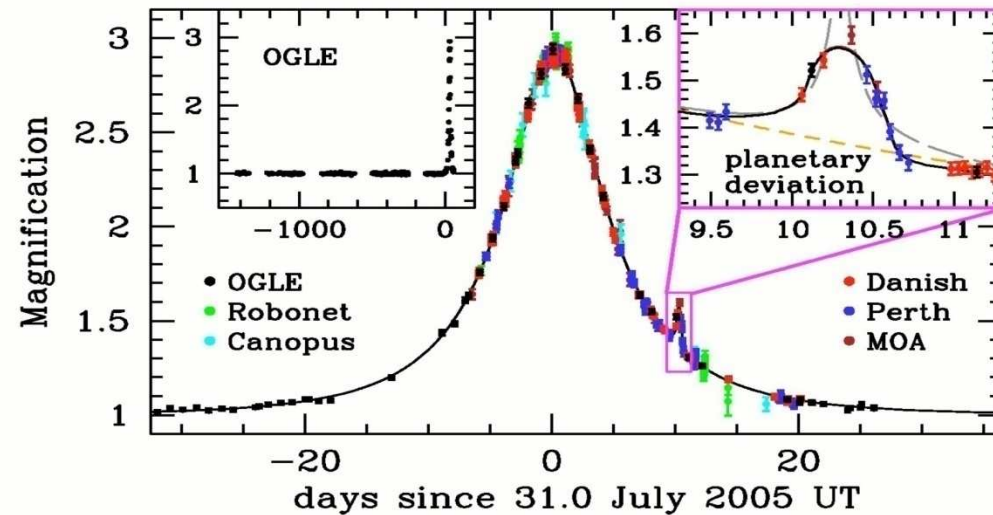
(J.-P. Beaulieu et al. Nature, 2006)

Figure 1 : The observed light curve of the OGLE-2005-BLG-390 microlensing event and best fit model plotted as a function of time. The data set consists of 650 data points from PLANET Danish (ESO La Silla, red points), PLANET Perth (blue), PLANET Canopus (Hobart, cyan), RoboNet Faulkes North (Hawaii, green), OGLE (Las Campanas, black), MOA (Mt John Observatory, brown). This photometric monitoring was done in the I band (with the exception of Faulkes R band data and MOA custom red passband) and real-time data reduction was performed with the different OGLE, PLANET and MOA data reduction pipelines. Danish and Perth data were finally reduced by the image subtraction technique[19] with the OGLE pipeline. The top left inset shows the OGLE light curve extending over the previous 4 years, whereas the top right one shows a zoom of the planetary deviation, covering a time interval of 1.5 days. The solid curve is the best binary lens model described in the text with a planet-to-star mass ratio of $q = 7.6 \pm 0.7 \times 10^{-5}$, and a projected separation $d = 1.610 \pm 0.008 \, R_E$ (where R_E is the Einstein ring radius). The dashed grey curve is the best binary source model that is rejected by the data, while the dashed orange line is the best single lens model.
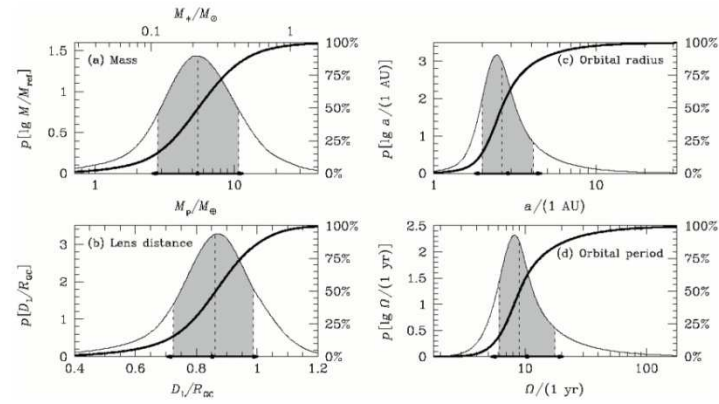
Figure 2 : Bayesian probability densities for the properties of the planet and its host star. The individual panels show the masses of the lens star and its planet (a), their distance from the observer (b), the three-dimensional separation or semi-major axis of an assumed circular planetary orbit (c) and the orbital period of the planet (d). The bold, curved line in each panel is the cumulative distribution, with the percentiles listed on the right. The dashed vertical lines indicate the medians, and the shading indicates the central 68.3% confidence intervals, while dots and arrows on the abscissa mark the expectation value and standard deviation. All estimates follow from a Bayesian analysis assuming a standard model for the disk and bulge population of the Milky Way and the stellar mass function of ref. [23], and a prior for the source distance D_S=1.05 ±0.25 R_{GC} (where R_{GC}= 7.62 ± 0.32 kpc for the Galactic Centre distance). The medians of these distributions yield a $5.5^{+5.5}_{-2.7}$ Earth mass planetary companion at a separation of $2.6^{+1.5}_{-0.6}$ AU from a $0.22^{+0.21}_{-0.11}M_\odot$ Galactic Bulge M-dwarf at a distance of 6.6 ± 1.0 kpc from the Sun. The median planetary period is 9^{+9}_{-3} years. The logarithmic means of these probability distributions (which obey Kepler's third law) are a separation of 2.9 AU, a period of 10.4 years, and masses of $0.22M_\odot$ and $5.5M_\oplus$ for the star and planet, respectively. In each plot, the independent variable for the probability density is listed within square brackets. The distribution of planet-star mass ratio was taken to be independent of the stellar mass, and a uniform prior was assumed for the planet-star separation distribution.

D.P. Bennett et al. A Low-Mass Planet with a Possible Sub-Stellar-Mass Host in Microlensing Event MOA-2007-BLG-192
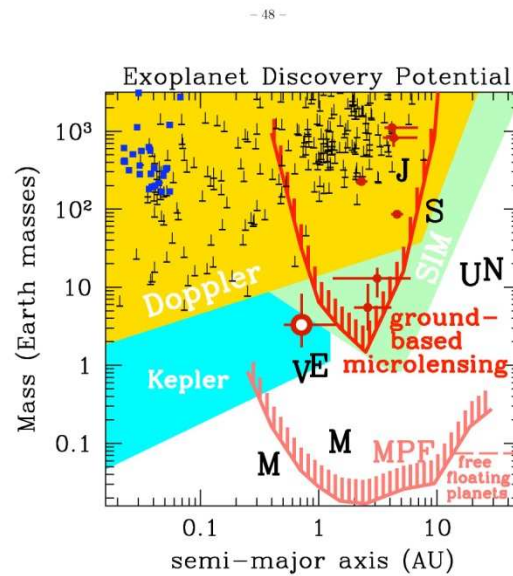Arxive:0806.0025[astro-ph] .

Fig. 16.— The known extrasolar planets are plotted as a function of mass vs. semi-major axis, along with the predicted sensitivity curves for a number of methods. The microlensing planets are indicated by dark red spots with error bars, and the large red spot with a white dot in the center is MOA-2007-BLG-192Lb. The blue dots indicate the planets first detected via transits, and the black bars with upward pointing error bars are the radial velocity planet detections. (The upward error bars indicate the 1-σ $\sin i$ uncertainty.) The gold, cyan, and light green shaded regions indicated the expected sensitivity of the radial velocity programs and the Kepler and SIM space missions. The dark and light red curves indicate the predicted lower sensitivity limits for a ground based and space-based (Bennett & Rhie 2002) microlensing planet search program, respectively. The Solar System's planets are indicated with black letters.

Table 2. Parameter Values and MCMC Uncertainties - without prior

parameter	value	2-σ range
M	$0.039^{+0.022}_{-0.012} M_\odot$	0.019–$0.113 M_\odot$
m	$2.3^{+2.5}_{-0.8} M_\oplus$	0.9–$14.4 M_\oplus$
$a_\perp$	$0.58^{+0.18}_{-0.14}$ AU	0.32–1.04 AU
D_L	1.3 ± 0.5 kpc	0.5–2.3 kpc
I_S	21.44 ± 0.08	21.30–21.60
q	$1.9 \pm 0.8 \times 10^{-4}$	0.6–6.4×10^{-4}

Table 3. Parameter Values and MCMC Uncertainties - with prior

parameter	value	2-σ range
M	$0.060^{+0.028}_{-0.021} M_\odot$	0.024–$0.128 M_\odot$
m	$3.3^{+4.9}_{-1.6} M_\oplus$	1.0–$17.8 M_\oplus$
$a_\perp$	$0.62^{+0.22}_{-0.16}$ AU	0.33–1.14 AU
D_L	1.0 ± 0.4 kpc	0.5–2.0 kpc
I_S	21.44 ± 0.08	21.31–21.61
q	$1.8^{+1.9}_{-0.8} \times 10^{-4}$	0.5–7.1×10^{-4}

The POINT-AGAPE collaboration

(Pixels Observation at INT)   (Andromeda Galaxy Amplified Pixel Experiment)

ARI – Liverpool, IoA – Cambridge, ITP – Zurich, OMP – Toulouse, Oxford University
PCC-Collège de France – Paris, QWM – London, Université Bretagne-sud – Vannes

Photometric survey of M31:

- **Isaac Newton Telescope (INT) $\varnothing$=2,5m (La Palma, Canaries)**

- **Wide Field Camera (WFC)**

- **180 observation nights (1 h/night between aug. 1999 and jan. 2002)**

- **3 filters : Sloan i', r' et g'**

- **field : 0,55 deg²**
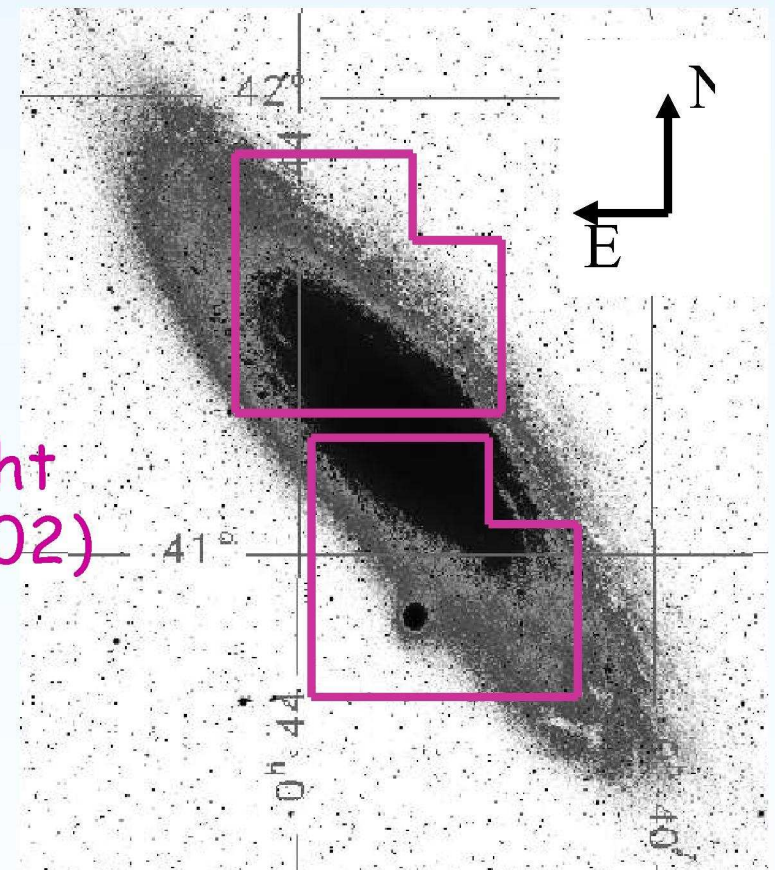
Pixel lensing

Microlensing towards M31

S. Calchi Novati

Abstract Pixel lensing is gravitational microlensing of unresolved stars. The main target explored up to now has been the nearby galaxy of Andromeda, M31. The scientific issues of interest are the search for dark matter in form of compact halo objects, the study of the characteristics of the luminous lens and source populations and the possibility of detecting extra-solar (and extra-galactic) planets. In the present work we intend to give an updated overview of the observational status in this field.

Table 1 Completed and ongoing microlensing campaigns towards M31. Fifth column: number of microlensing candidate events, in bracket those that are no longer considered as such (see text for details) and in particular not reported in Table 2 and in Fig. 2.

collaboration	years	telescope	f.o.v.	# events	ref
VATT/Columbia	1997	1.8m VATT	$2 \times (11.3' \times 11.3')$	(3)+3	(36; 37)
	1997-1999	1.3m MDM	$2 \times (17' \times 17')$		
MEGA	1999-2002	2.5m INT	$2 \times (33' \times 33')$	(4)+14	(38; 39)
AGAPE	1994-1996	2.0m TBL	$6 \times (4.5' \times 4.5')$	1	(26; 40)
SLOTT-AGAPE	1997-1999	1.3m MDM	$2 \times (17' \times 17')$	(5)+3	(41; 42)
POINT-AGAPE	1999-2001	2.5m INT	$2 \times (33' \times 33')$	7	(44; 49; 45; 46; 34)
WeCAPP	1997-2008	1.23m CA	$17.2' \times 17.2'$	2	(47; 48)
		0.80m We	$8.3' \times 8.3'$		
Nainital	1998-2002	1.04m Sa	$13' \times 13'$	1	(43)
ANGSTROM	2004-	2m LT & FTN	$4.6' \times 4.6'$	-	(50)
PLAN	2006-	1.5m OAB	$2 \times (13' \times 12.6')$	2	(51; 35)

Table 2 Candidate microlensing events reported towards M31, as shown in Fig. 2. Seventh column: '$*$' indicates that the colour is $V - R$, '$**$' indicates that the colour is $B - R$.

id	RA (deg)	DEC (deg)	d_{M31} (arcmin)	t_{FWHM} (days)	ΔR_{MAX}	$R - I$	name	REF
1	10.672917	41.277528	0.72	5.3	17.9	0.8(**)	AGAPE-Z1	(40)
2	10.713333	41.398972	7.89	1.8	20.8	1.2(*)	PA-N1/MEGA-ML16	(44; 39)
3	11.087083	41.479111	22.07	22.0	19.1	1.0(*)	PA-N2/MEGA-ML7	(45; 38)
4	10.626250	41.216833	4.10	2.3	18.8	0.6	PA-S3/GL1	(45; 48; 46)
5	10.625000	40.896139	22.55	2.0	20.7	0.0	PA-S4/MEGA-ML11	(49; 38; 46)
6	10.552083	41.358333	8.01	16.0	21.0	2.2	C3	(42)
7	10.606667	41.440833	10.87	13.0	21.3	1.1	C4	(42)
8	10.470000	41.288333	9.74	14.0	21.8	0.5	C5	(42)
9	10.636667	41.332361	4.36	5.4	-	1.1	GL2	(48)
10	10.845417	41.091667	12.90	26.5	22.2	-	97-1267	(37)
11	10.762083	41.120694	9.58	17.3	20.3	-	97-3230	(37)
12	10.988750	41.198972	14.36	2.2	21.8	-	99-3688	(37)
13	10.793750	41.296611	5.19	5.4	21.8	0.6	MEGA-ML1	(38)
14	10.799583	41.295444	5.42	4.2	21.5	0.3	MEGA-ML2	(38)
15	10.815833	41.347833	7.56	2.3	21.6	0.4	MEGA-ML3	(38)
16	10.852083	41.630667	22.95	27.5	22.3	0.6	MEGA-ML8	(38)
17	11.195000	41.685194	33.90	2.3	22.0	0.2	MEGA-ML9	(38)
18	10.978750	41.175917	14.41	44.7	22.2	1.1	MEGA-ML10	(38)
19	10.760417	40.752556	31.19	26.8	23.3	0.8	MEGA-ML13	(38)
20	10.927083	40.709417	35.34	25.4	22.5	0.4	MEGA-ML14	(38)
21	10.509583	40.909722	22.98	3.4	19.5	-0.1	(PA-S16)	(46)
22	10.544583	41.329278	7.27	1.8	20.8	0.5	PA-N6	(34)
23	10.677500	41.211889	3.46	4.1	20.8	0.8(*)	PA-S7	(34)
24	10.888750	41.128889	12.49	59.0	20.1	1.3	NMS-E1	(43)
25	10.788750	41.348167	6.67	16.1	21.6	0.5	MEGA-ML15	(39)
26	10.481667	40.938889	21.85	10.1	22.2	0.4	MEGA-ML17	(39)
27	10.822083	41.037139	15.25	33.4	22.7	0.5	MEGA-ML18	(39)
28	10.737500	41.380556	7.09	7.1	21.1	1.0	OAB-N1	(35)
29	10.708333	41.311111	2.73	2.6	19.1	1.1	OAB-N2	(35)

Note added in proof

The WeCAPP collaboration (A. Riffeser and S. Seitz, private communication) is currently completing the final analysis of their 11-years campaign (Riffeser et al., 2010, in preparation and Koppenhöfer et al., 2010, in preparation). They report the detection of 10 microlensing events (all of them with very short duration and specifically, 8 out of 10 with $t_{\mathrm{FWHM}} < 5$ days). Their preliminar results on the expected rate indicate that the self-lensing signal alone is not sufficient to explain all of the observed events.
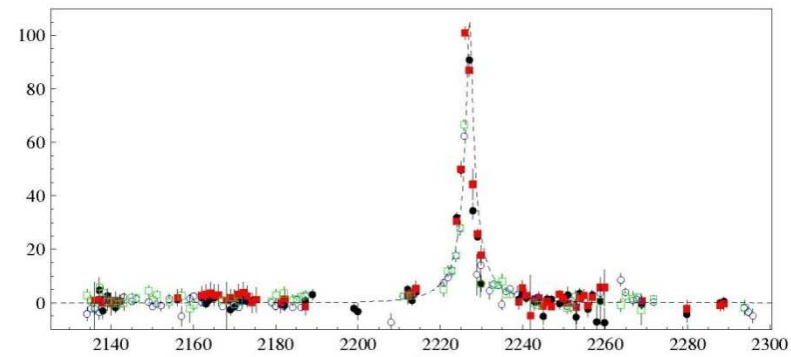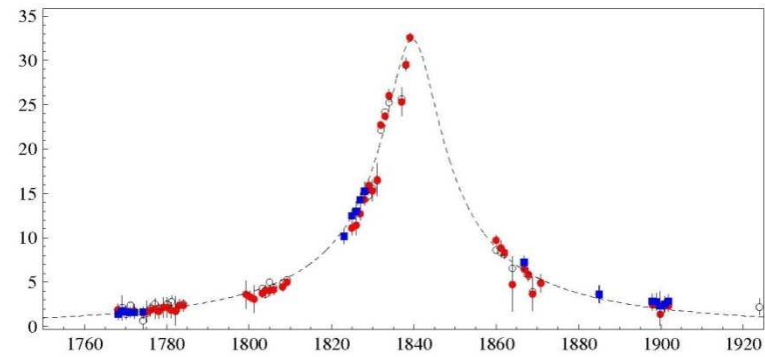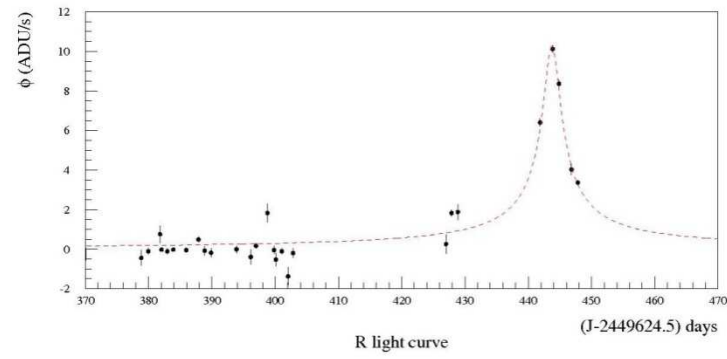
Fig. 4 The light curves for three pixel lensing (candidate) events observed towards M31. From top to bottom: AGAPE-Z1 (Figure reproduced from Fig. 3 of (40)); POINT-AGAPE PA-N2/MEGA ML7 (Figure adapted from (45)); POINT-AGAPE S3/WeCAPP GL1 (Figure adapted from (45; 48)). The dashed curves represent the best Paczyński light curve fits. The units on the axes (middle and bottom panels) are the same as in the top panel. Middle panel: empty/filled circles and filled boxes are for g', r' and i' band data respectively (black, red and blue in the colour version). Bottom panel: circles and boxes are for R and I band data, filled and empty symbols for the POINT-AGAPE and WeCAPP data sets.

Astronomy
&
Astrophysics

Influence of magnification threshold on pixel lensing optical depth, event rate and time scale distributions towards M 31

F. De Paolis[1], G. Ingrosso[1], A. A. Nucita[1], and A. F. Zakharov[2,3]

[1] Dipartimento di Fisica, Università di Lecce and INFN, Sezione di Lecce, CP 193, 73100 Lecce, Italy
e-mail: ingrosso@le.infn.it
[2] Institute of Theoretical and Experimental Physics, 25, B. Cheremushkinskaya St., Moscow 117259, Russia
[3] Astro Space Centre of Lebedev Physics Institute, Moscow

Abstract. Pixel lensing is the gravitational microlensing of light from unresolved stars contributing to the luminosity flux collected by a single pixel. A star must be sufficiently magnified, that is, the lens impact parameter must be less than a threshold value u_T if the excess photon flux in a pixel is to be detected over the background. Assuming the parameters of the Isaac Newton Telescope and typical observing conditions, we present maps in the sky plane towards M 31 of threshold impact parameter, optical depth, event number and event time scale, analyzing in particular how these quantities depend on u_T in pixel lensing searches. We use an analytical approach consisting of averaging on u_T and the star column density the optical depth, microlensing rate and event duration time scale. An overall decrease in the expected optical depth and event number with respect to the classical microlensing results is found, particularly towards the high luminosity M 31 inner regions. As expected, pixel lensing events towards the inner region of M 31 are mostly due to self-lensing, while in the outer region dark events dominate even for a 20% MACHO halo fraction. We also find a far-disk/near-disk asymmetry in the expected event number, smaller than that found by Kerins (2004). Both for self and dark lensing events, the pixel lensing time scale we obtain is ≃1−7 days, dark events lasting roughly twice as long as self-lensing events. The shortest events are found to occur towards the M 31 South Semisphere. We also note that the pixel lensing results depend on $\langle u_T \rangle$ and $\langle u_T^2 \rangle$ values and ultimately on the observing conditions and telescope capabilities.

Key words. gravitational lensing – Galaxy: halo – cosmology: dark matter – galaxies: individual: M 31
– methods: observational

1. Introduction

Pixel lensing surveys towards M 31 (Crotts 1992; Baillon et al. 1993) can give valuable information to probe the nature of MACHOs (Massive Astrophysical Compact Halo Objects) discovered in microlensing experiments towards the LMC and SMC (Large and Small Magellanic Clouds) (Alcock et al. 1993; Aubourg et al. 1993) and also address the question of the fraction of halo dark matter in the form of MACHOs in spiral galaxies (Alcock et al. 2000).

This may be possible due to both the increase in the number of expected events and because the M 31 disk is highly inclined with respect to the line of sight and so microlensing by MACHOs distributed in a roughly spherical M 31 halo give rise to an unambiguous signature: an excess of events on the far side of the M 31 disk relative to the near side (Crotts 1992).

Moreover, M 31 surveys probe the MACHO distribution in a different direction to the LMC and SMC and observations are made from the North Earth hemisphere, probing the entire halo extension.

The Pixel lensing technique studies the gravitational microlensing of unresolved stars (Ansari et al. 1997). In a dense field of stars, many of them contribute to each pixel. However, if one unresolved star is sufficiently magnified, the increase of the total flux will be large enough to be detected. Therefore, instead of monitoring individual stars as in classical microlensing, one follows the luminosity intensity of each pixel in the image. When a significative (above the background and the pixel noise) photon number excess repeatedly occurs, it is attributed to an ongoing microlensing event if the pixel luminosity curve follows (as a function of time) a Paczynski like curve (Paczynski 1996).

Clearly, variable stars could mimic a microlensing curve. These events can be recognized by performing observations in several spectral bands and monitoring the signal from the same pixel for several observing seasons to identify the source.

Two collaborations, MEGA (preceded by the VATT/Columbia survey) and AGAPE have produced a number of microlensing event candidates, which show a rise in pixel luminosity in M 31 (Crotts & Tomaney 1996; Ansari et al. 1999; Auriere et al. 2001; Calchi Novati et al. 2002).
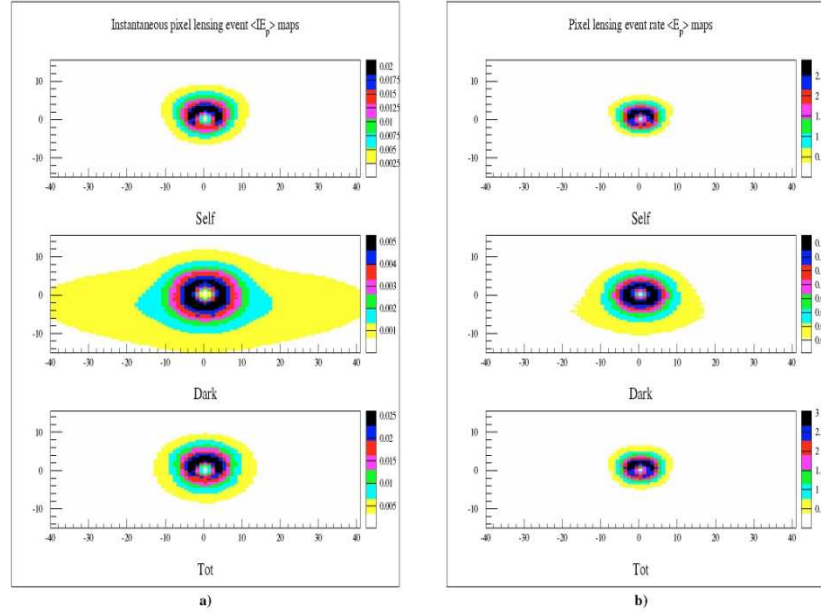
Fig. 5. In panel **a)**, the instantaneous pixel lensing event number density $\langle IE_p(x,y)\rangle$ maps (events per arcmin^2) towards M 31 are given for self, dark and total lensing. In panel **b)** maps of pixel lensing event rate $\langle E_p(x,y)\rangle$ (events per year and per arcmin^2) are given, in the same cases.

expected total number of events detectable by monitoring for 1 year the 100×70 arcmin^2 region oriented along the major axis of M 31 (events within 8 arcmin from the center are excluded). The first four lines refer to the models considered in Table 1 and to the parameters in the third row of Table 2. As one can see, the obtained results for the Reference model are intermediate with respect to those for the other more extreme models.

In the last row of Table 3, for the Reference model we show how the expected event number changes considering a different value of $\langle u_T \rangle_\phi \simeq 1.44 \times 10^{-2}$ (see 5th row in Table 2). As expected, one can verify that roughly the event number scales as $\langle u_T \rangle_\phi$.

Similar results have been obtained in previous simulations (see, e.g. Kerins 2004, and references therein). We also note that our numerical results scale with the fraction of halo dark matter in form of MACHOs and with the MACHO mass by a factor $(f_{\mathrm{MACHO}}/0.2) \sqrt{0.5\,M_\odot/m_l}$.

In Table 4 we give the total event number $\langle E_p \rangle$ for different lens populations (bulge, disk and halo) located in M 31. As one can see, the ratio dark/total events depends on the considered model, varying from 0.07 (for the massive disk model) to 0.40 for the massive halo model.

To study the far-disk/near-disk asymmetry, in the last three columns of Table 4 we give results for the South/North M 31 Semispheres and in brackets their ratio. For the Reference model, we find that self-lensing events are roughly symmetric (the same is true for lenses located in the MW disk and halo, not given in the table), while events due to lenses in M 31 halo are asymmetrically distributed with a ratio of about 2. The asymmetry is particularly evident (in the last column of the table) for sources located in the disk.

In Table 5 the instantaneous total number of events $\langle IE_p \rangle$ within the considered M 31 region is given. The first four rows refer to the parameter values $\langle m_b \rangle \simeq 0.31\,M_\odot$, $\langle m_d \rangle \simeq 0.53\,M_\odot$, $f_{\mathrm{MACHO}} = 0.2$ and $\langle u_T^2 \rangle_\phi \simeq 9.56 \times 10^{-3}$ (used throughout the paper). For comparison with the results obtained by Kerins (2004), in the last four rows of Table 5 we present our results for $\langle m_b \rangle \simeq 0.5\,M_\odot$, $\langle m_d \rangle \simeq 0.5\,M_\odot$, $f_{\mathrm{MACHO}} = 1$ and $\langle u_T^2 \rangle_\phi \simeq 1.17 \times 10^{-3}$. The asymmetry ratio we obtain is always rather smaller than that quoted by Kerins (2004).

As it has been mentioned by several authors, in order to discriminate between self and dark lensing events, it is important to analyze the event duration. Indeed self-lensing events are expected to have, on average, shorter duration with respect to events due to halo MACHOs.
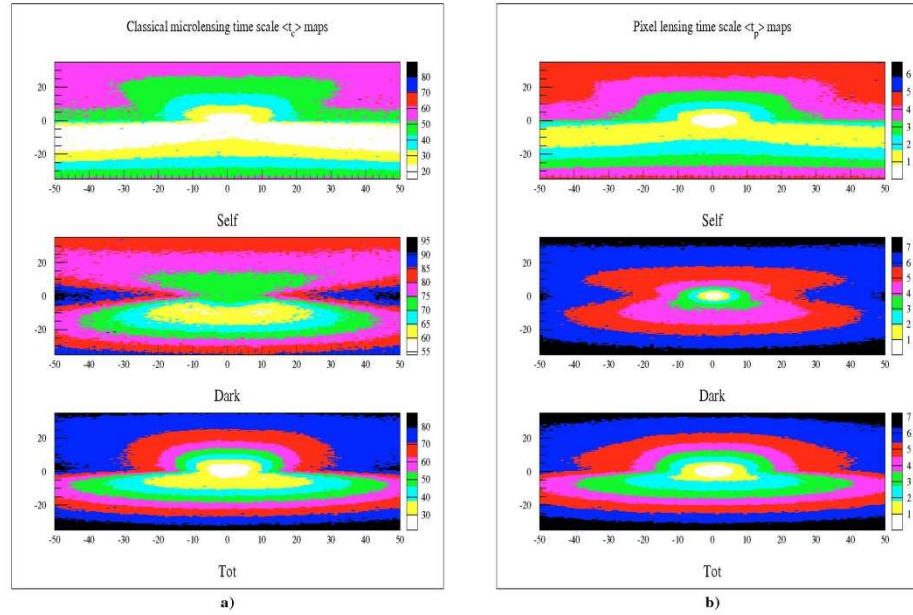
Fig. 6. In panel **a)**, mean classical event duration time $\langle t_c(x, y)\rangle$ (in days) maps towards M 31 are given for self, dark and total lensing. In panel **b)** for pixel lensing, maps of $\langle t_p(x, y)\rangle$ are given, in the same cases.
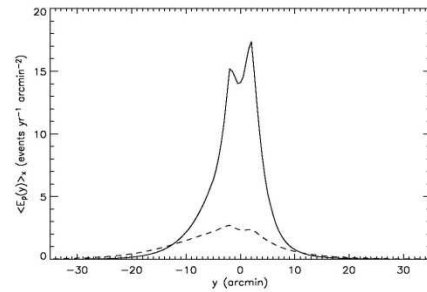

Fig. 7. The projected (along the x axis) mean event number $\langle E_p(y)\rangle_x$ is given as a function of the coordinate y for the Reference model. The dashed line refers to dark lensing events by MACHOs in M 31 and MW halos while the solid line is for self-lensing events by stars in M 31 bulge and disk.

6.4. Pixel lensing event time scale

Maps of mean event duration time scale in classical and pixel lensing are shown in Figs. 6a and 6b.

Here we use the probability, for each location of sources and lenses given in Eq. (26), of obtaining event duration maps for self and dark microlensing events.

As expected, short duration events are mainly distributed towards the inner regions of the galaxy and this occurs for both $\langle t_c(x, y)\rangle$ and $\langle t_p(x, y)\rangle$. The main effect of $\langle u_T(x, y)\rangle_\phi$ is to decrease the event time scale, in particular towards the inner regions of M 31, giving a larger number of short duration events with respect to expectations based on $\langle t_c(x, y)\rangle$ calculations.

Both for self and dark events the pixel lensing time scale we obtain is $\simeq 1-7$ days, in agreement with results in Kerins (2004), but much shorter with respect to the duration of the events observed by the MEGA Collaboration (de Jong et al. 2004). This is most likely due to the fact that current experiments may not detect events shorter than a few days.

However, the pixel lensing time scale values depend on $\langle u_T(x, y)\rangle_\phi$ and ultimately on the observational conditions and the adopted analysis procedure. Indeed from Table 2 one can see that the $\langle u_T(x, y)\rangle_\phi$ value may be easily doubled, changing the adopted parameters and therefore giving longer events.

In Fig. 8 the pixel lensing event duration $\langle t_p(y)\rangle$ averaged along the x direction is given as a function of the y coordinate. The dashed line refers to dark lensing events by MACHOs

Pixel-lensing and extra-solar searches
G. Ingrosso, S. Calchi-Novati, F. De Paolis, P. Jetzer, A. Nucita, AFZ
(MNRAS, 399, 219)

Planets with masses 0.1 Earth masses may be detected in M31

There were two claims in the article.

•Exoplanets with masses less than Earth mass may be detected with pixel lensing using present observational facilities.

•The pixel lensing event candidate observed by PLANET—AGAPE collaboration in 1999 may be fitted by a planetary system in Andromeda galaxy with a mass exoplanet about 5—7 Jupiter masses.

New Scientist
http://www.newscientist.com/article/dn17287-first-extragalactic-exoplanet-may-have-been-found.html

http://www.newscientist.com/section/science-news

Technology Review (Published by MIT)
http://www.technologyreview.com/blog/arxiv/23619/

FOX News
http://www.foxnews.com/story/0,2933,525886,00.html

BBC
http://news.bbc.co.uk/2/hi/science/nature/8097141.stm

Universe Today
http://www.universetoday.com/2009/06/10/first-extra-galactic-planet-may-have-been-detected/

Scientific American

http://www.scientificamerican.com/article.cfm?id=planet-spotted-in-andromeda-galaxy-2009-06

Daily Telegraph

http://www.telegraph.co.uk/science/science-news/5534891/Planet-six-times-the-mass-of-Jupiter-spotted-by-astronomers.html

World News

http://article.wn.com/view/2009/06/14/Hint_of_planet_outside_our_galaxy/

Russian Press

http://www.gazeta.ru/science/2009/06/10_a_3209024.shtml?lj2

http://www.rian.ru/science/20090618/174737604.html
(with an interview to Alexander Zakharov)

http://rian.ru/science/20090609/173875820.html

Intervista con il Prof. Jetzer (University of Zurich)

http://www.spektrum.de/artikel/1008445

Spanish Press
http://www.terra.cl/actualidad/index.cfm?id_cat=1167&id_reg=1199230

ANSA Italia
http://ansa.it/opencms/export/site/visualizza_fdg.html_989646565.html

Le Stelle
http://www.lestelle-astronomia.it/news.asp

Le Stelle (articolo apparso sul Numero di Agosto 2009 e qui riprodotto)
http://www.fisica.unisalento.it/tagroup/download/LeStelle2009.pdf

Thaindian News
http://www.thaindian.com/newsportal/health/first-extragalactic-exoplanet-may-have-been-found-by-gravitational-microlensing_100203542.html

Wired
http://www.wired.it/news/archivio/2009-06/15/i-misteri-fuori-dalla-nostra-galassia.aspx

Il Corriere del Mezzogiorno
http://corrieredelmezzogiorno.corriere.it/lecce/notizie/universita/2009/15-giugno-2009/astrofisici-salentini-osservano-primo-pianeta-fuori-nostra-galassia--1601467322460.shtml

La Repubblica
http://www.repubblica.it/2008/12/gallerie/scienze/pianeta-extragalattico/1.html

Il Mattino
http://www.ilmattino.it/articolo.php?id=62260&sez=SCIENZA

La Gazzetta di Parma
http://www.gazzettadiparma.it/primapagina/dettaglio/7/22044/Astronomia:_italiani_scoprono_prima_pianeta_extragalattico.html

Quotidiano di Lecce
http://www.lecceprima.it/articolo.asp?articolo=14980

Quotidiano di Puglia
http://www.quotidianopuglia.it/leggi_notizia.asp?ID=8034

http://www.fisica.unisalento.it/tagroup/images/Quotidiano160609.jpg

http://blogs.discovermagazine.com/80beats/2009/06/16/have-astronomers-spotted-the-first-exoplanet-in-another-galaxy/

http://www.lifeinitaly.com/node/6145

http://news.webindia123.com/news/printer.asp?story=/news/Articles/India/20090615/1275300.html

RAI
http://www.radio.rai.it/grr/grcontinua.cfm?GR=1&L_DATA=2009-06-15&L_ORA=19:00#

Il nostro paper e' attualmente disponibile al link:

http://arxiv.org/PS_cache/arxiv/pdf/0906/0906.1050v1.pdf

Il pianeta possibilmente identificato (PA-99-N2) e' stato aggiunto alla ben nota "extrasolar planet encyclopedia" con i dati riportati nel nostro paper.

Per maggiori informazioni:
http://exoplanet.eu/planet.php?p1=PA-99-N2&p2=b&showPubli=yes&sortByDate

European Association for Astronomical Education

http://eaae-astronomy.org/blog/?p=508

JPL (Pasadena, USA)

http://planetquest.jpl.nasa.gov/news/roundUp.cfm

(Indian Top News)

http://www.topnews.in/first-planet-spotted-outside-milky-way-may-lie-andromeda-galaxy-2177884

http://www.ask.com/wiki/Extragalactic_planet

SOFTPEDIA

http://news.softpedia.com/news/First-Exoplanet-in-Another-Galaxy-Found-113678.shtml

ASTRONOMIND

http://www.astronomind.com/faces-of-exoplanets

EXOPLANETZ

http://exoplanetz.com/exoplanet-discovered-in-another-galaxy

FRESHNEWS (INDIA)

http://www.freshnews.in/first-planet-spotted-outside-the-milky-way-may-lie-in-andromeda-galaxy-149525

Pixel lensing as a way to detect extrasolar planets in M31

G. Ingrosso,[1][*] S. Calchi Novati,[2] F. De Paolis,[1] Ph. Jetzer,[3] A. A. Nucita[4] and A. F. Zakharov[5,6]

[1]*Dipartimento di Fisica, Università del Salento and INFN Sezione di Lecce, CP 193, I-73100 Lecce, Italy*
[2]*Dipartimento di Fisica, Università di Salerno, I-84081 Baronissi (SA) and INFN Sezione di Napoli, Italy*
[3]*Institute for Theoretical Physics, University of Zürich, Winterthurerstrasse 190, CH-8057 Zürich, Switzerland*
[4]*XMM-Newton Science Operations Centre, ESAC, ESA, PO Box 50727, 28080 Madrid, Spain*
[5]*Institute of Theoretical and Experimental Physics, B. Cheremushkinskaya 25, 117259 Moscow, Russia*
[6]*Bogoliubov Laboratory of Theoretical Physics, Joint Institute for Nuclear Research, 141980 Dubna, Russia*

ABSTRACT

We study the possibility to detect extrasolar planets in M31 through pixel-lensing observations. Using a Monte Carlo approach, we select the physical parameters of the binary lens system, a star hosting a planet, and we calculate the pixel-lensing light curve taking into account the finite source effects. Indeed, their inclusion is crucial since the sources in M31 microlensing events are mainly giant stars. Light curves with detectable planetary features are selected by looking for significant deviations from the corresponding Paczyński shapes. We find that the time-scale of planetary deviations in light curves increase (up to 3–4 d) as the source size increases. This means that only few exposures per day, depending also on the required accuracy, may be sufficient to reveal in the light curve a planetary companion. Although the mean planet mass for the selected events is about $2\,M_{\rm Jupiter}$, even small mass planets ($M_{\rm P} < 20\,{\rm M}_{\oplus}$) can cause significant deviations, at least in the observations with large telescopes. However, even in the former case, the probability to find detectable planetary features in pixel-lensing light curves is at most a few per cent of the detectable events, and therefore many events have to be collected in order to detect an extrasolar planet in M31. Our analysis also supports the claim that the anomaly found in the candidate event PA-99-N2 towards M31 can be explained by a companion object orbiting the lens star.

Key words: gravitational lensing – Galaxy: halo – galaxies: individual: M31.

NASA

Hint of planet outside our galaxy

By Jason Palmer

Science and technology reporter, BBC News

Astronomers believe they have seen hints of the first planet to be spotted outside of our galaxy.

Situated in the Andromeda galaxy, the planet appears to be about six times the mass of Jupiter.

The method hinges on gravitational lensing, whereby a nearer object can bend the light of a distant star when the two align with an observer.

The results will be published in Monthly Notices of the Royal Astronomical Society (MNRAS).

The team, made up of researchers from the National Institute of Nuclear Physics (INFN) in Italy and collaborators in Switzerland, Spain, and Russia, exploited a type of gravitational lensing called microlensing.

The effect of large, massive objects between an observer and a distant planet or star can cause distortion or multiple images as the

First Planet in Another Galaxy Possibly Found

Friday, June 12, 2009

FOX NEWS

The Andromeda galaxy in a NASA composite image.
Astronomers may have found the first planet in another galaxy, according to New Scientist magazine.

SCIENTIFIC AMERICAN

SkyMania - June 14, 2009

Planet 'spotted' in Andromeda galaxy

Astronomers believe they may have discovered the first planet ever detected in another galaxy. The new world was apparently glimpsed in the closest giant spiral galaxy to the Milky Way, Messier 31 in the constellation of Andromeda. It lies an incredible 2.5 million light-years away - too far normally to be seen. But it revealed itself thanks to a phenomenon called microlensing where the gravitational field of an object closer to Earth acts like a magnifying glass.

Astronomers believe they may have discovered the first planet ever detected in another galaxy. The new world was apparently glimpsed in the closest giant spiral galaxy to the Milky Way, Messier 31 in the constellation of Andromeda.

It lies an incredible 2.5 million light-years away - too far normally to be seen.

But it revealed itself thanks to a phenomenon called microlensing where the gravitational field of an object closer to Earth acts like a magnifying glass.

Amazingly, it has taken the astronomers five years to realise that they probably netted an extra-galactic planet. They observed a peculiar microlensing event while studying the Andromeda galaxy - which can be seen as a dim blur with the unaided eye - in 2004.

The international team, using the UK's Isaac Newton Telescope on the Canary Island of La Palma, thought at the time that they had recorded a pair of stars orbiting each other.

But computer simulations and other calculations have persuaded them that they actually observed a star with a smaller, planet sized companion about six times bigger than Jupiter.

More than 300 so-called exoplanets have been found orbiting other stars in our own galaxy. And NASA has launched a $595 million spaceprobe called Kepler to watch 100,000 stars for signs of world like Earth.

Picture: A photo of the galaxy M31 in visible light. (Photo: John Lanoue).

• Discover space for yourself and do fun science with a telescope. Here is Skymania's advice on how to choose a telescope. We also have a guide to the different types of telescope available.

©PAUL SUTHERLAND, Skymania.com

European Association for Astronomy Education

- search
- skip to content ↓

rss

- EAAE Home

The quest for Extragalactic Exoplanets begins…

by Alexandre Costa on Jan.14, 2010, under Extrasolar Planets

Source: arXiv:1001.2105v1

While the most distant exoplanets detected until today are OGLE-05-390L b, MOA-2007-BLG-400-L b at around 6,500 & 6,000 parsecs, which roughly means ~21,190 & ~19,500 light-years away respectively, an international team of astronomers proposes a new observational method that they believe will allow the detection of exoplanets in the Andromeda galaxy (M31) that is at a distance of 2.9 million light-years from us.
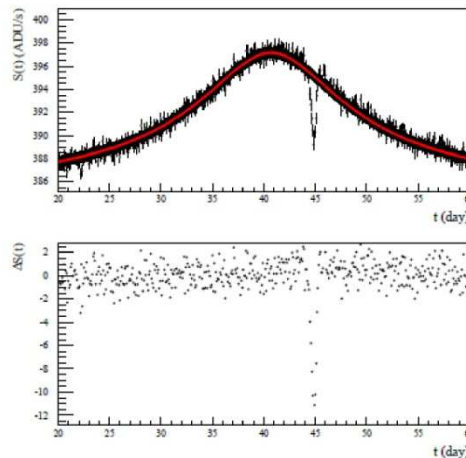
A simulation of the expected microlensing event. Credit: Ingrosso *et al.* (2009)

The authors think that that exoplanets in the M31 galaxy may be detected with the pixel-lensing method by using telescopes making high cadence observations of an ongoing microlensing event.Although the mean mass for detectable exoplanets is about 2 M_J, even small mass exoplanets (inferior to 20 Earth masses) can cause significant deviations, which are observable with large telescopes. (read more)

Link:

Planet : PA-99-N2 b

Basic data :

Name	PA-99-N2 b
Discovered in	2009
M.sin i	6.34 M_J
Update	16/06/09

ref

http://exoplanet.eu/planet.php?p1=PA-99-N2&p2=b&showPubli=yes&sortByDate

Remarks :

Reanalysis of data by An et al 2004

4 related publications :

AN J., EVANS N., KERINS E., BAILLON P., CALCHI NOVATI S., CARR J., CREZE M., GIRAUD-HERAUD Y., GOULD A., HEWETT P., JETZER Ph., KAPLAN J., PAULIN-HENRIKSSON S., SMARTT S., TSAPRAS Y. & VALLS-GABAUD D. (The POINT-AGAPE Collaboration) , 2004

The anomaly in the candidate microlensing event PA-99-N2

ApJ. , **601** , 845

paper

INGROSSO G., CALCHI NOVATI S., DE PAOLIS F., JETZER Ph., NUCITA A. & ZAKHAROV A. , 2009

Pixel-lensing as a way to detect extrasolar planets in M31

MNRAS , **399** , 219

accepted

preprint

WRIGHT J., MARCY G. & the California Planet Survey consortium , 2010

Exoplanet Data Explorer

web page

INGROSSO G., CALCHI NOVATI S., DE PAOLIS F., JETZER Ph., NUCITA A. & ZAKHAROV A. , 2010

Search for exoplanets in M31 with pixel-lensing and the PA-99-N2 event revisited

in *II Italian-Pakistani Workshop on Relativistic Astrophysics*, Pescara 2009

Paper: **arXiv:1001.4342**

THE STAR
in M31

Name	_ PA-99N2
Distance	670000 pc
Mass	0.5 M_{sun}

Andromeda Galaxy
From Wikipedia, the free encyclopedia

In 2009, the first planet may have been discovered in the Andromeda Galaxy. This candidate was detected using a technique called microlensing, which is caused by the deflection of light by a massive object.[26]

26. Ingrosso, G.; Calchi Novati, S.; De Paolis, F.; Jetzer, Ph.; Nucita, A. A.; Zakharov, A. F.. "Pixel-lensing as a way to detect extrasolar planets in M31". arXiv. http://arxiv.org/abs/0906.1050.
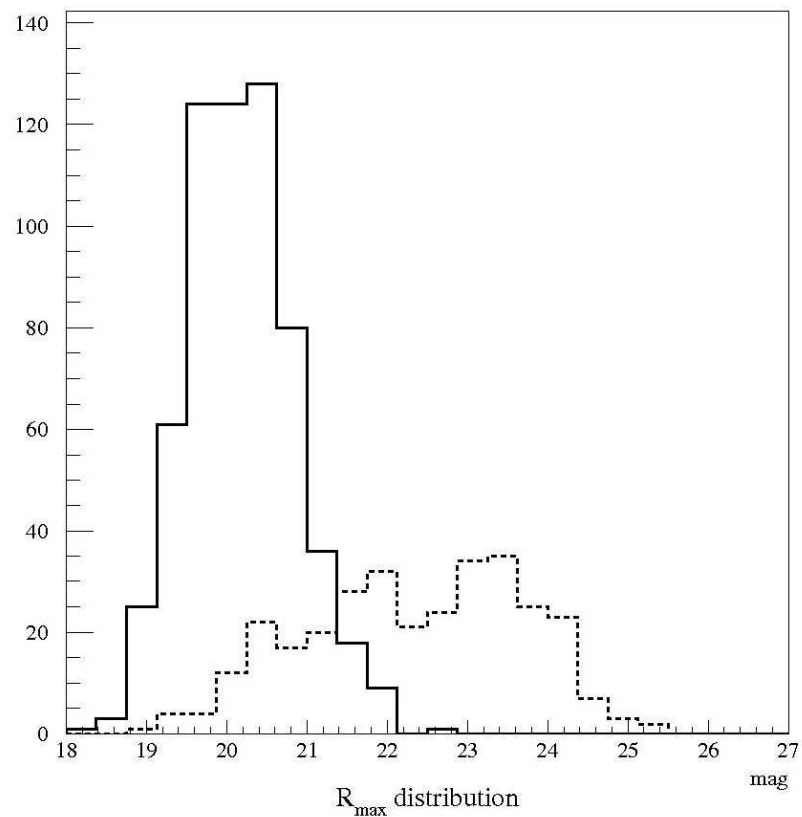
Figure 3. Normalized distributions of R_{max} for events with $\chi_r^2 > 4$ and $N_{good} > 3$, assuming a telescope diameter $D = 8$ m. Events with $\rho/u_0 > 1$ (solid line) and $\rho/u_0 < 1$ (dashed line) are shown.
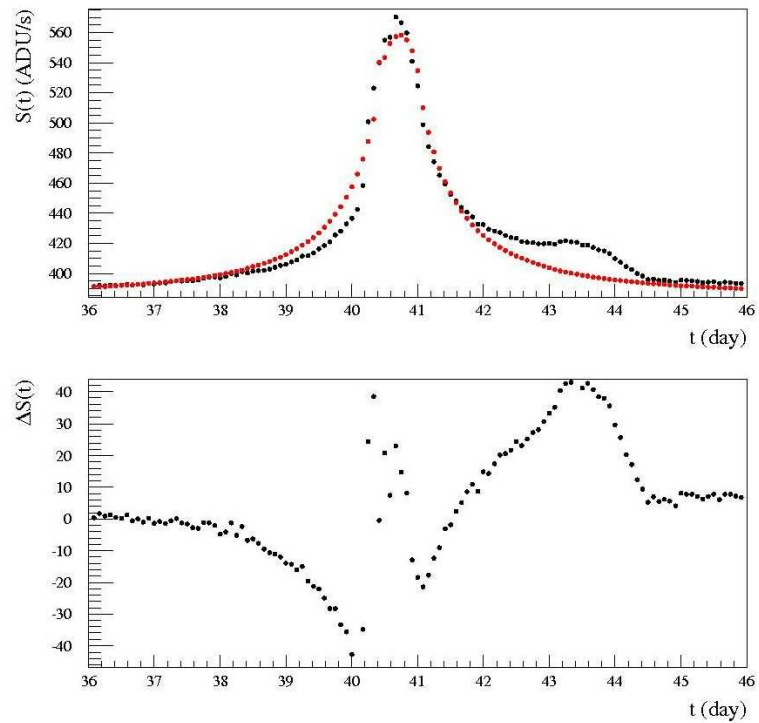
Figure 4. Event of the I class #1 (see Table 2). The upper panel shows the simulated light curve and the corresponding best fit model (a Paczyński light curve modified for finite source effects). The lower panel gives the difference.
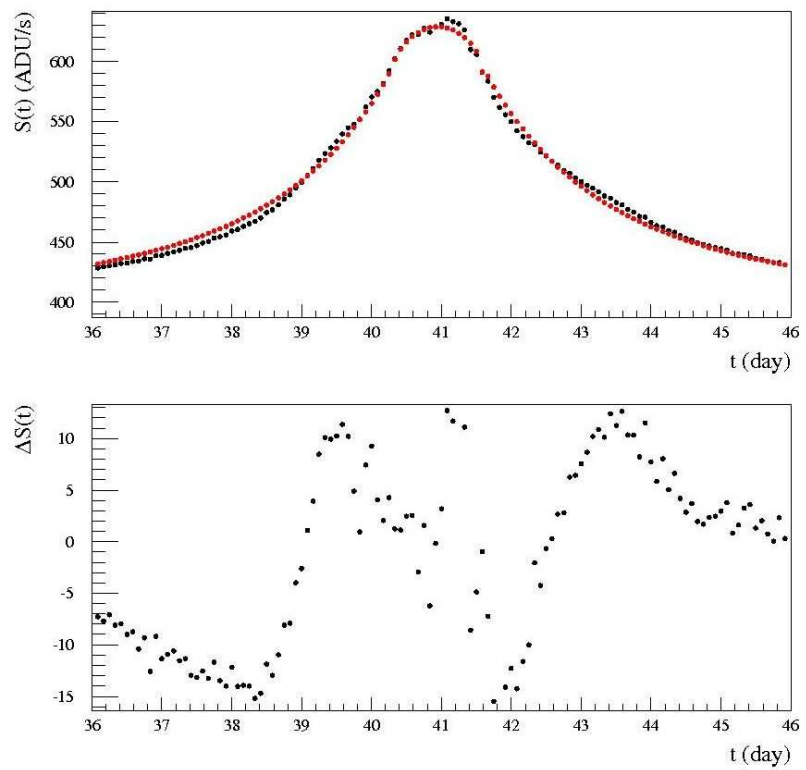
Figure 5. The same as in Fig. 4 for the I class event #2 (see Table 2).
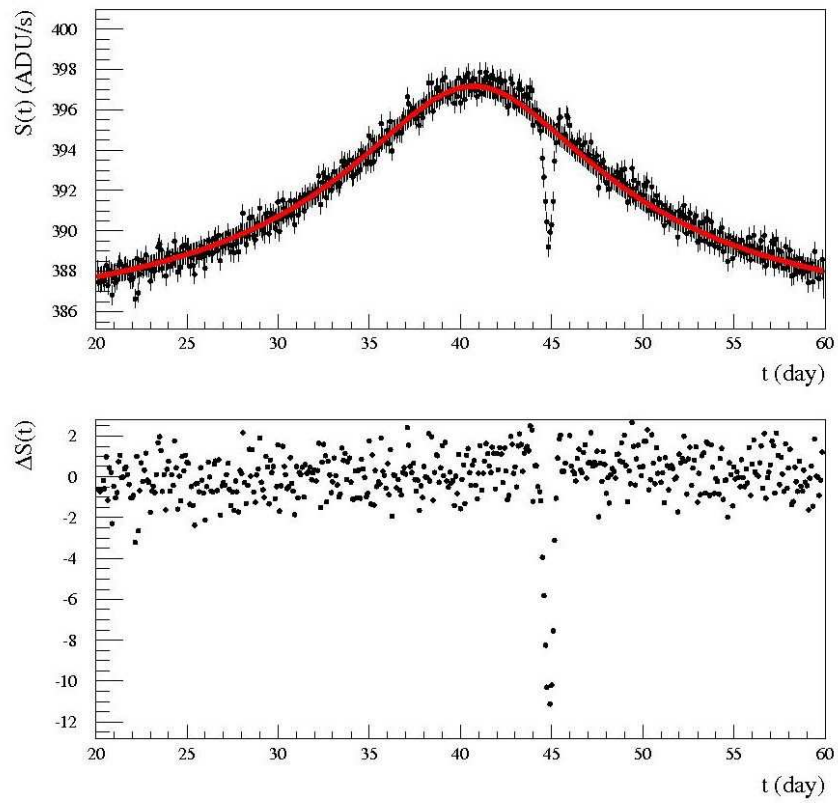
Figure 6. The same as in Fig. 4 for the second class event #3 (see Table 2).
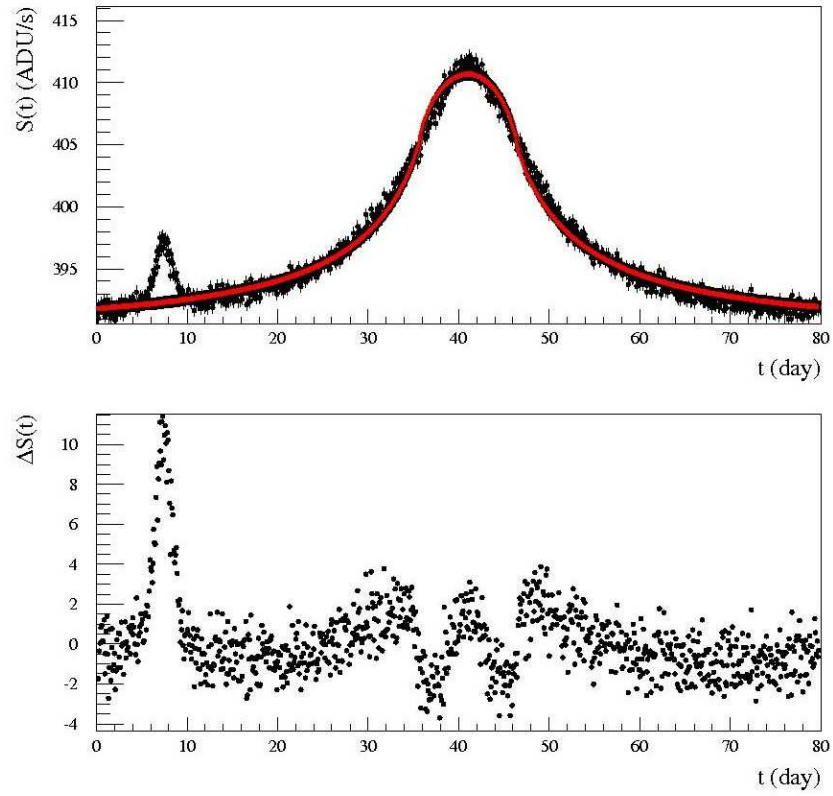
Figure 7. The same as in Fig. 4 for the second class event #4 (see Table 2).
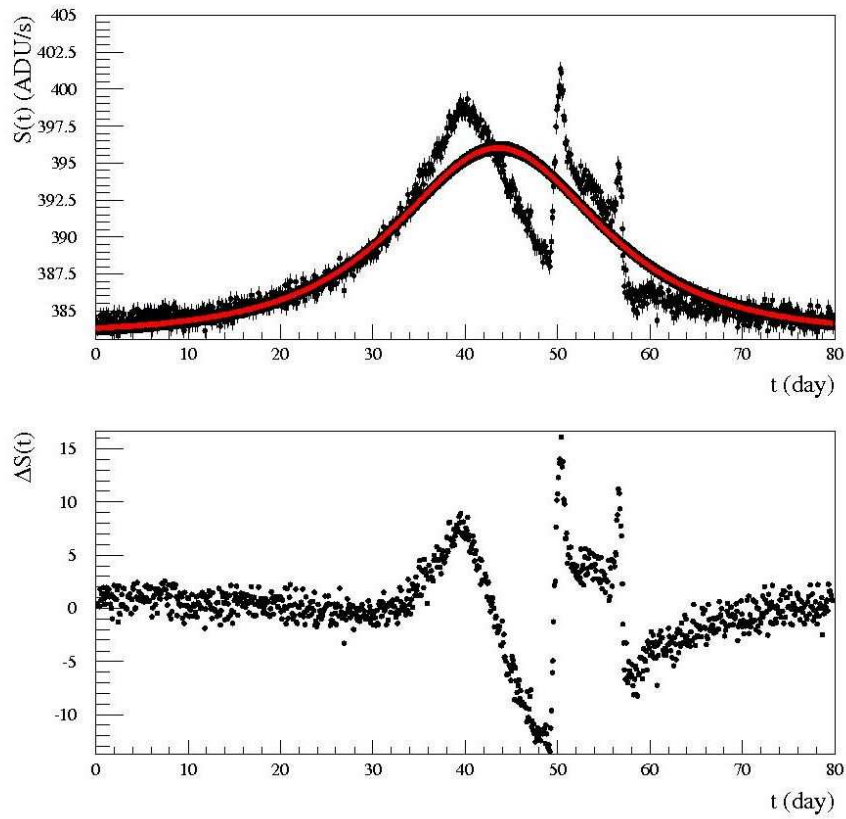
Figure 8. The same as in Fig. 4 for the second class event #5 (see Table 2).
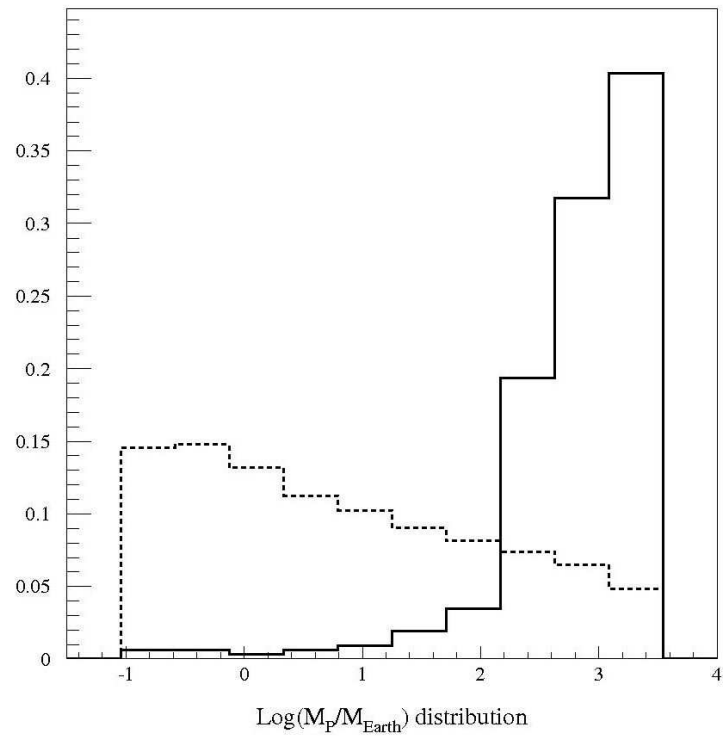
Figure 8. The distribution of the planet mass M_P for the second class of events is shown (solid line). For comparison, the M_P distribution of the generated events is also shown (dashed line). Here we take $N_{im} = 12$ day^{-1} and $D = 8$ m.
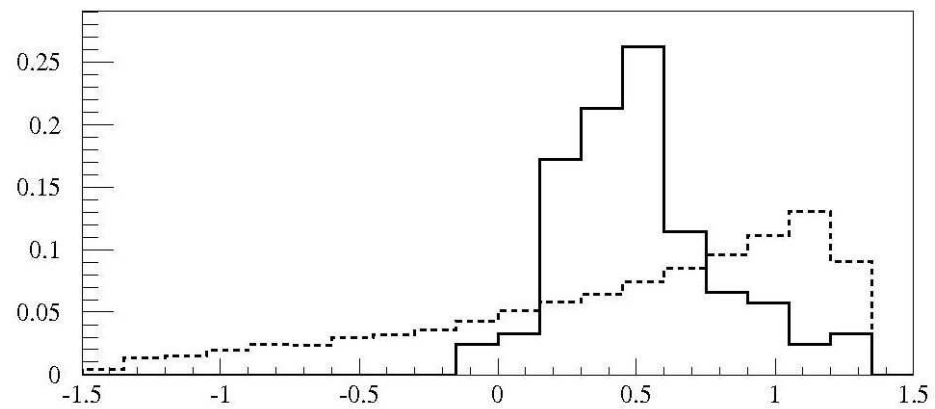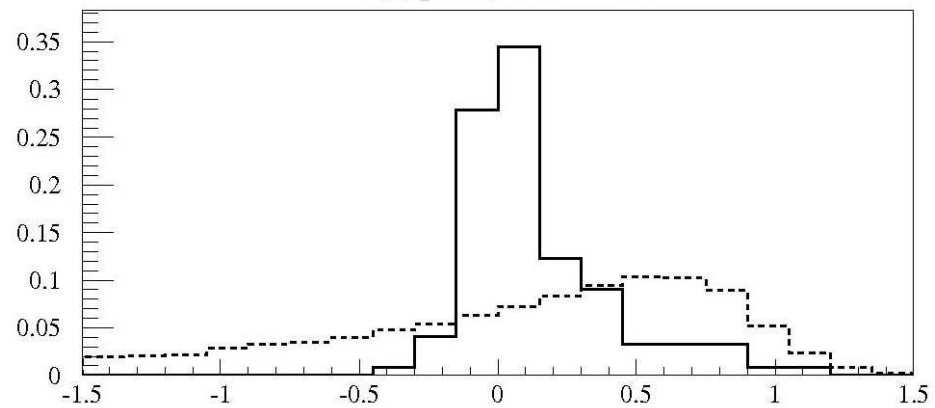
Fig. 6 Upper panel: normalised distributions of the star-to-planet separation $d_{\rm P}$ (in AU units) for the events with detectable planetary deviations (solid line) and for the generated events (dashed line). Bottom panel: distribution of $d_{\rm P}/R_{\rm E}$ for events as before.
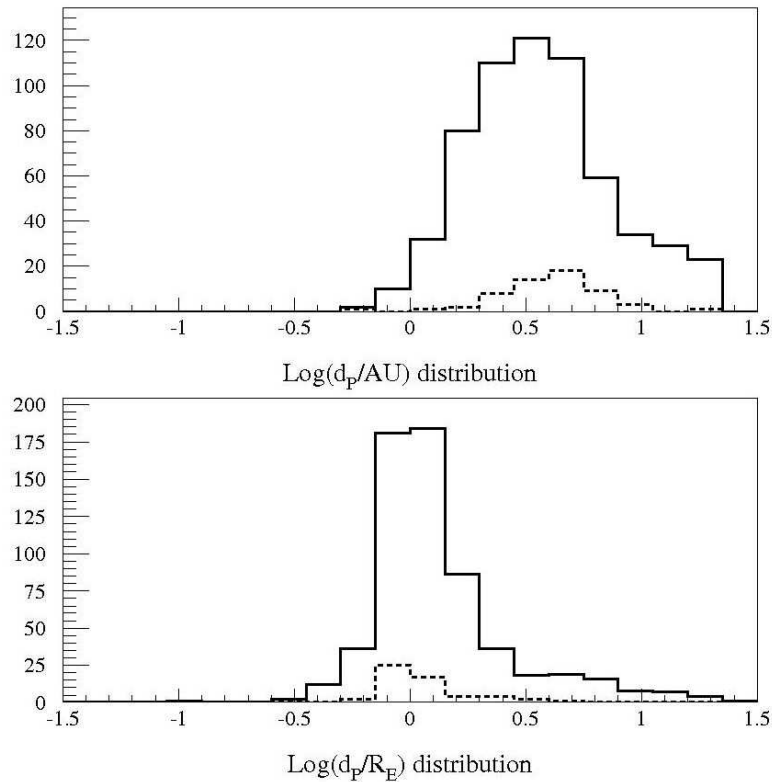
Figure 9. Upper panel: for the second class of events, distributions of the star-to-planet separation d_P (in AU units) for all (solid line) and small planetary mass ($M_P < 20\ M_\oplus$, dashed line). Lower panel: distributions of $s = d_P/R_E$ for events as before.
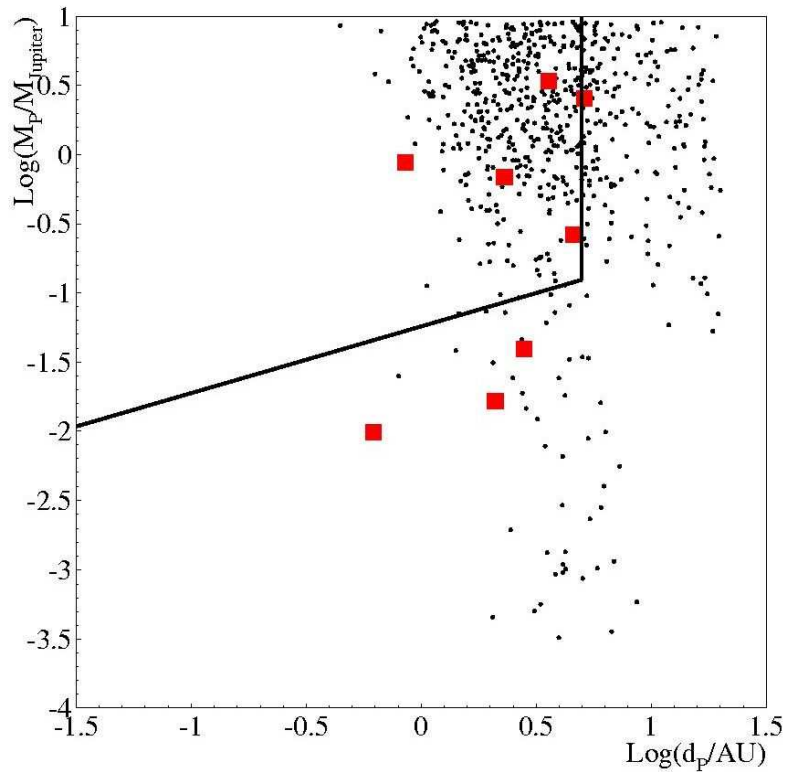
Figure 11. Scatter plot of the planet mass (in unit of Earth mass) vs planet distance (in Astronomical Units). The solid thick line delimits the region (upper and left) of planet detection accessible by the radial velocities, transit and direct imaging methods. The eight small boxes are the planets detected by the microlensing technique. Starting from a sample of **40,000** detectable pixel-lensing events ($D = 8$ m), **630** selected events (indicated by black dots) with $\chi_r > 4$, $N_{good} > 3$ and $\langle \epsilon \rangle_{max} > 0.1$ show planetary features and among these **48** events have $M_P < 20 \ M_{\oplus}$.
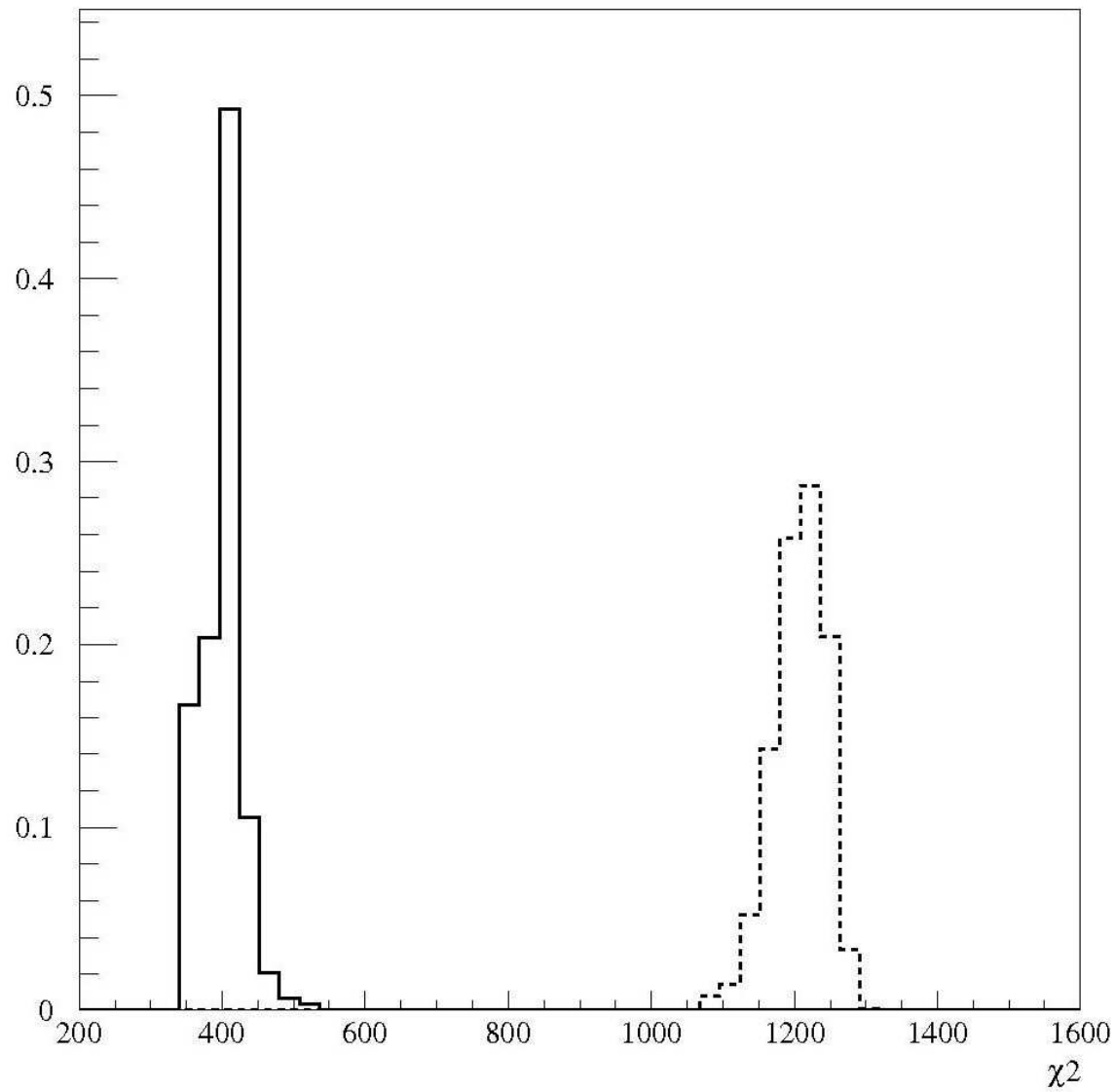
Fig. 7 Normalised distributions of the χ^2 for binary (solid line) and single lens fit (dashed line).
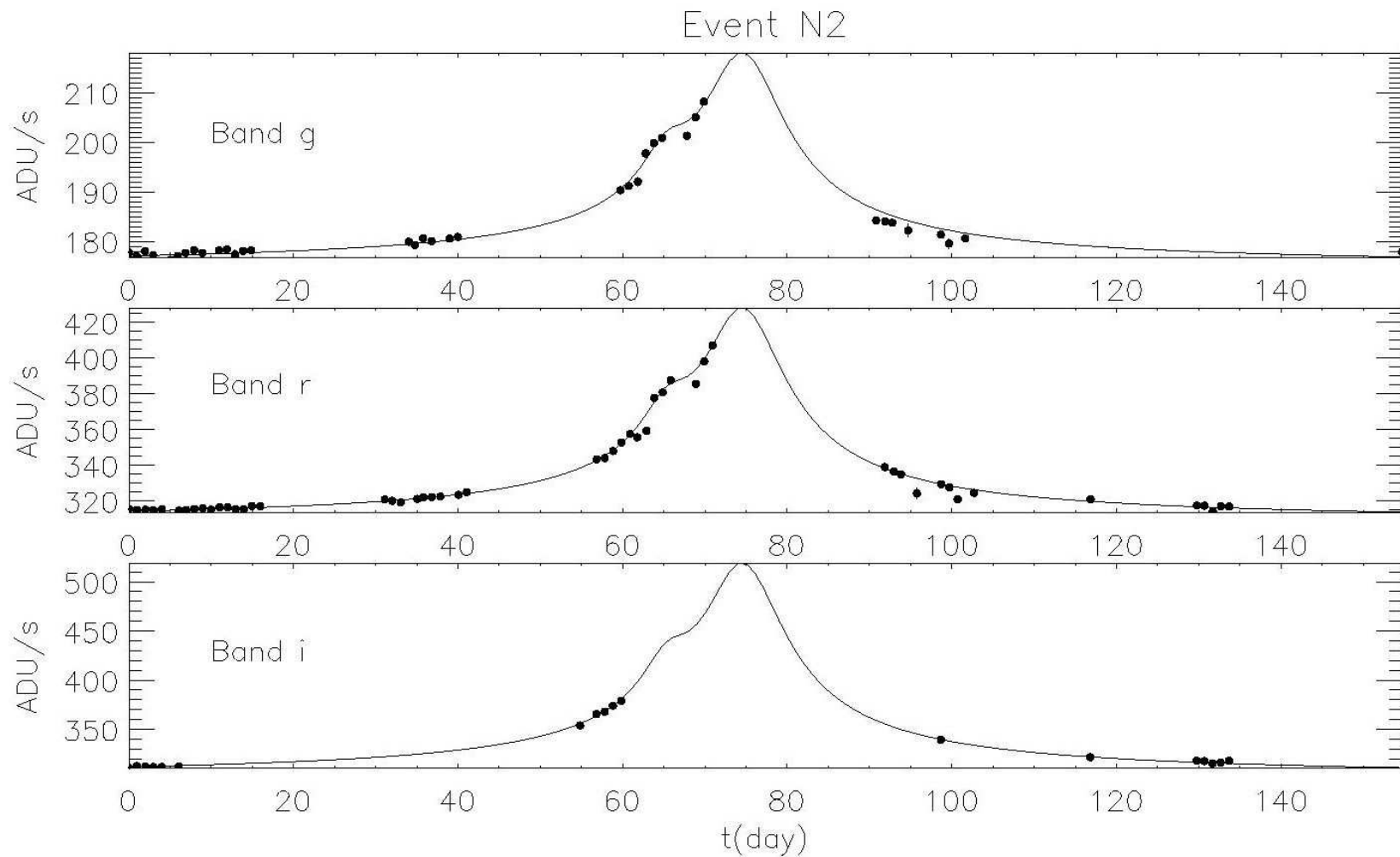
Fig. 8 The binary light curves corresponding to the C1 model [12] for g, r and i bands.

"A Giant Planet Around a Metal-Poor Star of Extragalactic Origin" by Setiawan et al at
http://www.sciencemag.org/content/early/2010/11/17/science.1193342

M = 1.25 M_Jup
P = 16.3 days:
http://exoplanet.eu/planet.php?p1=HIP+13044&p2=b

Personal note (JS): the extra-galactic origin of the star does not prove that the planet b is also of extragalactic origin.
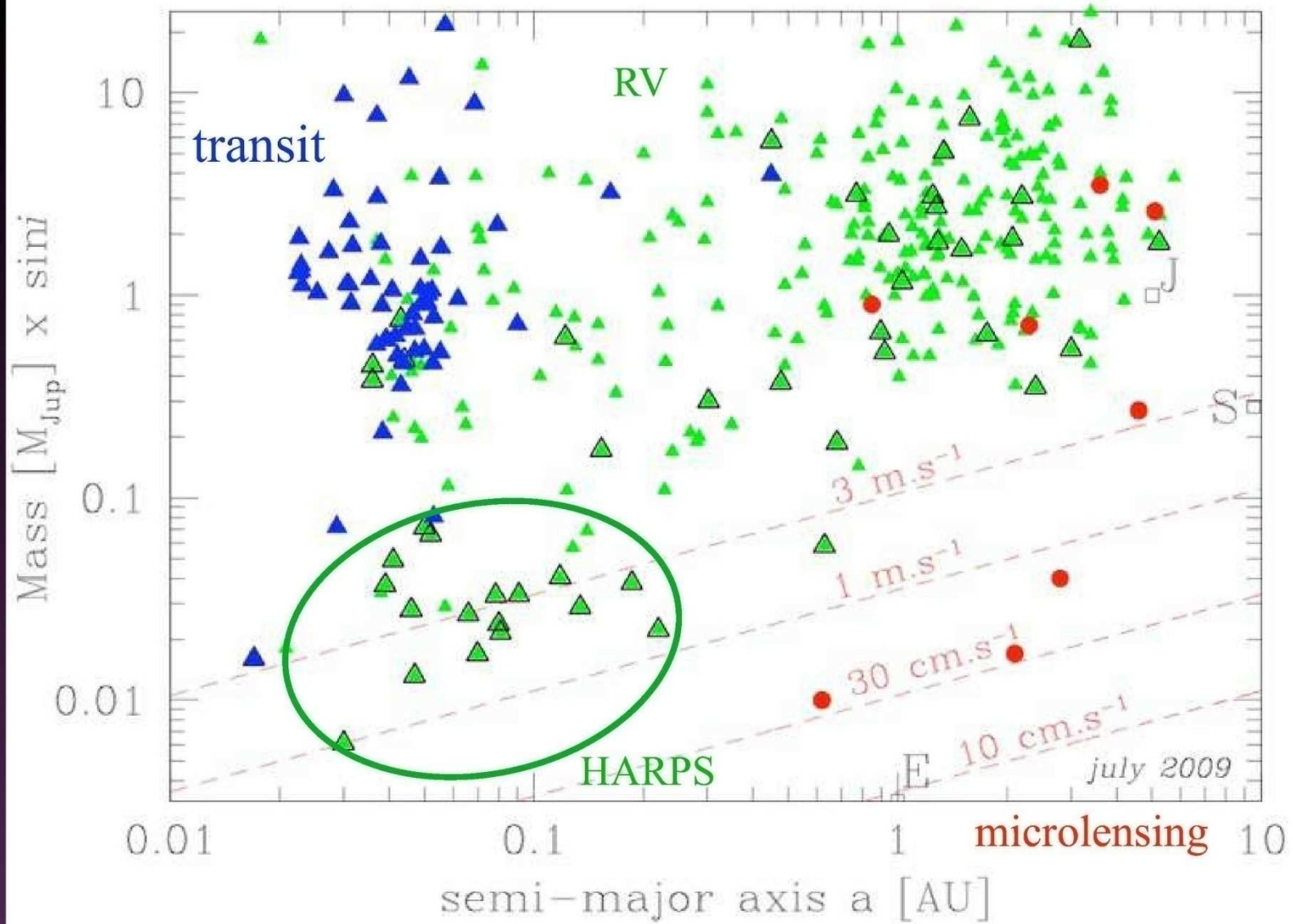
Temporal evolution of the discoveries
II. Towards longer-period and multi-planet systems

NASA Exoplanet Archive   2013 May 13   exoplanetarchive.ipac.caltech.edu

Number of Detections vs. Discovery Year

Legend:
- Radial Velocity
- Transits
- Microlensing
- Imaging
- Pulsar Timing
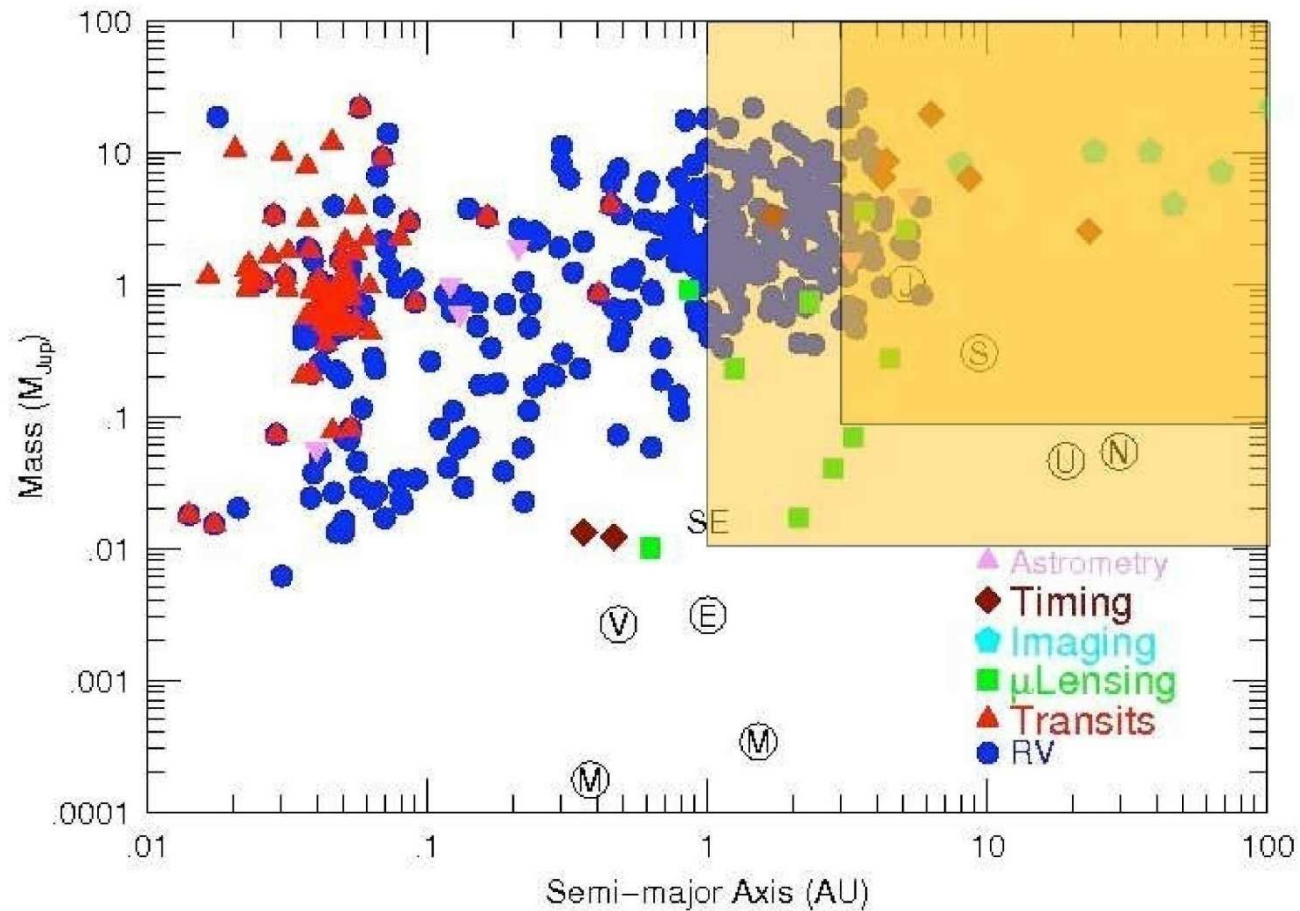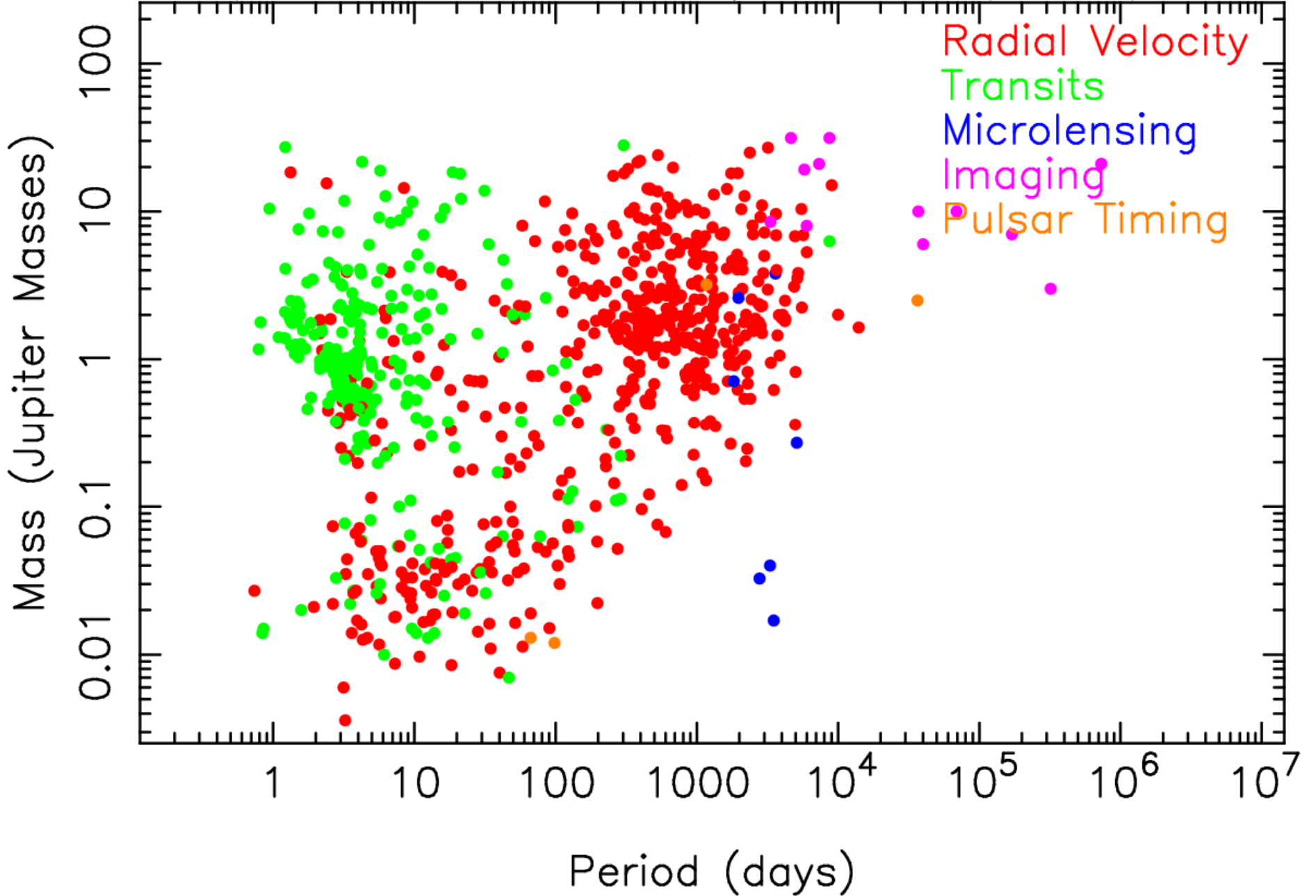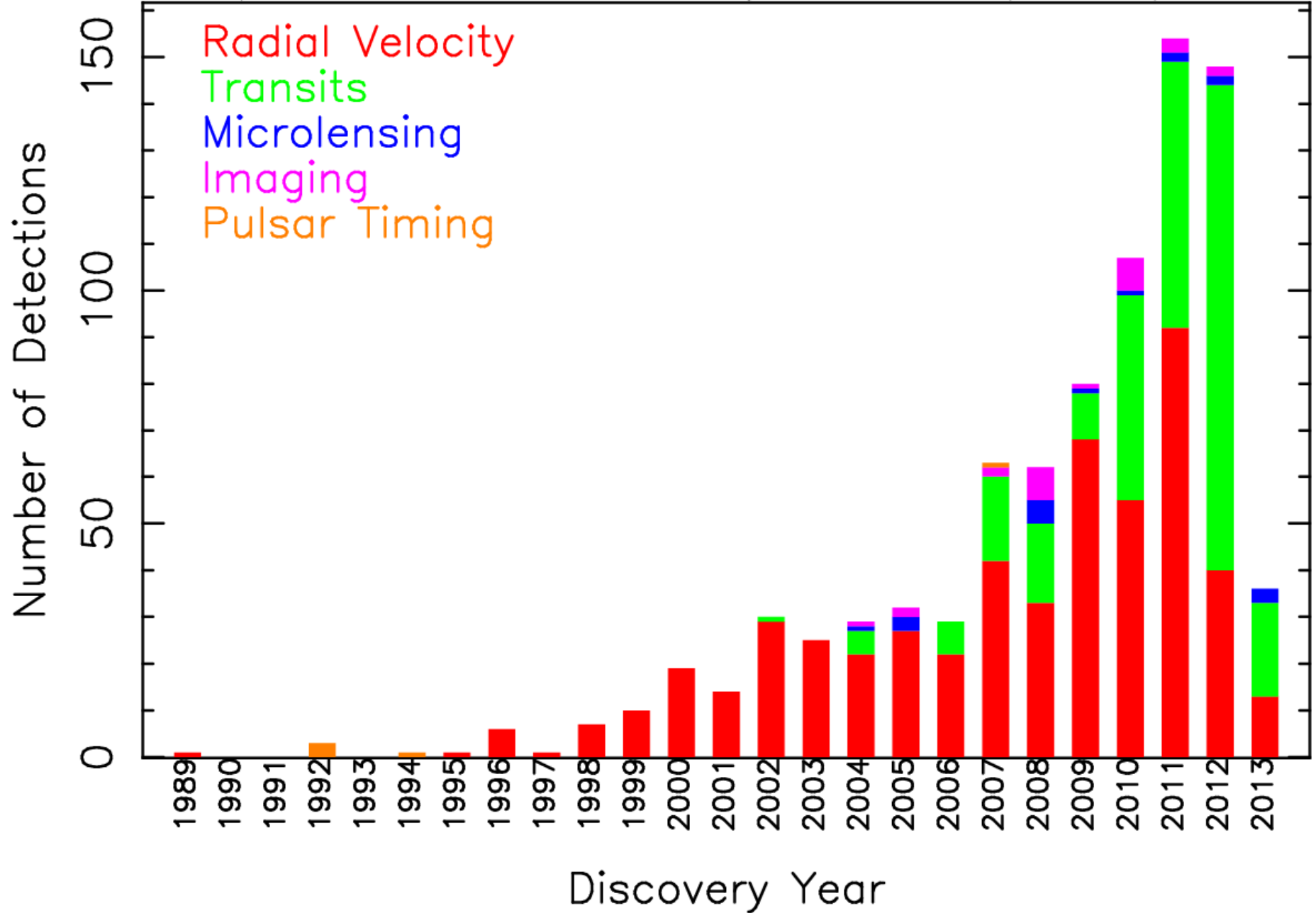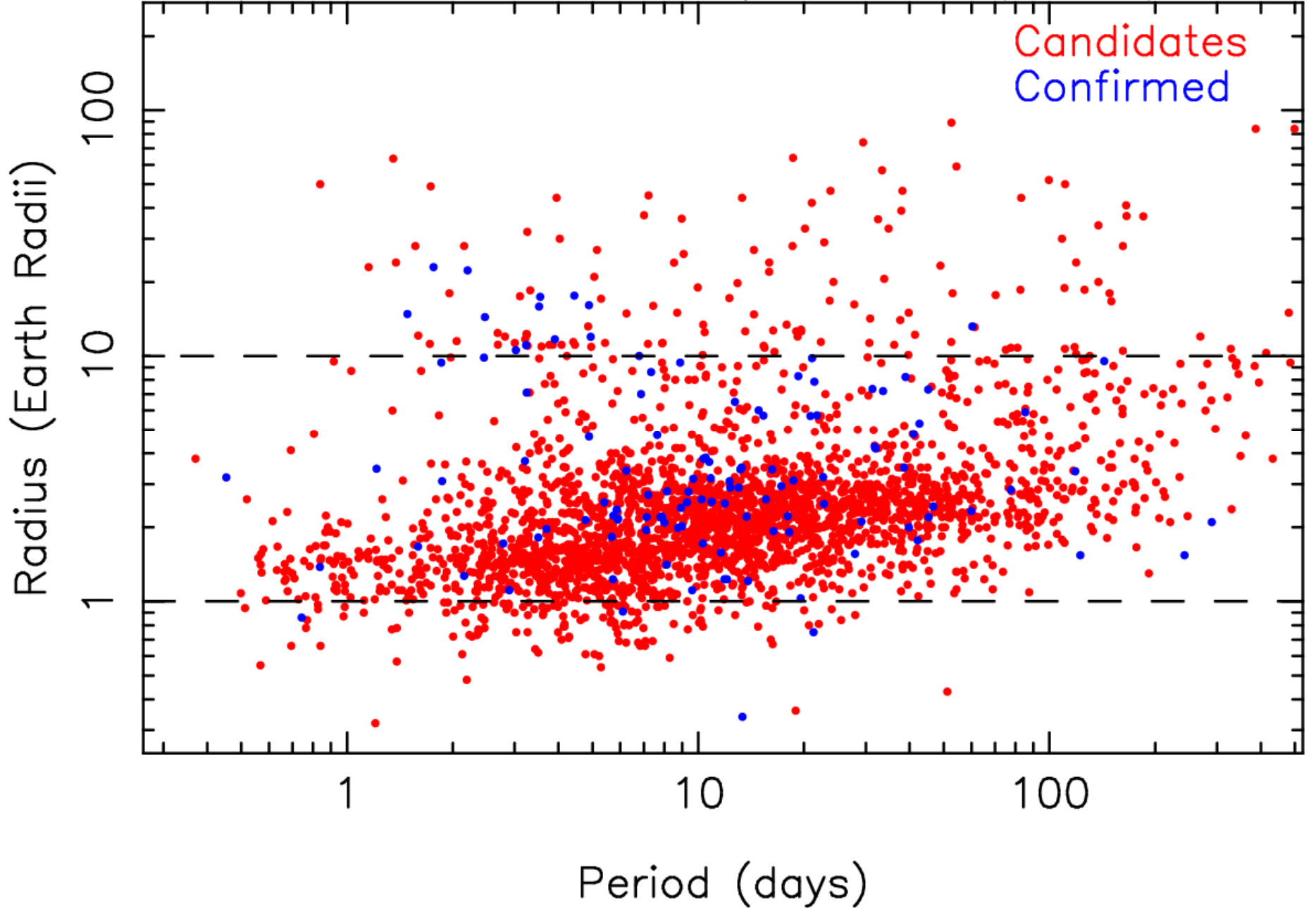
Polarization for pixel microlensing

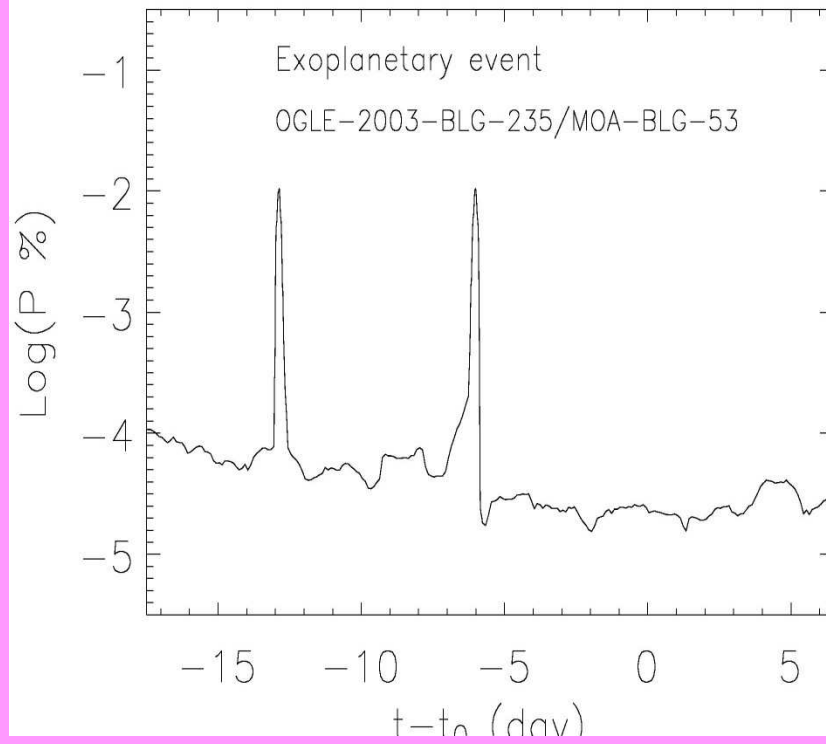G. Ingrosso, S. Calchi-Novati, F. De Paolis, P. Jetzer, A. Nucita, F. Strafella, AFZ (MNRAS, 2012)

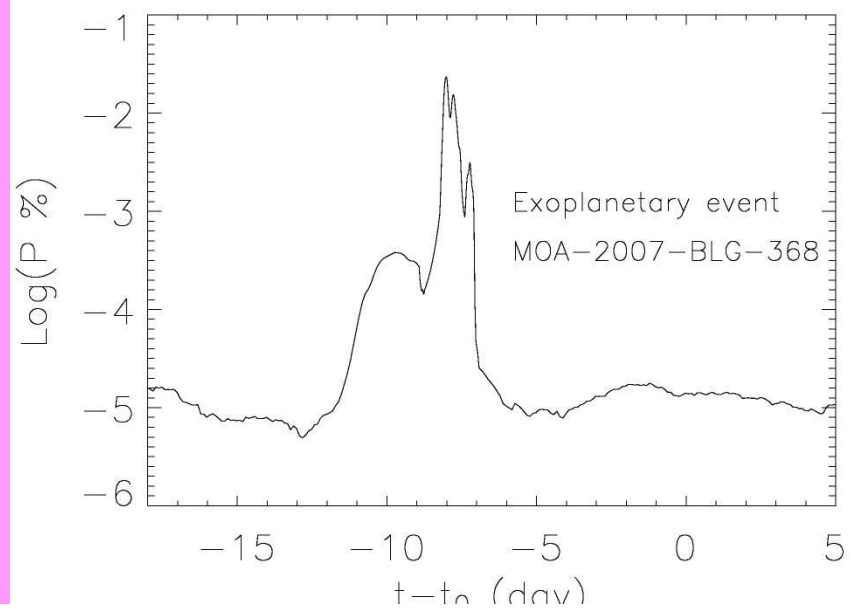Exoplanetary events

MOA−2008−BLG−310

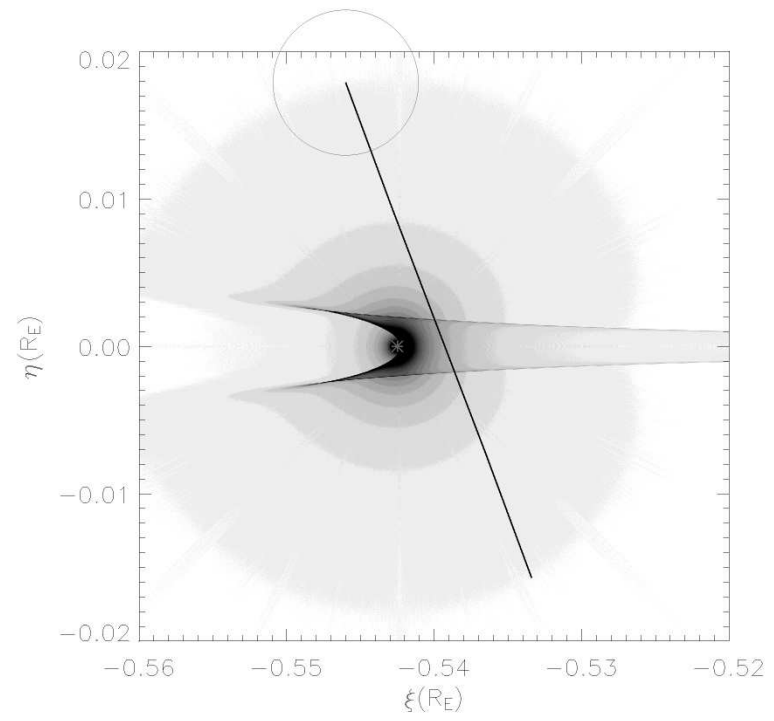MOA−2007−BLG−400

t−t₀ (day)

Exoplanetary event
OGLE-2005-BLG-390

Exoplanetary event
OGLE−2005−BLG−169

t−t₀ (day)

Exoplanetary event
OGLE-2003-BLG-235/MOA-BLG-53

Log(P %)

Exoplanetary event
MOA-2007-BLG-368

t−t₀ (day)

MOA−2008−BLG−310

A(t)

400

300

200

100

Log(P(t)%)

−1.0

−1.5

−2.0

−2.5

−3.0

$\theta_P(t)$

50

0

−50

−0.20   −0.10   0.00   0.10   0.20
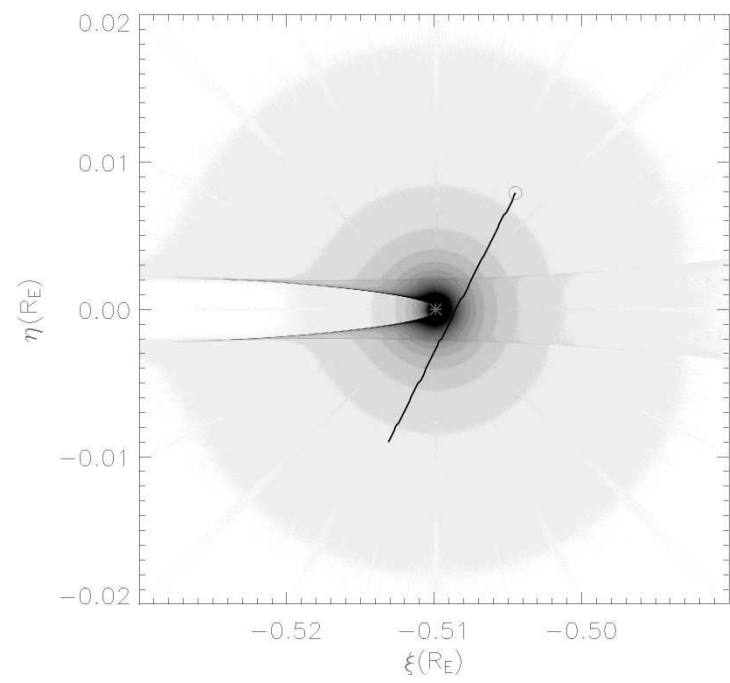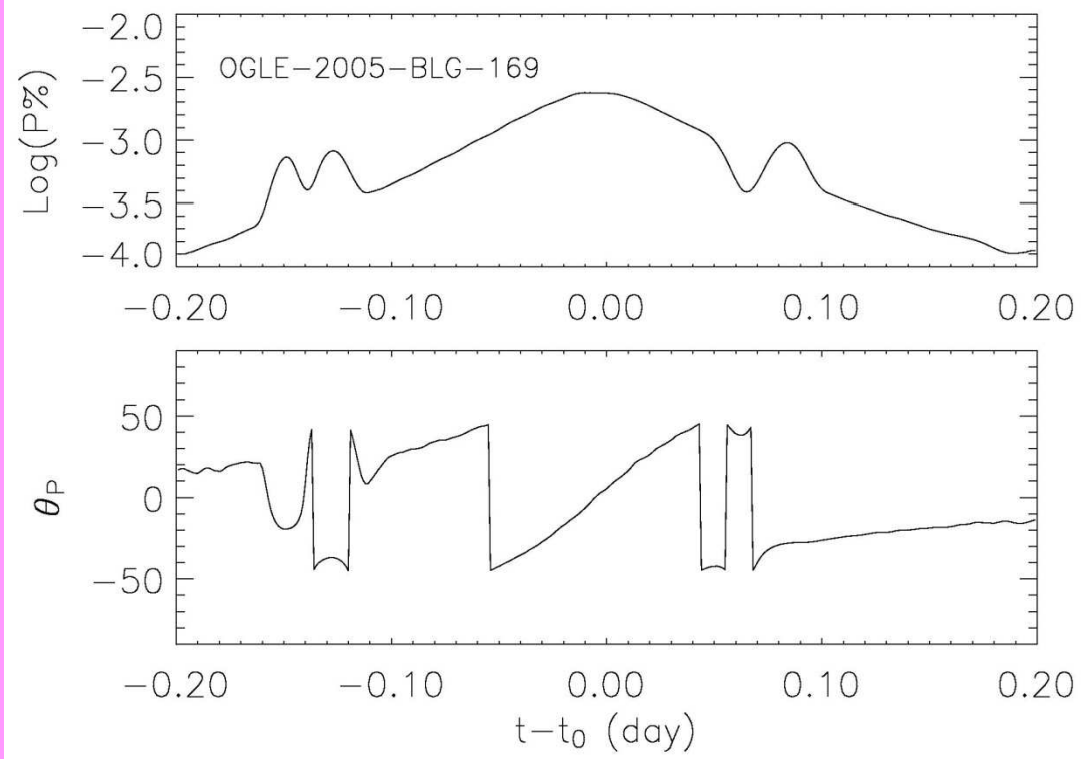
t−t$_0$ (day)

OGLE−2005−BLG−169
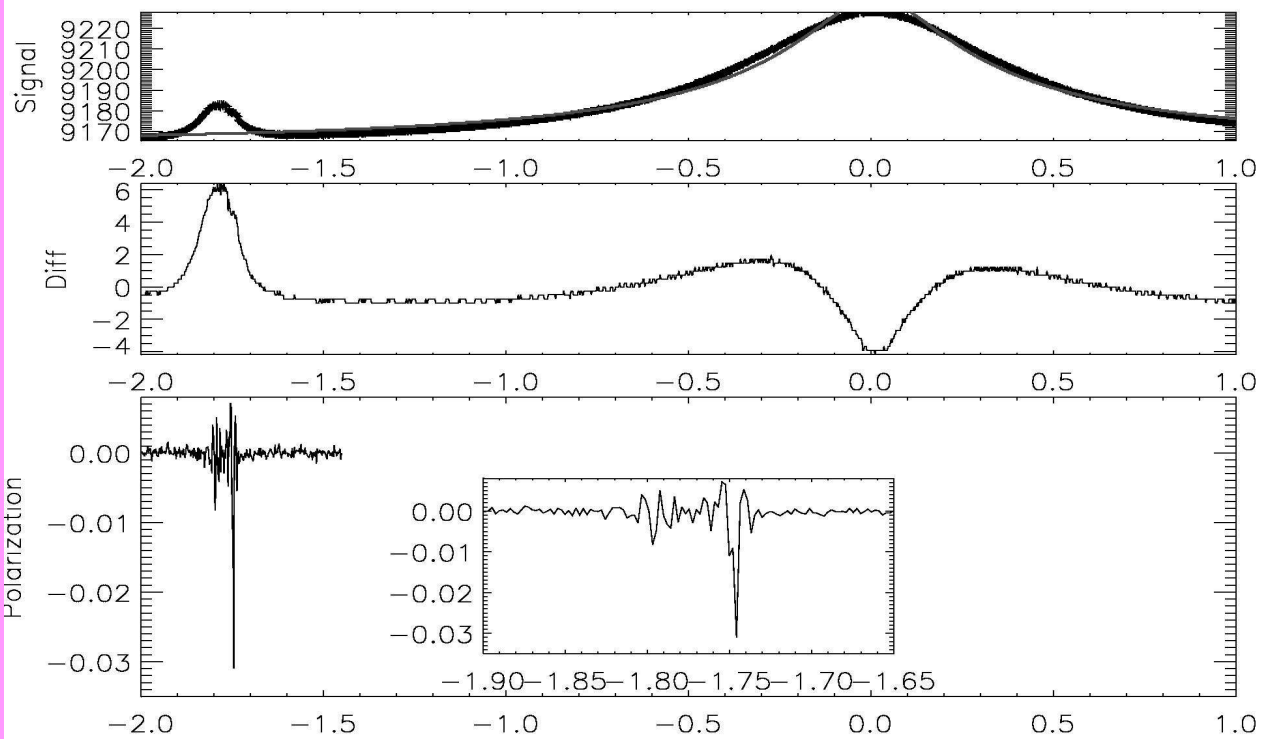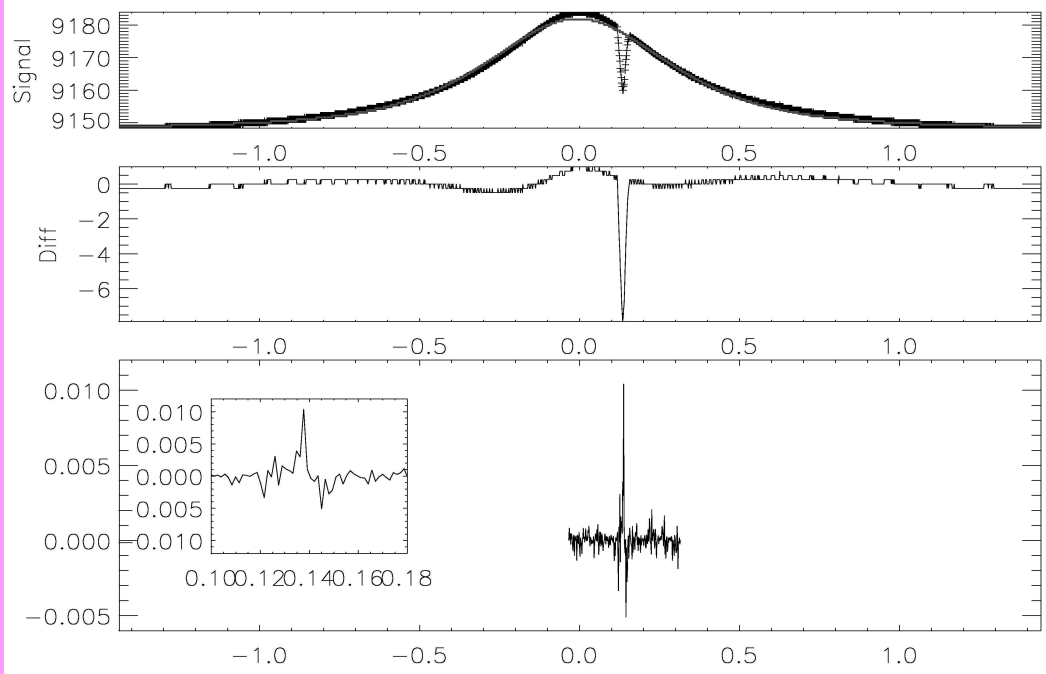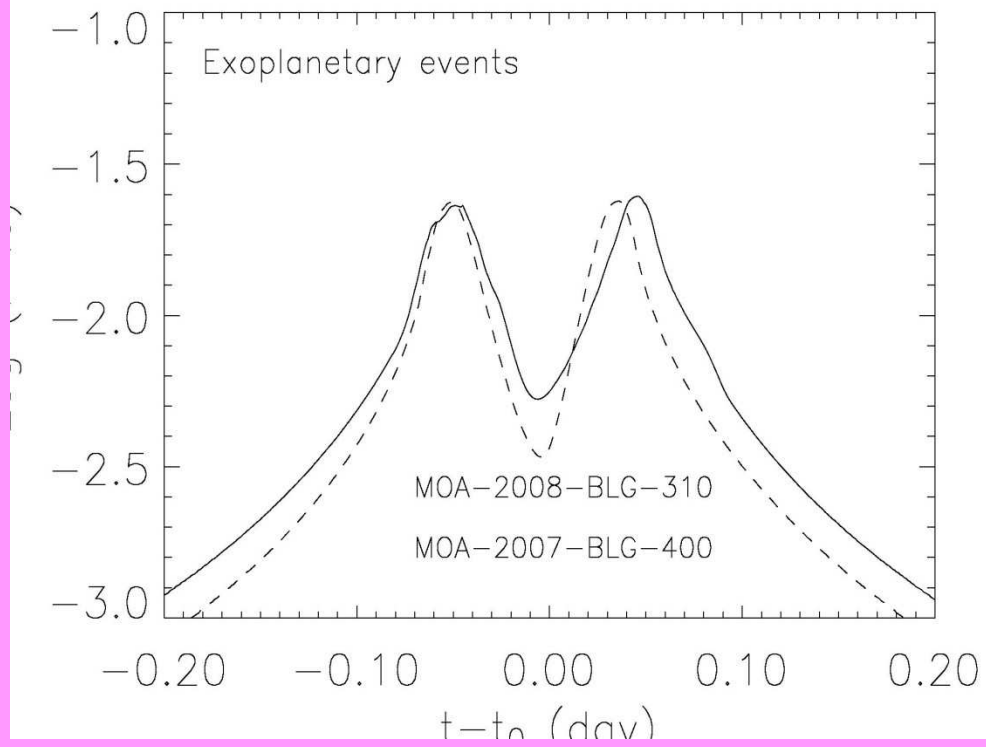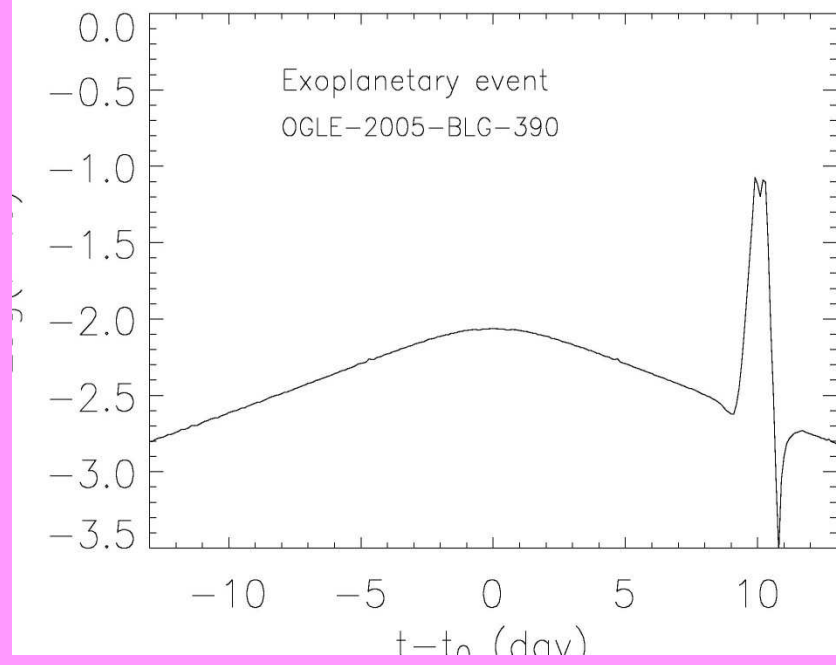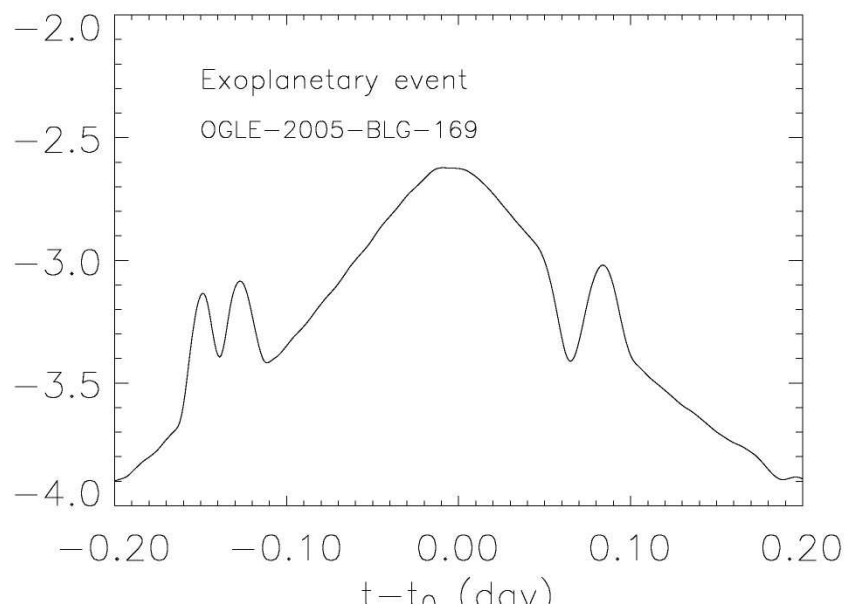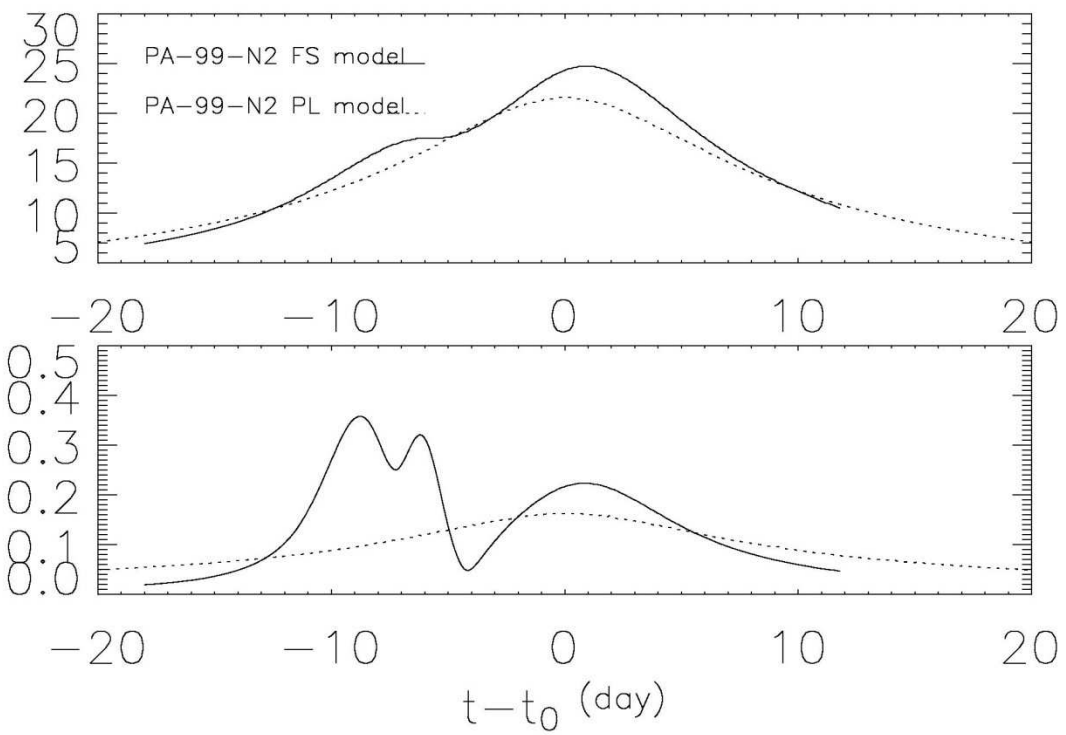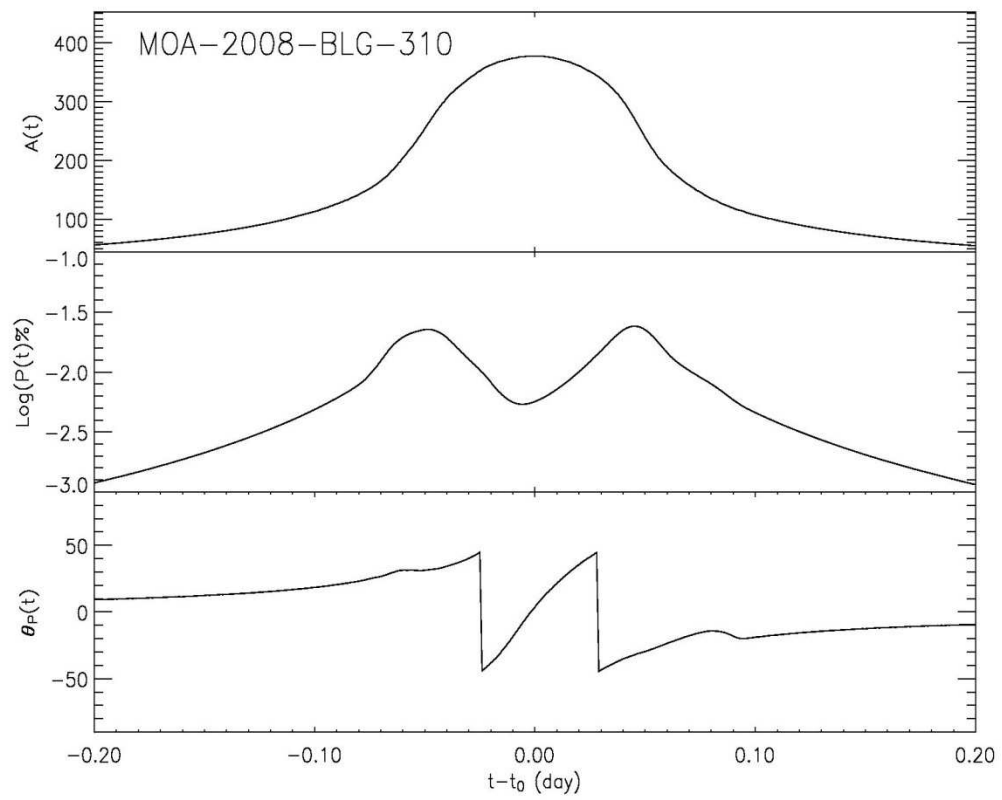
S. Mao & B. Paczynski (1991), Paczynski (1996) claimed that the most efficient technique to find light exoplanets at large distances (near the so-called snow line) from host stars is **microlensing.**

Conclusions

- **Polarization is a very important tool to verify of binary ML model (or star+planet as a microlens) for detected candidates**

- **Model parameters could be clarified (including information about a proper motion of a source in respect of gravitational microlens system) with the technique**
-

Thanks for your kind attention!